Alma Mater Studiorum – Università di Bologna

DOTTORATO DI RICERCA IN

Scienze e Tecnologie Agrarie Ambientali e Alimentari

Ciclo XXXII

Settore Concorsuale: 07/D1

Settore Scientifico Disciplinare: AGR/12

STUDY OF RAPID ALKALINIZATION FACTOR (RALF) GENES AS PLANT SUSCEPTIBILITY AGENTS DURING PLANT PATHOGEN INTERACTION IN STRAWBERRY

Presentata da: Francesca Negrini

Coordinatore Dottorato

Prof. Massimiliano Petracci

Supervisore

Prof. Elena Baraldi

Esame finale anno 2020

Table of Contents

Abstract

Rapid Alkalinization Factor (RALF) are cysteins-rich peptides ubiquitous in plant kingdom. They play multiple roles as hormone signals and recently their involvement in host-pathogen crosstalk as negative regulator of immunity in *Arabidopsis* has also been recognized. In addition, RALF homologue peptides are secreted by different fungal pathogens as effectors during early stages of infections. The aim of this work was to characterize RALF genes as susceptibility factors during plant pathogen interaction in strawberry. For this, the genomic organization of the RALF gene families in the octoploid strawberry (*Fragaria × ananassa)* and the re-annotated genome of *Fragaria vesca* were described , identifying 13 member in *F. vesca* (*FvRALF*) and 50 members in *F. x ananassa* (*FaRALF*). The changes in expression of fruit *FaRALF* genes was investigated upon infection with *C.acutatum* and B. cinerea showing that, among RALF genes expressed in fruit, *FaRALF3* was the only one upregulated by fungal infection in the ripe stage. A role of *FaRALF3* as susceptibility gene was then assessed trough *Agrobacterium*-mediated transient *FaRALF3* overexpression and silencing in fruits, revealing that *FaRALF3* expression promotes fungal growth and hyphae penetration in host tissues. *In silico* analysis was used to identify distinct pathogen inducible elements upstream of the *FaRALF3* gene. Agroinfiltration of strawberry fruit with deletion constructs of the *FaRALF3* promoter identified a 5' region required for *FaRALF3* expression in fruit, but failed to identify a region responsible for fungal induced expression. Furthermore, FaRALF3 and strawberry receptor FERONIA (FaMRLK47) were heterologously expressed in *E. coli* in order to purify active proteins forms and study RALF-FERONIA interaction in strawberry. However, it was not possible to obtain pure and active proteins. Finally RNAi transgenic plants silenced for the *FvRALF13* gene were genotypically and phenotypically characterized suggesting a role of *FvRALF13* in flowering time regulation and reproductive organs development.

1. General Introduction

1.1 Strawberry crop

Strawberry (*Fragaria spp*.) is one of the most consumed and produced fruits in the world with more than 35,000 ha of strawberries harvested each year and an average yield of 29.2 t/ha only in Europe. Due to the characteristic morphological softening, fruits are highly perishable and susceptible to several fungal pathogens which affect this crop both in field and at postharvest stage, causing severe economic losses every year (Boa, 2003). Management of strawberry diseases implies the use of multiple pesticides which have unwanted side effects on human health and environment, thus it is becoming urgent to study plant-pathogen interaction mechanisms in order to find alternatives plant protection strategies.

The cultivated strawberry *Fragaria x ananassa* is an allo-octoploid (2n=8x=56) species obtained from interspecific hybridization between octoploid (2n=8x=56) *Fragaria virginiana* (originally from North American) and octoploid (2n=8x=56) *Fragaria chiloensis* (originally from South African). The genomes of *Fragaria x ananassa* progenitors originated from multiple polyploidy events caused by fusion and interactions among genomes from four diploid ancestors species (namely subgenomes) (Duchesne, 1766). Identities of the four *Fragaria x ananassa* diploid progenitors have remained obscure until the release of the *Fragaria x ananassa* whole genome sequence (*Edger et al.,* in 2019). *Fragaria x ananassa* genome is composed of four diploid subgenomes inherited from respectively *Fragaria vesca, Fragaria iinumae, Fragaria nipponica* and *Fragaria viridis* species; each subgenome provides seven couples of chromosomes for a total of four sets of seven couples of chromosomes (Fig.1.1) (Folta & Barbey, 2019). Studies conducted by *Edger et al.* (2019) showed also that *F. vesca* inherited subgenome is the most influent and active in terms of genes number and at transcriptional level, revealing a subgenomical regulation among progenitor inherited genomes.

Strawberry and in particular the diploid woodland strawberry *Fragaria vesca* are also model species for Rosaceae crops and knowledge on this species can have important drawbacks in other main fruits crops. Genome of woodland strawberry was first sequenced in 2011 (Shulaev et

al., 2011) and recently re-annotated (Y. Li, Pi, Gao, Liu, & Kang, 2019) improving basic research and commercial strawberry.

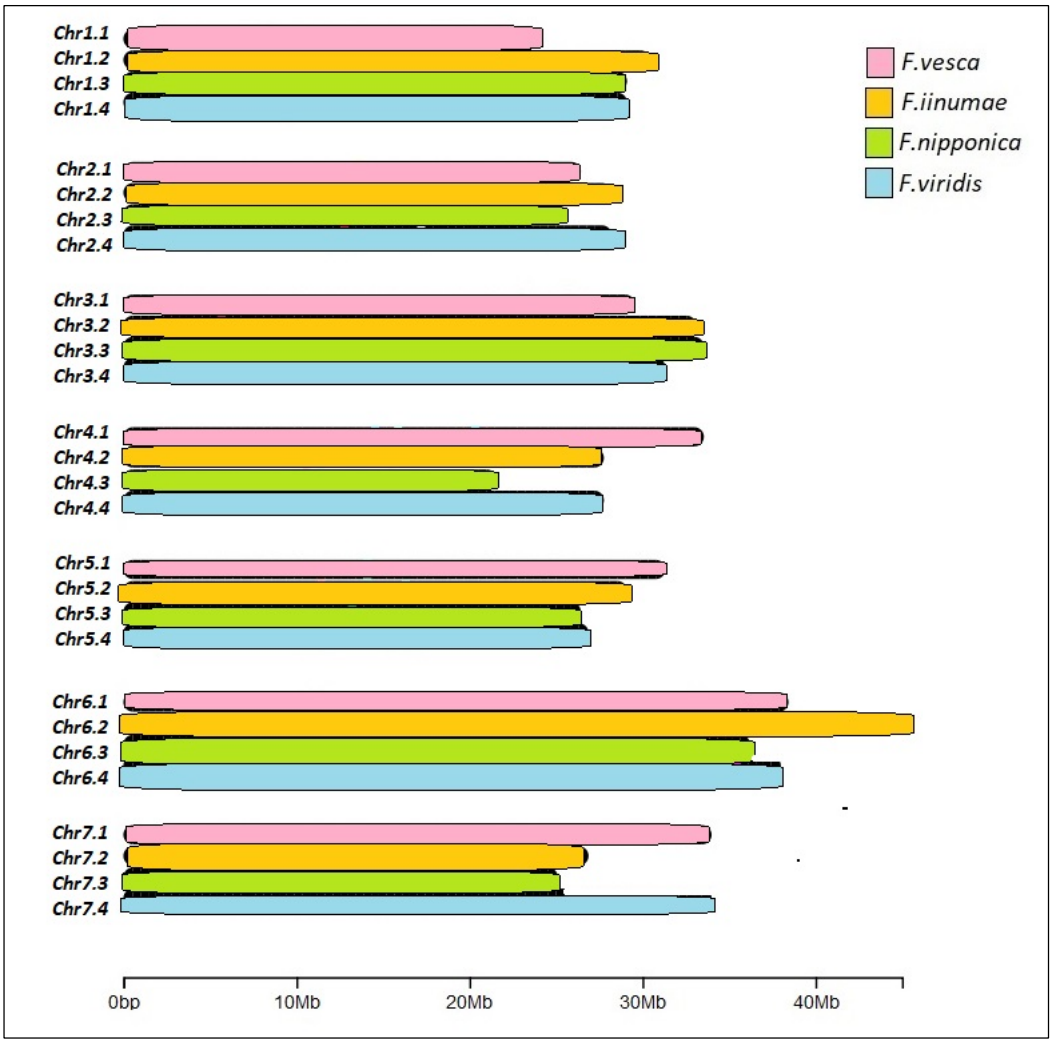

Fig.1.1 ***Fragaria x ananassa*** **octoploid genome chromosomes map.** Four sets of seven chromosomes are represented as colored bars, respectively pink belongs to *F. vesca* subgenome, orange to *F. iinumae* subgenome, green to *F. nipponica* subgenome and light blue to *F. viridis* subgenome. Bars length is represented in Megabases (Mb) scale.

1.2 Strawberry diseases

Strawberry fruit are particularly perishable, especially after harvest they can commonly undergo fungal spoilage. The main strawberry pathogen is *Botrytis cinerea*, followed by *Colletotrichum spp*., *Penicillium spp*., *Rhizopus stolonifer*, *Mucor spp*., which are the major pathogens responsible for postharvest decay of strawberry fruit (Feliziani & Romanazzi, 2016).

Colletotrichum spp. and in particular *C. acutatum* are the causal agents of strawberry (*Fragaria x ananassa*) anthracnose (Smith and Black, 1990; Howard, 1992). This fungal pathogen can affect most parts of the plant, such as fruits, flowers, roots, stolons, leaves and crown (Fig.1.2). Symptoms on fruits are visible as brown sunken lesions (Fig.1.2A), which can eventually develop mycelium and orange spore masses (Fig.1.2B). Infected flowers appear brown (Fig.1.2C) and stolons and petioles develop oval, elongated dark lesions (Fig.1.2D), while infected leaves show dark brown spots (Fig.1.2.E). Pathogen infection is favoured in the field by warm and humidity weather and generally the inoculum source are infected transplants and contaminated soil (Feliziani & Romanazzi, 2016). The fungi have an hemibiotrophic colonization strategy characterized by an initial biotrophic stage, which switch to a necrotrophic behaviour. After spore germination and appressoria formation, *C. acutatum* can stay quiescent inside the host tissue until fruit ripens (Prusky, 1996) developing visible symptoms only during post-harvest period, when fruit production reaches its highest value. *C. acutatum* can infect both white and red fruits, but on white fruits, *C. acutatum* becomes quiescent as melanized appressoria after 24 h of interaction (Guidarelli et al., 2011) and only when fruit ripens (red stage) the pathogen restores its growth and symptoms become apparent within 3 days.

B. cinerea is the causal agents of grey mold and infect strawberry fruits and flowers. Symptoms are visible on fruits as dark circular area characterized by softer tissues which develop abundant sporulation and mycelium turning from white to grey depending on light exposure. (Feliziani & Romanazzi, 2016). Upon penetration in the strawberry floral organs or unripe fruits, *B. cinerea* enters a quiescent state and resumes its activity exclusively when the fruit ripens (Jarvis, 1962; Williamson et al., 2007; Prusky and Lichter, 2007).

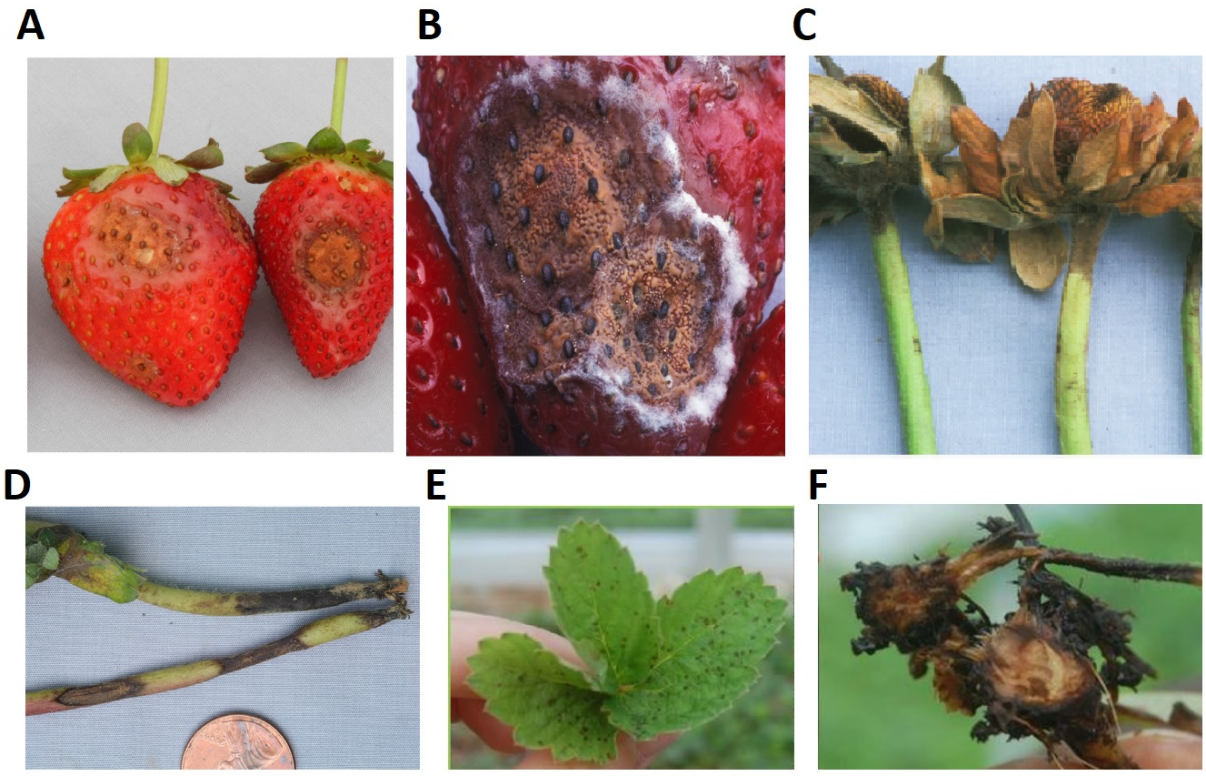

Fig.1.2 Anthracnose symptoms on strawberry organs (*Fragaria x ananassa*). a) Strawberry fruits symptoms are visible as brown lesions and severe infections can develop mycelium and orange spores (b). Anthracnose symptoms on flowers (c), stolons (d), leaves (e) and crown (f). Pictures were adapted from *Production Guideline,* www.CalStrawberry.com, https://ucanr.edu/blogs/strawberries_caneberries/blogfiles/47929.pdf .

It has been suggested that the ability of *C. acutatum* and *B. cinerea* to enter a quiescent state is influenced by: i) deficiency in the host nutritional resources required for pathogen development; ii) the presence of preformed or inducible fungistatic antifungal compounds in resistant unripe fruits; and iii) an unsuitable environment for the activation of fungal pathogenicity factors (Prusky & Lichter, 2007). Due to latent infection by the two pathogens, the control and management of anthracnose and gray mould disease becomes more complex (Vicente, Martínez, Civello, & Chaves, 2002).

1.3 Rapid Alkalinization Factor (RALF) gene family

Plants are naturally provided with very sophisticated and strong immune mechanisms and the development of the disease is generally dependent on the 'switch off' state of these mechanisms or, in turn, on the 'switch on' state of susceptibility mechanisms. Besides suppression or plant immunity-evasion, pathogens, in particular biotrophs and hemibiotrophs, require cooperation of the host for establishment of a compatible interaction. Accommodating the pathogen involves enabling it to establish feeding structures, inside the host cell to obtain nutrients. All plant genes that facilitate infection and support compatibility can be considered susceptibility genes. Mutation or silencing of a susceptibility gene can therefore limit the ability of the pathogen to cause disease (van Schie & Takken, 2014). Lately, the possibility to control susceptibility genes has emerged as a more promising approach to develop resistant crops than the control of resistant genes. However, the knowledge about the susceptibility factors present in the plants favouring pathogens invasion, and/or growth, remains limited.

Rapid Alkalinization Factors (RALF) are small signal peptides (SSP) which regulate a variety of different functions such as cell expansion (Haruta, Sabat, Stecker, Minkoff, & Sussman, 2014), root growth (Murphy et al., 2016), root hair differentiation (Wu et al., 2007; Bergonci et al., 2014; Du et al., 2016), stress response (Atkinson et al., 2013), pollen tube elongation and fertilization (Covey et al., 2010 ; Mecchia et al., 2017; Ge et al., 2017,2019). Recently, it was reported that in *A. thaliana,* RALF peptides act as negative regulators of the plant immune response to bacterial infection (Stegmann et al., 2017), since the binding of processed RALF23 to the FER receptor inhibits the formation of the complex between the immune receptor kinases EF-TU RECEPTOR (EFR) and FLAGELLIN-SENSING 2 (FLS2) with their co-receptor BRASSINOSTEROID INSENSITIVE 1–ASSOCIATED KINASE 1 (BAK1), which is necessary to initiate immune signalling. Interestingly, biologically-active RALF homologs have also been identified in fungal plant pathogens, possibly following interspecies horizontal gene transfer, pointing to a role for fungal RALF genes as virulence factors (Thynne et al., 2017). In facts, a RALF-homolog fungal peptide is fundamental for *Fusarium oxysporum* ability to induce host alkalinisation and infection (Masachis et al., 2016). Since for many pathogenic fungi alkalinisation is important to activate virulence factors and successfully infect plant tissues, RALF secreted peptides may act as initial effectors to promote

host alkalinisation at early stage infection, when hyphal biomass is not sufficient to secrete a huge amount of ammonia (Fernandes et al. 2017))

Expression analysis conducted on *Fragaria x ananassa (Fxa)* fruits infected with *C. acutatum* at two different ripening stages revealed an increase in the expression of a RALF gene in the susceptible fruit at early stage infection (Guidarelli et al., 2011). Upregulation of RALF genes during plant infection has also been observed in mature red tomato fruits (*Solanum lycopersicum)* infection by *Colletotrichum gleosporioides* and in rice upon *Magnaporthe oryzae* infection (Wang et al., 2019). This suggests a role for RALF gene expression as a susceptibility factor in fungal infection (Alkan, Prusky, Fluhr, Friedlander, & Ment, 2014). Furthermore Dobón et al. (2015), studying the expression pattern of four *Arabidopsis* transcription factors mutants (*at1g66810, pap2, bhlh99, zpf2)* characterized by the increased susceptibility to *B. cinerea* and *Plectosphaerella cucumerina*, observed an upregulation of *RALF23, RALF24, RALF32* and *RALF33* genes expression.

these previous evidences suggested to further characterized RALF genes as susceptibility genes also in strawberry.

1.4 RALF signalling pathway

In plants, several small secreted peptides (SSPs) function as hormone signalling molecules to respond to internal and external stimuli (Olsson et al., 2019). SSPs are known to be involved in different processes, ranging from organs growth to biotic and abiotic responses (Murphy et al., 2012; Tavormina et al., 2015).

RALFs are cysteins-rich SSPs originally identified for their ability to rapidly alkalinize tobacco cell culture (G. Pearce, Moura, Stratmann, & Ryan, 2001). They are ubiquitous in plant kingdom with 37 members identified in *Arabidopsis thaliana* (Sharma et al., 2016; Campbell and Turner, 2017). *RALF* genes are translated as pre-pro-peptides and activated in the apoplast through proteolytic cleavage. Besides the signal sequence necessary for extracellular extrusion, RALF proteins contain distinctive amino acid motifs, such as the RRILA motif for S1P protease recognition (Srivastava, Liu, Guo, Yin, & Howell, 2009) and the YISY motif, important for signaling cascade activation (Pearce et al., 2010; Xiao et al., 2019). In addition four conserved cysteines

forming two disulfide bonds are present in RALF sequences (Fig.1.3A). Based on these features, RALF peptides were classified in four major clades (Campbell and Turner, 2017) Campbell and Turner, 2017); clades I, II and III contain typical RALF peptides, whereas clade IV groups the most divergent RALF peptides, lacking RRILA and YISY motifs, and in some cases containing only three cysteines.

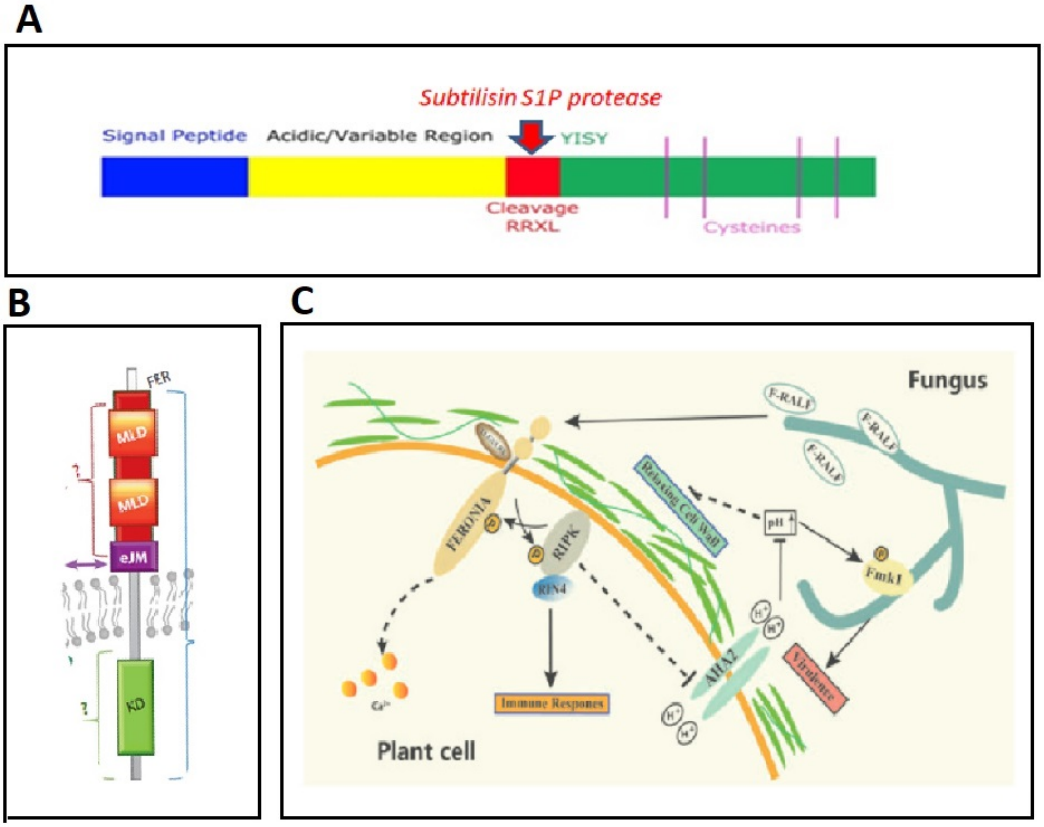

Fig.1.3 RALF and FERONIA protein structure and signaling pathway. a) RALF peptide structure scheme. Peptides are usually characterized by signal sequence peptide for apoplastic localization (blue), an acidic variable region (yellow), the Subtilisin S1P protease cleavage recognition motif RRXL (red), and the mature peptide (green) characterized by four conserved cysteines (magenta lines) and YISY conserved active site fundamental for interaction with receptor. Propeptide RALF sequence refers to yellow-red-green sequence boxes, while mature peptide to green box sequence. Picture adapted from Campbell and Turner (2017). b) FERONIA protein structure is composed of intracellular kinetic domain (KD), external juxtamembrane portion (eJM) and the extracellular domain (red) formed by two tandem Malectin-like motifs (MLD). c) A hypothetical model for RALF–FER-mediated pathogen response. The RALF-like peptides secreted by pathogens activate the FER–RIPKcomplex that would inhibit rhizosphere acidification through phosphorylation of AHA2. RALF-induced pH elevation promotes the activity of Fmk1 and enhances pathogenicity. RIPK-regulated RIN4 protein also participates in effector-triggered immunity (ETI). Arrows denote activation, and bars indicate repression. Picture adapted from Liao *et al.,*(2017).

RALF peptides bind to the *Catharanthus roseus* Receptor Like Kinases 1 - like family protein (CrRLK1L), characterized by two tandem malectin-like motif in the extracellular domain (Fig.1.3B) and known to be involved in cell expansion and reproduction throughout the plant kingdom (Galindo-Trigo *et al.,* 2016)(Galindo-Trigo et al., 2016). The large CrRLK1L receptor family includes FERONIA (FER) receptors, previously reported to interact with *Arabidopsis RALF1* and *RALF23* (Haruta *et al.*, 2014(Haruta et al., 2014; Stegmann *et al.*, 2017)Stegmann et al., 2017), Buddah's Paper Seal 1, 2 (BUPS1/2), ANXUR1, 2 (ANX1/2) protein, which interact through their ectodomain and bind to RALF4 and 19 in pollen the tube (Ge et al., 2017)(Ge et al., 2017) and THESEUS1 (THE1), the RALF34 receptor in roots (Gonneau et al., 2018)(Gonneau et al., 2018). RALF peptides binding to *CrRLK1L* receptors also involve other interacting partners such as Lorelei-like-Glycosylphosphatidylinositol-Anchored protein (LLG1,2,3) (Li *et al.*, 2015(Li et al., 2015; Xiao *et al.*, 2019)Xiao et al., 2019) and Leucin-Rich Repeat Extensins (LRX) reported to bind RALF4/19 in the pollen tube (Mecchia *et al.*, 2017(Mecchia et al., 2017;Moussu *et al.*, 2019)Moussu et al., 2019) and to interact with FER, as part of cell wall sensing system responsible for vacuolar expansion and cellular elongation (Dünser et al., 2019)(Dünser et al., 2019). RALF binding to receptors leads to a number of different intracellular signaling events involving different molecular components, mostly still unidentified. However, it is known that in Arabidopsis binding of RALF1 to FER receptor results in plasma membrane H(+)-adenosine triphosphatase 2 phosphorylation, causing the inhibition of protein transport and subsequent apoplastic alkalinization (Haruta et al., 2014)(Haruta et al., 2014) (Fig.1.3C).

1.5 Aim of the study

Considering the important role played by RALF family genes and the receptor FERONIA during plant-pathogen interaction, the aim of this study was to characterize the role of *FaRALF* genes and proteins as susceptibility factors in infected strawberry.

1. Characterization of RALF family genes in octoploid and diploid strawberries considering sequence variability and tissues specific transcriptional regulation.
2. RALFs expression analysis during pathogens infections.
3. Study of the role played by *FaRALF3-1* during *C. acutatum* strawberry fruits infection, through Agro-infiltration mediated *FaRALF3-1* silencing and overexpression.
4. Pathogen-responsive regulatory elements identification in *FaRALF3-1* promoter, through *in silico* and *in vivo* analysis.
5. FaRALF3 and FaMRLK47 (FERONIA strawberry homolog) proteins purification from *E. coli* heterologous expression, in order to study strawberry RALF-FERONIA ligand-receptor interaction.
6. Genotypic and phenotypic characterization of *F. vesca* transgenic RNAi plants silenced for *FvRALF13* gene, considering plants growth traits and *C. acutatum* plants susceptibility.

2. Rapid Alkalinization Factor (RALF) gene family characterization in strawberry

2.1 Introduction

Nine RALF genes have been previously identified in the Fragaria vesca v1 genome by Campbell and Turner (2017). In order to classify the members of RALF gene family in *F. vesca*, the recent genome annotation (v4.0.a2) (Y. Li et al., 2019) was searched using 'RALF' as keyword gene name, revealing the presence of 13 RALF genes. Then, *F. vesca* RALF gene sequences were used as query against a database of predicted proteins (v1.0.a1 Proteins source) in *Fragaria x ananassa cv. Camarosa* (*Fxa*). For this, genome localization, phylogenetic and transcriptional analysis were conducted, based on available genomic and trascriptomic sources, with the aim to get insights into the different RALF gene functional roles.

2.2 Materials and Methods

2.2.1 RALF family genes identification, phylogenetic analysis, and chromosome map generation

F.vesca RALF genes already reported by Campbell and Turner (2017) were implemented using the keyword 'RALF' as query for GDR search (v4.0.a2). The output was compared and integrated. Nucleotide sequences of the 13 *Fragaria vesca* RALF members were used as query for BLASTx against *Fragaria x ananassa cv. Camarosa* Genome v1.0.a1 proteome (Yuan et al., 2019)(Yuan et al., 2019) to find octoploid RALF homologs. *Fragaria x ananassa* RALF peptide sequences were aligned by MUSCLE (Edgar, 2004)(Edgar, 2004) and the phylogeny was inferred using the Maximum Likelihood method and JTT matrix-based model (Jones, Taylor, & Thornton, 1992)(Jones et al., 1992). The tree with the highest log likelihood was chosen. The Initial tree was obtained automatically by applying Neighbor-Join and BioNJ algorithms to a matrix of pairwise distances estimated using a JTT model, and then selecting the topology with superior log likelihood value. Evolutionary analyses were conducted MEGA X (Kumar, Stecher, Li, Knyaz, & Tamura, 2018)(Kumar et al., 2018). To classify the new members in clades, all the RALF peptide sequences available from Campbell and Turner Campbell and Turner plus the updated *F. vesca* genes were aligned and phylogentic tree were designed as mentioned above. *Fragaria x ananassa* genes annotation and position were retrieved from GDR (*Fragaria x ananassa* cv. Camarosa genome v1.0.a1), and progenitor lineage were inferred according to Edger *et al.*, 2019. Chromomap package in R (Anand, 2019)(Anand, 2019) was used to design FaRALF gene chromosome map.

2.2.2 RALF family genes expression profile in *F. vesca and qRTPCR in F.x ananassa*

Heatmap expression profile of RALF family genes in different *F.vesca* tissues were obtained using heatmap3 package in R (Zhao, Guo, Sheng, & Shyr, 2014)(Zhao et al., 2014) from Transcripts Per Kilobase Million (TPM) values calculated by Li et al. (2019)Li et al. (2019).

2.3 Results and Discussion

2.3.1 Identification of RALF gene family members in *Fragaria vesca*

RALF peptides belonging to 51 plant species have been previously classified in four clades depending on the sequence similarity (Campbell & Turner, 2017)(Campbell & Turner, 2017). Typical distinctive amino acid sequence motifs, such as the RRILA proteolitic cleavage site (Srivastava et al., 2009)(Srivastava et al., 2009) and the YISY receptor binding site , are present in RALF peptides of clade I to III, and missing in clade IV, which contains divergent peptides. Among the different plant species, nine RALF genes were identified in the *Fragaria vesca* v1 genome.

In order to identify new members of RALF gene family in the recent *Fragaria vesca* genome annotation (v4.0.a2) (Y. Li et al., 2019)(, *F. vesca* v4.0.a2 genes and transcripts annotation was scored using the gene name 'RALF' as query, revealing the presence of 13 RALF genes in woodland strawberry. The identified *F. vesca* RALF (*FvRALF*) genes were named with progressive numbers according to their chromosome position, from Chr1 to 6 (Table 2.1), with one RALF gene in Chr1, two in Chr2, -3, and -5, and three in Chr4, and -6. No RALF genes are found in Chr7. Out of the nine RALF genes previously reported by Campbell and Turner (2017), eight genes are confirmed both for identity and chromosome position. These are the gene08146 (corresponding to *FvRALF2*), *gene10567 (FvRALF3)*, *gene02376 (FvRALF4)*, *gene02377 (FvRALF5), gene06579 (FvRALF6), gene06890 (FvRALF8), gene10483 (FvRALF9), gene22211 (FvRALF13)* (Table 2.1). The *gene00145*, previously annotated as gene encoding for peptide with the typical RALF motifs RRILA and YISY (Cambell and Turner, 2017), was discarded since in the new v4.0.a2 annotation its sequence corresponds to gene *FvH4_6g07633* encoding for a shorter peptide lacking most of RALF conserved motifs.

RALF genes	v4.0.a2	Former annotation	Chromosome localization	clade	Arabidopsis homology	%id
FvRALF1	FvH4_1g16140	gene23829	Fvb1:9232850..9233915	IV	*RALF34*	60.58%
FvRALF2	FvH4_2g13590	gene08146*	Fvb2:11869901..11870362	III	*RALF4*	48.65%
FvRALF3	FvH4_2g25351	gene10567*	Fvb2:20606722..20607381	II	*RALF33*	64.91%
FvRALF4	FvH4_3g09010	gene02376*	Fvb3:5266873..5268430	III	*RALF19*	51.69%
FvRALF5	FvH4_3g09020	gene02377*	Fvb3:5269449..5270363	III	*RALF19*	50.00%
FvRALF6	FvH4_4g13190	gene06579*	Fvb4:16794712..16795349	II	*RALF32*	49.54%
FvRALF7	FvH4_4g13250	gene06566	Fvb4:16854377..16855101	III	*RALF24*	47.71%
FvRALF8	FvH4_4g18001	gene06890*	Fvb4:21972673..21974193	II	*RALF33*	61.32%
FvRALF9	FvH4_5g21290	gene10483*	Fvb5:12816493..12816858	II	*RALF33*	33.63%
FvRALF10	FvH4_5g26840	gene41610	Fvb5:18214922..18215453	IV	*RALF25*	34.18%
FvRALF11	FvH4_6g36290	gene42389	Fvb6:28540907..28541125	IV	*RALF32*	36.62%
FvRALF12	FvH4_6g41850	gene42489	Fvb6:32780751..32781347	IV	*RALF5*	35.63%
FvRALF13	FvH4_6g06520	gene22211*	Fvb6:3818620..3820001	I	*RALF33*	58.88%

Table 2.1 *F. vesca RALF genes*. List of RALF genes identified in *F.vesca*, with the relative gene codes in the new F. vesca gene annotation (v4.0.a2) and old annotation version (Schulev et al. 2011), the chromosome localization v4.0.a2, the clade classification according to Campbell and Turner (2017) and the homology to Arabiodopsis RALF genes. Asteriscs indicate the RALF genes previously identified in v1 F. vesca genome by Campbell and Turner (2017) and confirmed in the v4.0.a2 gene annotation. Percentage of identity with *A. thaliana* genes is shown (%id).

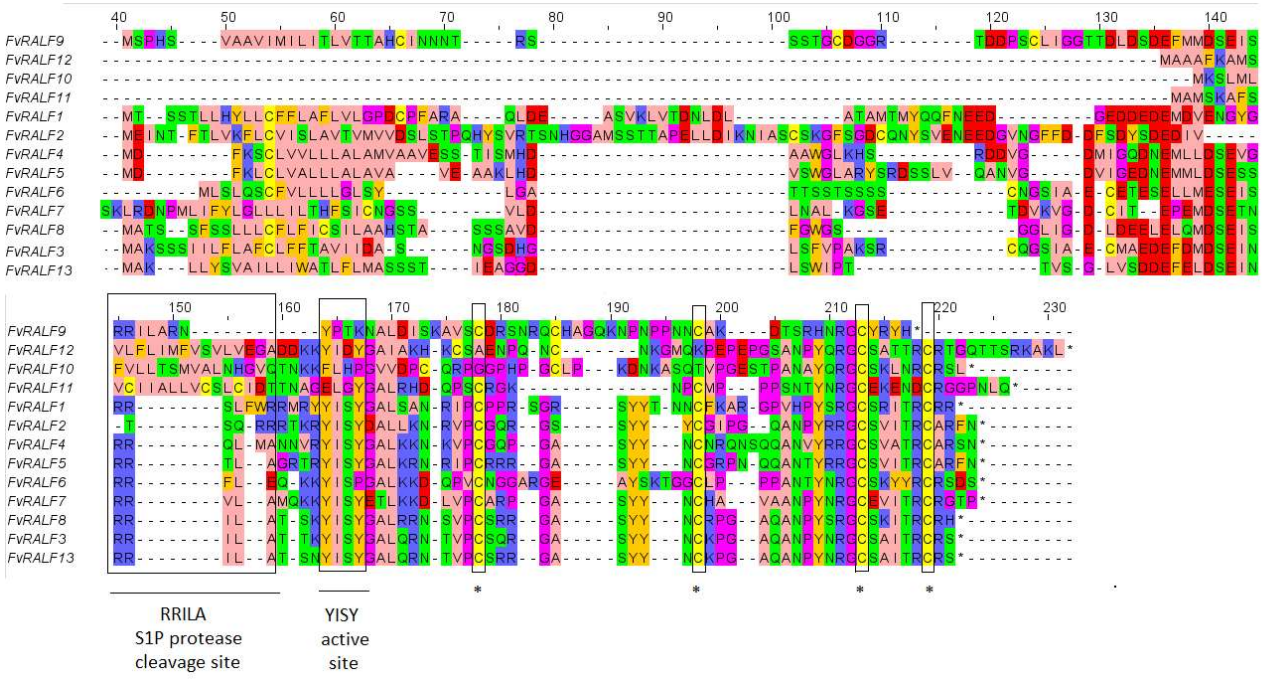

Figure 2.1 *F.vesca* RALF peptide sequences aligned in MEGA-X. The alignment is shown for the mature peptide fragment to highlight the conserved sites like RRILA cleavage site and YISY active site.

The *FvRALF* genes members were aligned using MUSCLE (Edgar, 2004) and classified in four clades according to Campbell and Turner (2017) (Fig.2.1). Genes belonging to clade I, II and III share conserved motifs such as RRILA cleavage site and YISI active site, while clade IV genes are more divergent and have the RALF conserved domain in the latest part of the mature peptide. Overall, one gene (*FvRALF13*) was included in clade I, four in clade II (*FvRALF3, FvRALF6, FvRALF8, FvRALF9*), four in clade III (*FvRALF2, FvRALF4,FvRALF5, FvRALF7*) and four (*FvRALF1, FvRALF10, FvRALF11, FvRALF12*) in clade IV. The *FvRALF* genes include two members homologous to *Arabidopsis AtRALF32* (*FvRALF11, FvRALF6*), two homologous to *AtRALF19* (*FvRALF4, FvRALF5*), four homologous to *AtRALF33* (*FvRALF3, FvRALF8 ,FvRALF13 and FvRALF9*), and one respectively to *AtRALF4* (*FvRALF2*), *AtRALF5* (*FvRALF12), AtRALF24* (*FvRALF7*)*, AtRALF25* (*FvRALF10*) and *AtRALF34* (*FvRALF1*) (Tab.2.1). All *FvRALF* genes are predicted to contain a single exon and no introns. Interestingly, the gene *FvRALF3* is transcribed from a putative Natural Antisense Transcript (NAT) generating region and its complementary sequence encodes for the 3' untranslated region of a heat shock factor binding protein gene (*FvH4_2g25350*).

2.3.2 Identification, evolution and chromosome organization of RALF genes family member in *Fragaria x ananassa*

The thirteen *F. vesca* RALF genes sequences were used as query sequences against *Fragaria x ananassa cv. Camarosa* (*Fxa*) predicted proteins database. Fifty RALF members were identified in the *Fxa* octoploid strawberry (Table 2.2). *Fxa RALF* genes *(FaRALF)* were named based on corresponding *FvRALF* orthologs and the subgenome localization, with progressive numbers from 1 to 4 to indicate *F.ve*, *F.ii*, *F.ni* and *F.vi* progenitors respectively (accordingly to Edger et al., 2019) , and progressive letters to nominate genes orthologous to the same *FvRALF* genes and localized on the same chromosome (e.g. *FaRALF3-3* is the *Fxa* gene orthologous to *FvRALF3* mapping on *F.nipponica* subgneome). Paralogous genes (othologs to *FvRALF* genes) were identified in the *Fxa* subgenomes from alignment and phylogenetic analysis (Fig.2.2A) and progenitors lineage were inferred from chromosome localization (Fig. 2.2B) according to Edger *et al.* (2019). Fourteen genes out of these 50 belong to the *F. vesca* subgenome (*F.ve*), 15 members on the *F. nipponica* subgenome (*F.ni*), 13 on the *F. inumae* subgenome (*F.ii*) and only eight are localized on the *F .viridis* subgenome (*F.vi*) (Fig. 2.2C).

Gene homology and chromosome localization analysis showed that only four out of 13 *FvRALF* genes, namely *FvRALF1, FvRALF4, FvRALF7, FvRALF9,* have orthologs in all the four subgenomes. For all the other cases the *FvRALF* orthologs are not represented in all the different *Fxa* subgenomes, probably due to gene loss events occurred during evolution or polyploidy adjustment (Fig. 2.2A). In particular, the *F. viridis* derived subgenome has the lowest number of RALF gene members and is lacking genes othologous to *FvRALF5, FvRALF8, FvRALF6, FvRALF8, FvRALF11* and *FvRALF2*. On the other hand, similarly to *F. vesca*, no RALF genes are localized in Chr7 of the different progenitors. Moreover in *Fxa* genome some RALF genes probably underwent duplication events. For example *FaRALF11-1a* and *FaRALF11-1b* are both orthologous to *FvRALF11* and are positioned close together on Chr6 (*F.ve*). Another atypical gene organization is found for *FaRALF5-1a* and *FaRALF5-1b* genes, located on Chr3 (*F.ve*), which are annotated as single genes but contain two tandem RALF conserved domains, suggesting that a duplication event occurred during genome evolution. In addition, the *FaRALF7-4* gene is predicted to encode for a 325 aa protein containing a conserved RALF domain within the first 104 amino acids and a domain homologous to chloroplastic NADPH-dependent aldehyde-reductase like protein, from aa 124 to 325. This incongruous arrangement of typically unrelated protein domains suggest that this gene is a result of shuffling events during evolution. The genes *FaRALF9-3b* and *FaRALF9-3c,* occur as NAT element on Chr 5 (*F.ni*), as was observed in *F.vesca* for *FvRALF3*. The *F. viridis* derived subgenome contains the least number of RALF genes. This was also the case for R gene family in *Fxa* (Edger *et al.* Edger et al. 2019). However, in contrast to the R-gene family, there is not a clear dominance of *F.ve* progenitor in the *FaRALF* gene family composition, since genes are similarly distributed in the *F.ii, F.ni* and *F.ve* subgenomes (Fig.2.2C). The lack of RALF genes in *F. viridis* subgenome could be related to the higher TE content of this subgenome which can cause both higher mutation rates and gene loss, as was speculated by Edger *et al*. (2019). *Fxa* RALF genes classification in clades is consistent with diploid woodland strawberry respect to RALF clade distribution, with 15 genes in clade IV, 17 genes in clade III, 15 in clade II and three in clade I (Table 2).

Table 2.2: List of *Fragaria x ananassa* RALF genes identified in GDR through FvRALFs BLASTx . It is reported Chromosome localization (Chr.), chromosome corresponding progenitor lineage (progenitor), gene identification number used to name FaRALF in this work (geneID#) where *v1short name* reports gene v1 annotation abbreviation used to identify genes in Fig1A and *Orthology based* nomenclature was assigned according to FvRALF orthology and chromosome lineage using-1, -2,-3,-4 respectively for *F.vesca, F.iinumae, F.nipponica* and *F.viridis* progenitors, progressive letters was used to name genes orthologous to the same FvRALF gene and localized on the same chromosome. Whole name used to identify genes transcript in GDR *Fragaria x ananassa Camarosa* v1 transcript annotation (*Fragaria x anannassa Camarosa* v1 transcript annotation*)*, position coordinates in the genome (Location), classification in clades according to Campbell and Turner (2017) (clade); FvRALF Blastx against *Fragaria x ananassa* genome Output: *F. vesca* orthologous gene (Fv.Ort.), E-value and identity rate.

#	Chr.	Progenitor	gene ID#		*Fragaria x ananassa* Camarosa v1 transcript annotation	Location	Clade	Fv-Blastx-Fxa		
			v1 short name	*Orthology based*				*Fv Ort.*	*Evalue*	*Identity*
1	Fvb1-2	*F.iinumae*	gene103.4	FaRALF1-2	augustus_masked-Fvb1-2-processed-gene-103.4-mRNA-1	Fvb1-2:10325716..10326120	III	FvRALF1	1,45E-46	98,2
2	Fvb1-4	*F.vesca*	gene81.5	FaRALF1-1	augustus_masked-Fvb1-4-processed-gene-81.5-mRNA-1	Fvb1-4:8119520..8119924	III	FvRALF1	3,90E-46	96,4
3	Fvb1-1	*F.viridis*	gene196.6	FaRALF1-4	augustus_masked-Fvb1-1-processed-gene-196.6-mRNA-1	Fvb1-1:19637534..19637938	III	FvRALF1	8,85E-45	95,0
4	Fvb1-3	*F.nipponica*	gene90.5	FaRALF1-3	augustus_masked-Fvb1-3-processed-gene-90.5-mRNA-1	Fvb1-3:9086333..9086941	III	FvRALF1	3,25E-42	85,7
5	Fvb2-2	*F.vesca*	gene128.6	FaRALF2-1	augustus_masked-Fvb2-2-processed-gene-128.6-mRNA-1	Fvb2-2:12863406..12863804	III	FvRALF2	6,20E-74	99,2
6	Fvb2-4	*F.iinumae*	gene98.11	FaRALF2-2	augustus_masked-Fvb2-4-processed-gene-98.11-mRNA-1	Fvb2-4:9802842..9803250	III	FvRALF2	2,01E-33	87,5
7	Fvb2-1	*F.nipponica*	gene164.41	FaRALF3-3	snap_masked-Fvb2-1-processed-gene-164.41-mRNA-1	Fvb2-1:16467759..16468690	II	FvRALF3	2,7E-106	99,4
8	Fvb2-2	*F.vesca*	gene47.50	FaRALF3-1	snap_masked-Fvb2-2-processed-gene-47.50-mRNA-1	Fvb2-2:4766837..4767181	II	FvRALF3	6,56E-73	100,0
9	Fvb2-3	*F.viridis*	gene83.11	FaRALF3-4	augustus_masked-Fvb2-3-processed-gene-83.11-mRNA-1	Fvb2-3:8333608..8333952	II	FvRALF3	2,87E-71	98,2
10	Fvb3-2	*F.iinumae*	gene48.4	FaRALF4-2	augustus_masked-Fvb3-2-processed-gene-48.4-mRNA-1	Fvb3-2:4832788..4833141	III	FvRALF4	5,39E-62	97,4
11	Fvb3-1	*F.viridis*	gene270.42	FaRALF4-4	maker-Fvb3-1-augustus-gene-270.42-mRNA-1	Fvb3-1:27075197..27077721	III	FvRALF4	1,24E-60	98,3
12	Fvb3-3	*F.nipponica*	gene31.4	FaRALF4-3	augustus_masked-Fvb3-3-processed-gene-31.4-mRNA-1	Fvb3-3:3178618..3179037	III	FvRALF4	8,47E-64	100,0
13	Fvb3-3	*F.nipponica*	gene31.5	FaRALF5-3	augustus_masked-Fvb3-3-processed-gene-31.5-mRNA-1	Fvb3-3:3186944..3187300	III	FvRALF5	2,30E-59	95,8
14	Fvb3-2	*F.iinumae*	gene48.25	FaRALF5-2	snap_masked-Fvb3-2-processed-gene-48.25-mRNA-1	Fvb3-2:4834809..4835958	III	FvRALF5	2,87E-49	95,4
15	Fvb3-4	*F.vesca*	gene221.49	FaRALF5-1a	maker-Fvb3-4-augustus-gene-221.49-mRNA-1	Fvb3-4:22117395..22120230	III	FvRALF5	4,31E-42	75,8
16	Fvb3-4	*F.vesca*	gene246.64	FaRALF5-1b	maker-Fvb3-4-snap-gene-246.64-mRNA-1	Fvb3-4:24592271..24594558	III	FvRALF5	3,52E-57	99,0
17	Fvb4-4	*F.iinumae*	gene146.8	FaRALF6-2	augustus_masked-Fvb4-4-processed-gene-146.8-mRNA-1	Fvb4-4:14614753..14615082	II	FvRALF6	1,77E-42	96,1
18	Fvb4-3	*F.vesca*	gene152.8	FaRALF6-1	augustus_masked-Fvb4-3-processed-gene-152.8-mRNA-1	Fvb4-3:15250252..15250581	II	FvRALF6	2,58E-44	100,0
19	Fvb4-2	*F.nipponica*	gene135.5	FaRALF6-3	augustus_masked-Fvb4-2-processed-gene-135.5-mRNA-1	Fvb4-2:13577406..13577738	II	FvRALF6	1,25E-43	98,7
20	Fvb4-2	*F.nipponica*	gene134.10	FaRALF7-3	augustus_masked-Fvb4-2-processed-gene-134.10-mRNA-1	Fvb4-2:13450491..13450838	III	FvRALF7	1,53E-58	100,0
21	Fvb4-3	*F.vesca*	gene153.15	FaRALF7-1	snap_masked-Fvb4-3-processed-gene-153.15-mRNA-1	Fvb4-3:15307915..15308788	III	FvRALF7	3,03E-58	99,1
22	Fvb4-1	*F.viridis*	gene96.3	FaRALF7-4	augustus_masked-Fvb4-1-processed-gene-96.3-mRNA-1	Fvb4-1:9662627..9665750	III	FvRALF7	2,13E-56	99,0
23	Fvb4-4	*F.iinumae*	gene145.10	FaRALF7-2	augustus_masked-Fvb4-4-processed-gene-145.10-mRNA-1	Fvb4-4:14554980..14555327	III	FvRALF7	9,15E-58	98,1
24	Fvb4-3	*F.vesca*	gene192.46	FaRALF8-1a	maker-Fvb4-3-snap-gene-192.46-mRNA-1	Fvb4-3:19275637..19276150	II	FvRALF8	5,64E-35	100,0
25	Fvb4-4	*F.iinumae*	gene106.36	FaRALF8-2a	snap_masked-Fvb4-4-processed-gene-106.36-mRNA-1	Fvb4-4:10687227..10687816	II	FvRALF8	1,58E-28	98,6
26	Fvb4-2	*F.nipponica*	gene95.31	FaRALF8-3a	snap_masked-Fvb4-2-processed-gene-95.31-mRNA-1	Fvb4-2:9526037..9526632	II	FvRALF8	1,58E-28	98,6
27	Fvb4-4	*F.iinumae*	gene106.7	FaRALF8-2b	augustus_masked-Fvb4-4-processed-gene-106.7-mRNA-1	Fvb4-4:10687617..10687970	IV	FvRALF8	3,42E-07	100,0
28	Fvb4-3	*F.vesca*	gene138.3	FaRALF8-1b	augustus_masked-Fvb4-3-processed-gene-138.3-mRNA-1	Fvb4-3:13832048..13832290	IV	FvRALF8	1,18E-06	98,5
29	Fvb4-2	*F.nipponica*	gene95.2	FaRALF8-3b	augustus_masked-Fvb4-2-processed-gene-95.2-mRNA-1	Fvb4-2:9526433..9526786	IV	FvRALF8	2,65E-06	98,5

30	Fvb6-2	*F.nipponica*	gene274.62	FaRALF9-3a	maker-Fvb6-2-snap-gene-274.62-mRNA-1	Fvb6-2:27420383..27426133	II	FvRALF9	2,14E-92	82,3
31	Fvb5-3	*F.iinumae*	gene154.36	FaRALF9-2	maker-Fvb5-3-snap-gene-154.36-mRNA-1	Fvb5-3:15459676..15465543	II	FvRALF9	2,63E-56	81,8
32	Fvb5-4	*F.nipponica*	gene106.10	FaRALF9-3b	augustus_masked-Fvb5-4-processed-gene-106.10-mRNA-1	Fvb5-4:10651184..10651522	II	FvRALF9	8,43E-55	84,1
33	Fvb5-4	*F.nipponica*	gene106.26	FaRALF9-3c	snap_masked-Fvb5-4-processed-gene-106.26-mRNA-1	Fvb5-4:10651178..10651537	II	FvRALF9	1,57E-38	77,8
34	Fvb5-2	*F.viridis*	gene125.8	FaRALF9-4	augustus_masked-Fvb5-2-processed-gene-125.8-mRNA-1	Fvb5-2:12546292..12546654-	II	FvRALF9	1,45E-53	79,5
35	Fvb5-1	*F.vesca*	gene135.16	FaRALF9-1	snap_masked-Fvb5-1-processed-gene-135.16-mRNA-1	Fvb5-1:13539651..13540016-	II	FvRALF9	4,37E-58	82,0
36	Fvb2-4	*F.iinumae*	gene143.7	FaRALF10-2a	augustus_masked-Fvb2-4-processed-gene-143.7-mRNA-1	Fvb2-4:14363896..14364135	IV	FvRALF10	2,73E-17	63,0
37	Fvb2-1	*F.nipponica*	gene121.9	FaRALF10-3a	augustus_masked-Fvb2-1-processed-gene-121.9-mRNA-1	Fvb2-1:12175862..12176104	IV	FvRALF10	1,49E-16	61,7
38	Fvb5-4	*F.nipponica*	gene155.20	FaRALF10-3b	snap_masked-Fvb5-4-processed-gene-155.20-mRNA-1	Fvb5-4:15508684..15509008	IV	FvRALF10	7,43E-39	95,6
39	Fvb5-3	*F.iinumae*	gene107.25	FaRALF10-2b	snap_masked-Fvb5-3-processed-gene-107.25-mRNA-1	Fvb5-3:10738572..10738811	IV	FvRALF10	1,62E-48	97,5
40	Fvb6-4	*F.viridis*	gene55.10	FaRALF10-4	augustus_masked-Fvb6-4-processed-gene-55.10-mRNA-1	Fvb6-4:5587127..5587387	IV	FvRALF10	3,81E-06	43,0
41	Fvb6-1	*F.vesca*	gene317.62	FaRALF10-1	maker-Fvb6-1-snap-gene-317.62-mRNA-1	Fvb6-1:31717831..31719724	IV	FvRALF10	1,00E-07	44,3
42	Fvb6-1	*F.vesca*	gene103.2	FaRALF11-1a	augustus_masked-Fvb6-1-processed-gene-103.2-mRNA-1	Fvb6-1:10327835..10328053	IV	FvRALF11	2,77E-45	100,0
43	Fvb6-2	*F.nipponica*	gene12.12	FaRALF11-3	snap_masked-Fvb6-2-processed-gene-12.12-mRNA-1	Fvb6-2:1258093..1258311	IV	FvRALF11	9,20E-45	98,6
44	Fvb6-1	*F.vesca*	gene108.14	FaRALF11-b	snap_masked-Fvb6-1-processed-gene-108.14-mRNA-1	Fvb6-1:10825757..10825975	IV	FvRALF11	2,06E-44	98,6
45	Fvb6-3	*F.iinumae*	gene103.3	FaRALF11-2	augustus_masked-Fvb6-3-processed-gene-103.3-mRNA-1	Fvb6-3:10309960..10310253	IV	FvRALF11	1,13E-37	91,3
46	Fvb6-2	*F.nipponica*	gene340.18	FaRALF12-3	snap_masked-Fvb6-2-processed-gene-340.18-mRNA-1	Fvb6-2:33994441..33994692	IV	FvRALF12	7,17E-52	97,6
47	Fvb6-4	*F.viridis*	gene305.28	FaRALF12-4	snap_masked-Fvb6-4-processed-gene-305.28-mRNA-1	Fvb6-4:30509368..30509610	IV	FvRALF12	5,14E-36	84,1
48	Fvb6-1	*F.vesca*	gene322.10	FaRALF13-1	augustus_masked-Fvb6-1-processed-gene-322.10-mRNA-1	Fvb6-1:32210325..32210651	I	FvRALF13	2,44E-52	100,0
49	Fvb6-4	*F.viridis*	gene50.20	FaRALF13-4	snap_masked-Fvb6-4-processed-gene-50.20-mRNA-1	Fvb6-4:5019956..5030285	I	FvRALF13	5,07E-51	97,6
50	Fvb6-3	*F.iinumae*	gene378.1	FaRALF13-2	augustus_masked-Fvb6-3-processed-gene-378.1-mRNA-1	Fvb6-3:37802639..37803318	I	FvRALF13	4,95E-49	94,1

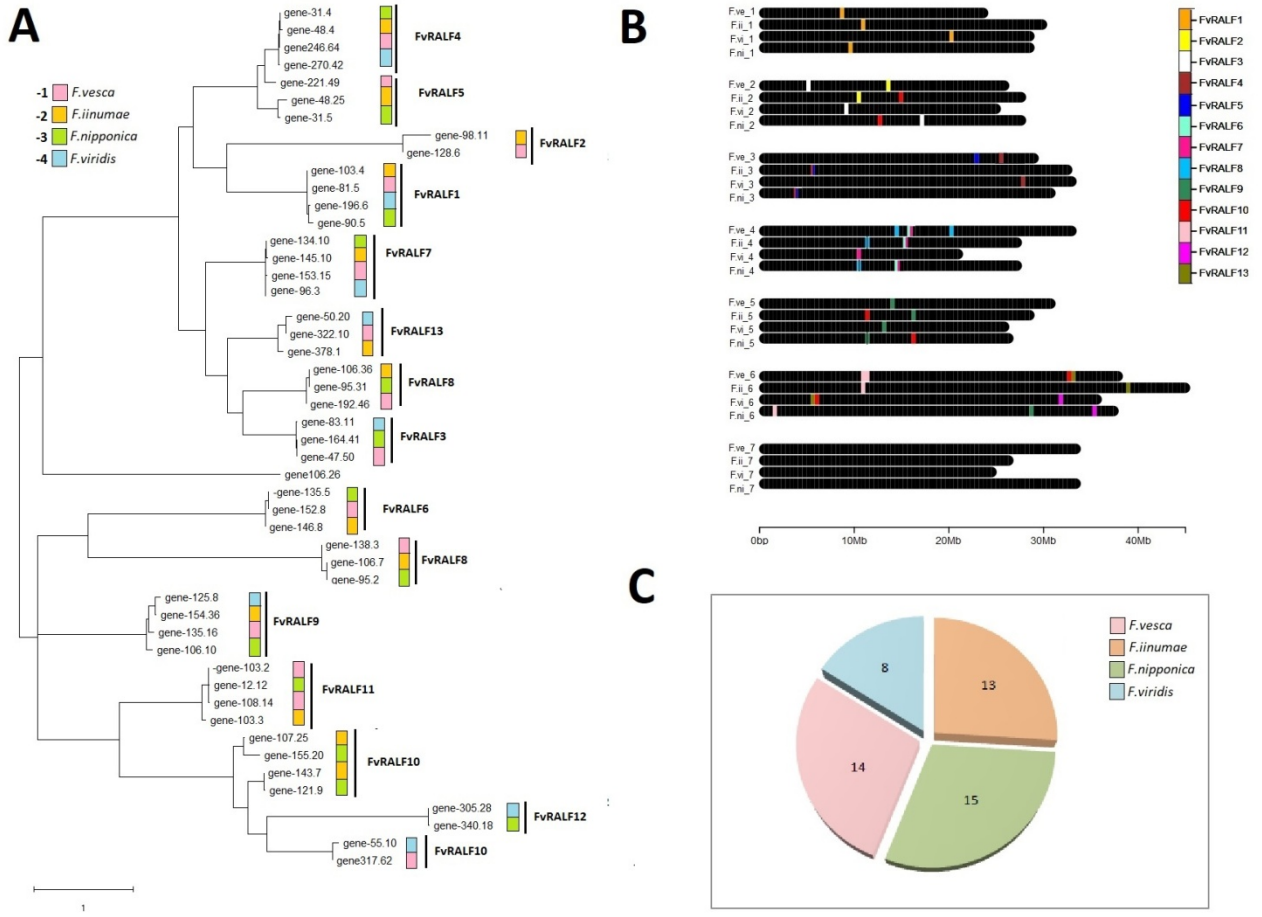

Figure2.2: *Fragaria x ananassa (Fxa)* RALF genes phylogentic analysis, evolution and chromosome organization. (a) Phylogenetic tree was built 50 *Fxa* RALF peptides sequences using MUSCLE . The neibour joining tree is drawn to scale, with branch lengths measured in the number of substitutions per amino acidic site in the peptide sequences. Gene annotations refer to *Fragaria x ananassa cv. Camarosa* v1.0.a1 and are listed in TableS1. Progenitor lineage were inferred from gene chromosome localization (b), and pink was used for *F.vesca* subgenome , green for *F.nipponica,* light blue for *F.viridis* and orange for *F.iinumae.* Color legend reports also code number used to name different *FaRALF* genes according to subgenome lineage, as is reported in TableS1. (b) *FaRALF* genes chromosome spatial organization in the octoploid genome. (c) Pie chart showing total FaRALF gene members present in the four subgenomes.

2.3.3 Transcriptional dataset analysis of RALF genes in *F.vesca*

To provide insights into the RALF genes members functions in strawberry, available RNA-seq datasets mapped onto the new genome annotation v4.0.a2 by Li *et al.* (2019), were analyzed in different tissues and developmental stages. RALF members were grouped based on similar expression profile and hierarchical clustering resulted in four major RALF expression groups (Fig.2.3): i) RALF genes specifically expressed in mature male gamete

(FvRALF4, FvRALF5, FVRALF10, FvRALF11); ii) a gene expressed only in two anther developmental stages (*FvRALF2)* iii) *FvRALF3* and *FvRALF12* genes mainly expressed in roots and in roots infected with *Phytophthora cactorum* iv) genes mainly expressed in different fruit developmental stages (*FvRALF1, FvRALF6, FvRALF7, FvRALF8, FvRALF9* and *FvRALF13)*.

Contrary to what has been observed in *Arabidopsis,* where clade IV RALF genes were highly expressed in flower tissues (Campbell & Turner, 2017), the woodland strawberry *FvRALF* genes included in each of the four expression groups belong to different clades, suggesting that members of the same clade are involved in different functions. The highly specific expression of four *FvRALF* genes in male gamete and late stage of anther development *(FvRALF4, FvRALF5, FVRALF10, FvRALF11,)* shown by the heatmap (Fig.2.3), suggests a role for these RALF genes in the ovule-pollen, cell-cell communication during the sequence of events precisely regulated during fertilization. A recent study reports that in Arabidopsis *At*RA*LF34* gene, expressed in the ovule, competes with *RALF4* and *RALF19*, expressed in the pollen tube, for binding to BUPs and ANXs receptors (Ge et al., 2017). The interaction between AtRALF34, expressed by the female gamete, and the receptor complex formed by BUPS1/2 and ANX1/2, present in pollen tube membrane leads to pollen tube rupture and sperm release (Ge et al., 2017). The competitive binding of AtRALF4 and AtRALF19 to this receptor complex suggest that they have a redundant function in regulating pollen tube growth and integrity (Mecchia *et al.,* 2017). It is possible that these RALF genes functional redundancy is conserved in woodland strawberry.

Among the *FvRALF* genes expressed in flower and fruit organs *FvRALF1* and *FvRALF7* are the most highly expressed at the early stage of development in shoot apical meristem (SAM), floral meristem (FM) and receptacle meristem (RM), with *FvRALF1* being also the family member most higly expressed in the leaves. As for fruit, *FvRALF8* is the most highly expressed gene in mature fruits, whereas *FvRALF6, FvRALF7, FvRALF9* are transcribed during fruit growth and in the mature organ at 15 days post anthesis (15 DPA) both in Yellow Yonder and Red Rugen genotypes (the two *F. vesca* genotypes used for RNA seq), while *FvRALF3* and *FvRALF13* are more expressed in the mature fruits at 20 DPA. In particular *FvRALF1, FvRALF6, FvRALF7* and *FvRALF13* expression decreases during fruit development both in the inner and the outer tissues of fruit. On the contrary *FvRALF9* expression gradually increases with fruit growth.

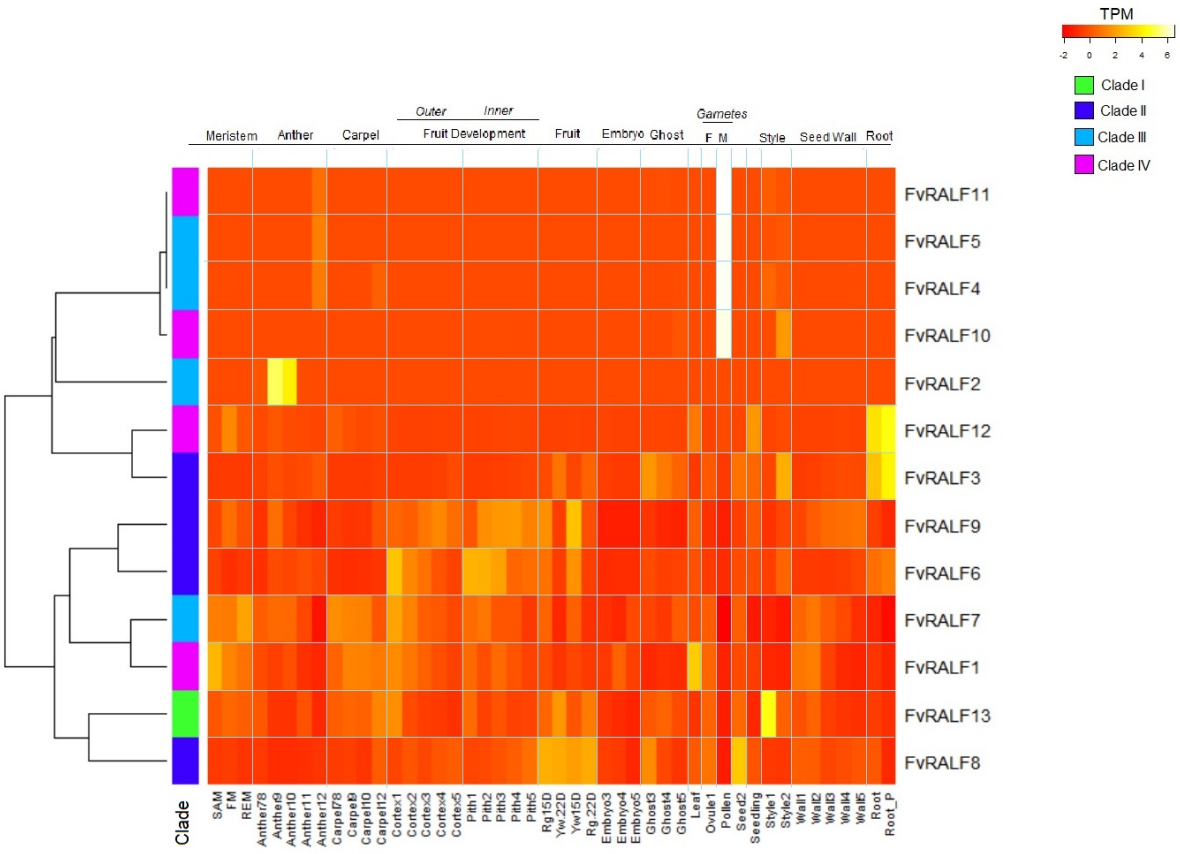

Figure2.3. RALF transcriptional analysis in *F. vesca.* Heatmap of the expression profile measured as Trascription per Kilobase Million (TPM) of *FvRALF* members (rows) in different tissues and developmental stages (column). Labels at the bottom specify the tissues and the stages, and light blue vertical lines divide organs labeled at the top. Dendrogram on the left shows rows relationship according to similar expression profile. RALF members classification in clades are shown: in green clade I, in blue clade II, in light blue clade III and magenta clade IV

In a recent work, Jia et al. (2017) analyzed the expression of the woodland strawberry (*F. vesca*) Malectin Receptor Like Kinases (MRLK) also known as the *Catharanthus roseus* RLK-like proteins (CrRLK1Ls). *F. vesca* MRLKs are encoded by more than 60 genes, and more than 50% of these are expressed during fruit development. The majority of fruit *FvMRLK* genes are expressed at high level only at the early stage of fruit ripening, and decrease at ripe stages. In particular, Jia et al. Jia et al. (2017), showed that transiently silencing and overexpression of *MRLK47* in strawberry fruit, severely affected ripening regulation.

Moreover, a recent report describes how MRKL47 changes the sensitivity of ripening-related genes to ABA, a key hormone for strawberry fruit ripening (Moya-león *et al.,* 2019)(Moya-león et al., 2019). Consistently, both RALF and ABA were found to be FERONIA-mediated cross-talk signals in stress-response and cell growth in *Arabidopsis* (Chen et al., 2016)(Chen et al., 2016). These data, together with an established role of FERONIA receptor in cell-wall integrity and Ca^{2+} signaling (Feng et al., 2018)(Feng et al., 2018) both known to be important during fruit growth and ripening (Forlani, *et al.,* 2019)(Forlani, et al., 2019)-, and with the similar expression profile of FvMRLKs to the one observed here for *FvRALF1, FvRALF6, FvRALF7* and *FvRALF13,* support an important role for the RALF-MRLK signalling also for strawberry fruit development. Future studies should be conducted in order to demonstrate that RALF peptides and FvMRLK receptors interact *in vivo*.

2.4 Conclusions

In conclusion, 13 RALF genes were identified in *F. vesca* re-annotated genome (v4.0.a2) and 50 RALF members were identified in *Fragaria x ananassa cv. Camarosa* genome (v1.0). RALF genes distribution among *Fragaria x ananassa* subgenomes is consistent with previous family genes distribution analysis and reflects the polyploidy adjustments and the genome remodelling occurred during evolution. In particular putative duplication events in *FaRALF* family and a reduced number of RALF genes in *F.viridis* subgenome, probably casused by more intensive TE elements activity, were observed. Transcriptional dataset analysis revealed that some members may be involved in tube-ovule crosstalk during fertilization, as was already showed in *Arabidopsis* (Ge et al., 2017), and a group of *FvRALF* member may be involved in fruit development. Furthermore, specific expression profiles were revealed for roots and meristem tissues. However, further analysis are required in order to assess RALF genes functional roles in different tissues.

3. RALFs expression analysis during pathogen infections

3.1 Introduction

RALF peptides are known to play a role in plant-pathogen interaction (Fernandes et al., 2017)(Fernandes et al., 2017) since they were found to negatively regulate plant immunity response in *Arabidopsis* (Stegmann et al., 2017). They were also found to be secreted by fungal pathogen as crucial virulence factors (Masachis et al., 2016; Thynne *et al.*, 2017)Thynne et al., 2017). Furthermore, it was reported that genes homologous to *AtRALF33* were upregulated both in tomato (*Solanum lycopersicon)* and in strawberry (*Fragaria x ananassa*) susceptible ripe fruits upon interaction with *Colletorichum gloeosporioides* and *C. acutatum,* respectively (Alkan et al., 2014) (Guidarelli et al., 2011).

To analyse *FvRALF* genes transcriptional regulation during infection and investigate their putative role as susceptibility factors, the transcript levels of *FaRALF* genes were assessed in *Fragaria* x *ananassa* fruit at two different ripening stages and upon infection with *C. acutatum* and *B. cinerea.* Fruit *FaRALF* gene targets were chosen based on the *FvRALF* gene homologs expressed in fruit (Fig. 2.3) since the *F.ve* progenitor is reported to have the most abundant expression level among the different subgenomes (Edger et al., 2019)(Edger et al., 2019). Therefore, primers were designed to amplify genes that are expressed in fruit (*FaRALF1-1, FaRALF3-1, FaRALF6-1, FaRALF7-1, FaRALF8-1, FaRALF9-1 and FaRALF13-1*), which included orthologs to *AtRALF33* (*FaRALF3-1, FaRALF8-1, FaRALF9-1* and *FaRALF13-1*).

3.2 Materials and Methods

3.2.1 *Fragaria x ananassa* fruits infection

Fragaria x ananassa cv. Alba plants were grown in the greenhouse at 25°C and 16 hours light. White (21 days after anthesis) and Red fruits (28 days after anthesis) were harvested and infected or not according to the experimental procedures. Each treatment contained at least three biological replicates. *Colletotrichum acutatum* (Isolate Maya-3, from CRIOF-UniBo fungi collection), *Botrytis cinerea* strain *B05.10* and *Penicillium expansum* (CRIOF collection) were grown on PDA plates at room temperature for 15 days. Detached fruits were dipped for 30 s in a 10^6 conidia per mL suspension or in water for control and incubated for 24 hours or 48 hours, according to experimental purpose, at room temperature in plastic bags

3.2.2 RNA extraction and qRT-PCR expression analysis

The surface of experimental fruits was excised with a scalpel and immediately frozen in liquid nitrogen. RNA was extracted according to Gambino *et al*. (2008), run on an 2% Agarose gel and quantified with NanoDrop™ 3300 for integrity and quality control. cDNA was made starting from 1µg of RNA using Promega ImProm-II™ Reverse Transcription system. qRT-PCR analysis was performed using ThermoFisher MAXIMA SYBR GREEN/ROX QPCR 2x supermix. RALF gene relative expression was calculated using ΔΔCt method and *Elongation Factor* gene as reference (*XM_004307362.2*). Primers for RALF genes expression analysis were designed on *Fragaria x ananassa, F. vesca* subgenome genes and specificity were checked observing a single peak in the dissociation curve for each primer pair. All the primers used for RALFs and transient transformation reporter genes expression analysis are listed in Table 3.1.

RALF1_For	GGACGATGAGGACGAGATGG	RALF7_Rev	CCTATTCGCCGAGAGAGCAC
RALF3_For	TGGCAAAGTCCTCTTCCA TT	RALF3_Rev	AACAAAGCTCAACCCGTGAT
RALF6_For	ATCTCACCTGGGGCTTTGAA	RALF9_Rev	GTTGTAAGTGTTGGCCGGAG
RALF7_For	TCCAAACTCAGAGACAATCCCA	RALF6_Rev	TGAGTGCATTGAGGTCCAGA
RALF8_For	ATGGCAACCTCCTCATTCTCC	RALF1_Rev	CAGCTCCTCATCCAAGTCTCC
RALF9_For	AAACTCCGGCACCAAGAATG	RALF10_Rev	CGGTTGTATTTGGCCTTGGT
RALF13_For	GCTCAGGCCAACCCGTATAA	RALF2_Rev	CAATAATAACAACAATACACCATCAC
EF_For	GCCCA GGTTGTTGAAAGTTTC	EF_Rev	GGCGCATGTCCCTCACA

Table3.1 . List of primers used for RALFs qRTPCR expression analysis In *Fragaria x ananassa* infected fruits, and for reporter gene expression in transient transformated fruits.

3.3 Results and Discussion

3.3.1 Expression profile of RALF genes in *Fragaria x ananassa* fruit and induction upon pathogen infection

Expression of predicted fruit *FvRALF* genes were measured in white and red fruits upon infection with *C. acutatum* and *B. cinerea* 24 hours post inoculation.

FaRALF3 expression shows a significant increase induced by infection with both pathogens at the susceptible ripe stage, whereas *FaRALF9* expression decreased in white fruits upon *C. acutatum* but not upon *B. cinerea* infections (Fig.3.1). The expression of *FaRALF8* and *FaRALF13* were not affected by infection, since no significant difference between infected and control samples was observed either in white or red fruits (Fig.3.1). Out of the other *FaRALF* genes analyzed, only *FaRALF6* shows a clear downregulation in infected fruits both at ripening stage and upon infection with pathogen species, while *FaRALF1 and FaRALF7* genes expression is significantly decreased only at ripe stage upon infection with *B. cinerea* and in white stage upon infection with *C. acutatum,* respectively.

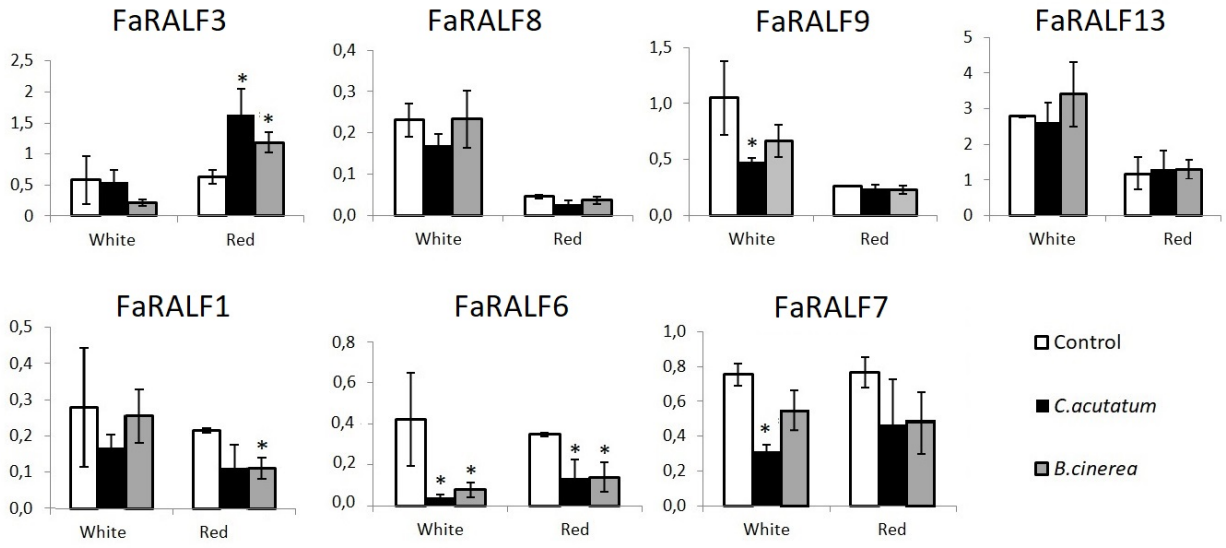

Figure3.1. *Fragaria x ananassa* RALF genes expression upon pathogens infection in fruits at different ripening stage. qRT-PCR analysis of different RALF genes (at the top the RALF-like 33: genes *FaRALF3, FaRALF9, FaRALF8* and *FaRALF13,* at the bottom *FaRALF1, FaRALF6, FaRALF7*) in *Fxa* strawberry fruits at different ripening stage (white and red) after 24 hours post infection with *C. acutatum* and *B. cinerea.* Histogram bars represent relative expression average and black lines represents standard deviations among three biological replicates. T-student test between infected samples and control was used to calculate statistical significance. $p < 0.05$ (*).

The expression profiles of fruit RALF genes in *Fxa* strawberry fruits infected with *C. acutatum* are consistent with our previous results (Guidarelli et al., 2011)(Guidarelli et al., 2011) showing that a *FaRALF33-like* gene expression (here now named *FaRALF3*) is upregulated in red susceptible fruits, while is costant in white fruits. Finally, the expression of *FaRALF1, FaRALF6* and *FaRALF9* is decreased during infection, thus it is possible that these *FaRALF* gene members may play different roles than *RALF3* homologs do upon plant-pathogen interaction and immune response.

Notably, the *FaRALF3* and *FaRALF13* genes, both expressed in strawberry fruits and homologous to *Arabidopsis RALF3*, encode for mature peptides differing only for two aminoacids but respond differently to pathogen infection (Fig.3.1), suggesting a different role for these peptides.

3.3.2 *FaRALF3* expression analysis upon *C. acutatum, B. cinerea* and *P. expansum* at 24 and 48 hours post infection.

In order to find out whether the up-regulation of *FaRALF3* gene is specifically related to the susceptibility of ripe stages or if it also occurs in white unripe fruits at later times of infection or in fruits inoculated with other fungal pathogens, *FaRALF3-1* gene expression analysis was performed in white and red fruits comparing samples at 24 and 48 hours post infection with *C. acutatum, B. cinerea* and *P. expansum*. Consistently with previous findings, a significant increase of the expression level of *FaRALF3* gene was observed at 24 hpi in red ripe *C. acutatum*-inoculated fruits when compared to the mock-inoculated strawberries whereas no difference was detected in white unripe fruits (Fig. 3.2). This indicates that the expression of the gene is indeed specific of the red ripe stage of the strawberry fruits interacting with actively growing *C. acutatum* as subcuticular intercellular hyphae, thereby suggesting a possible involvement of the gene in the susceptibility of the red ripe fruit. At 48 hpi *C acutatum* did not alter the expression level of *FaRALF3* gene neither in red ripe nor in white unripe fruits (Fig. 3.2).

When red ripe strawberry fruits were inoculated with *B. cinerea*, *FaRALF3* gene expression increased at 24 hpi, similarly to what was described for *C. acutatum* fruits, whereas no difference was observed in the white unripe stage neither at 24hpi nor at 48hpi (Fig. 3.2). This may indicate that *FaRALF3* gene participates in the susceptibility of the red ripe fruits against different

necritrophs. In contrast, neither white nor red strawberry fruits increase *FaRALF3* expression at 24h or 48 h post *P. expansum* inoculation (Fig. 3.2), the causal agent of blue mold.

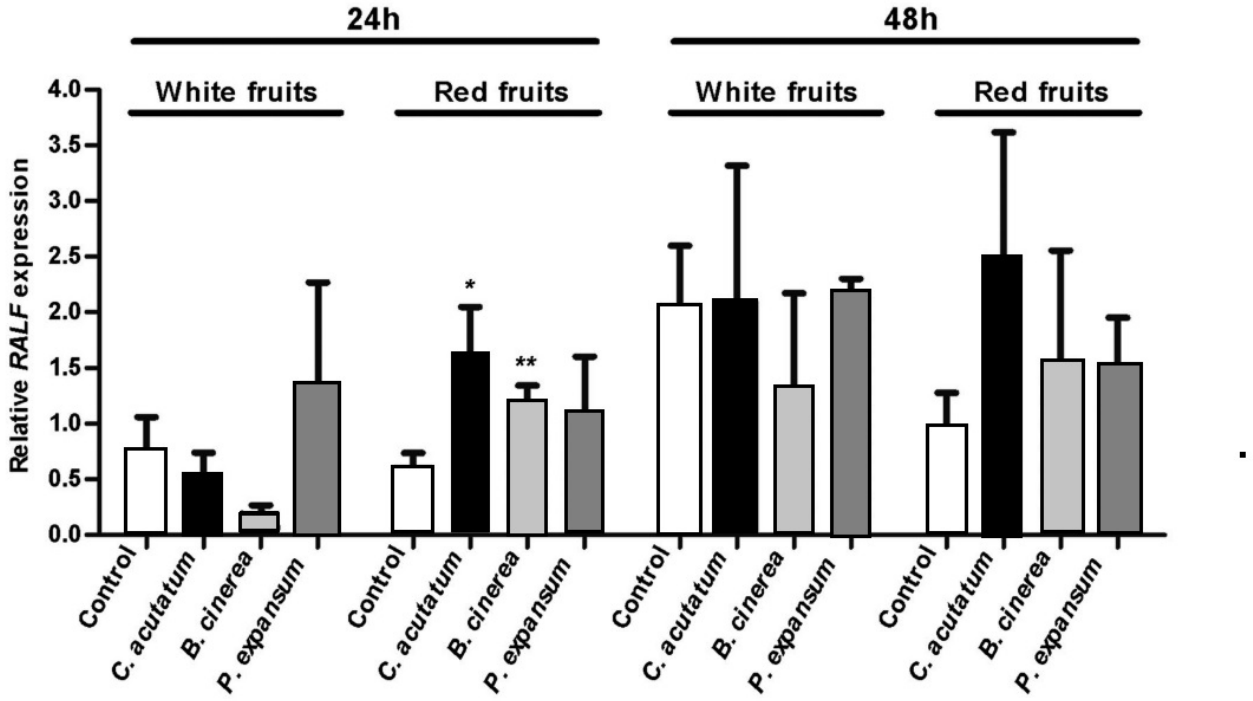

Figure3.2. ***FaRALF3-1 gene expressin anaylsis.*** Expression of *FaRALF3* gene at 24 h (left) or 48 h (right) after *C. acutatum* (black bar), *B. cinerea* (light grey) or *P. expansum* (dark grey) inoculation by white and red fruits. Expression levels in mock-inoculated white and red fruits are displayed in white histograms. Data were normalized against the transcript level of the housekeeping *elongation factor 1α gene*. The histogram show the means and the bars indicate the standard deviation among three biological replicates. The asterisks indicate significant difference compared with the control (Student's t-test: *P < 0.05, **P < 0.01)

3.4 Conclusions

Among *FaRALF* genes, *FaRALF3* is the only one which showed a significant induction within the first 24 hours upon infection with *C. acutatum* and *B. cinerea,* exclusively in ripe fruits. Already at 48 hpi, FaRALF3 expression was not significantly modulated by the fungus, suggesting a role of the gene during the first phases of fungus penetetration in host tissue. These data suggest a putative role of the gene in the establishment of susceptibility of ripe fruit, although this has to be proved.

Other *FaRALF* genes may be involved during plant- pathogen interaction, since *FaRALF6* showed a significant down regulation in white and red fruits upon *C. acutatum* and *B. cinerea* infections.

AKNOWLEDGMENT:

Paragraph 3.3.2 is a extracted from peer reviewed version of the following article:

Merino M. C., Guidarelli M., Negrini F., De Biase D., Baraldi E., Induced expression of the Fragaria × ananassa Rapid alkalinization factor-33-like gene decreases anthracnose ontogenic resistance of unripe strawberry fruit stages, *Molecular Plant Pathology*, 2019, 1-12.

which has been published in final form at DOI: 10.1111/mpp.12837.

4. *FaRALF3-1* role in *C. acutatum* infected strawberry: Agro-infilitration mediated gene induction and repression

This chapter is extracted from the peer reviewed version of the following open access article:

Molecular Plant Pathology

MOLECULAR PLANT PATHOLOGY (2019) DOI: 10.1111/mpp.12837

Induced expression of the *Fragaria* × *ananassa Rapid alkalinization factor-33-like* gene decreases anthracnose ontogenic resistance of unripe strawberry fruit stages

MARIA CECILIA MERINO[1,†], MICHELA GUIDARELLI[1], FRANCESCA NEGRINI[1], DARIO DE BIASE[2], ANNALISA PESSION[2] AND ELENA BARALDI [1,*]

[1]*Department of Agricultural and Food Sciences (DISTAL), University of Bologna, viale Fanin 44, Bologna, Italy*
[2]*Department of Pharmacy and Biotechnology, University of Bologna, Via San Giacomo 14, Bologna, 40126, Italy*

Which has been published in final form at DOI: 10.1111/mpp.12837. This article may be used for non-commercial purposes in accordance with Wiley Terms and Conditions for Use of Self-Archived Versions."

My contributions to this paper were:

RNA extraction, retro-transcription and qRTPCR analysis of *FaRALF* genes upon pathogen infections. (Paragraph 3.3.2); fungal growth evaluation trough fungal β-tubulin expression in Agroinfilitarted fruits; immunity related genes expression analysis in Agroinfilitrated fruits. Togheter with Dr. M.Guidarelli, contribution in evaluating fungal penetration in histological analysis and together with Dr. M.C. Merino paper revision.

4.1 Introduction

Guidarelli et *al.* (2011) found that a RALF gene homologue to *AtRALF33* (here named *FaRALF3-1),* is up-regulated at 24 h upon *C. acutatum* inoculation of red ripe strawberry fruits, where the pathogen is active, whereas no difference in the expression of this gene was found in inoculated white unripe fruits. Furthermore, *FaRALF* gene expression analysis conducted in strawberry frtuis infected with *C. acutatum* and *B. cinerea*, revealed that *FaRALF3-1* is the only RALF family member upregulated gene during early stage infection.

To analyze the putative role of *FaRALF3-1* in anthracnose development in strawberry, the *Agrobacterium tumefaciens*-mediated transient transformation was used to silence *FaRALF3-1* gene in red ripe strawberry fruits, and in parallel, to overexpress this gene in white unripe fruits, all inoculated with *C. acutatum.* Anthracnose symptoms of transfected white and red strawberries inoculated with *C. acutatum* were monitored, following histological analysis of the infected tissues.

4.2 Materials and Methods

4.2.1 Fungal material

Colletotrichum acutatum was isolated from strawberry fruits of different strawberry cultivars showing severe anthracnose symp- toms. Monoconidial cultures were identified by morphological analysis and sequencing of ribosomal DNA internal transcribed spacer (ITS) regions. Isolate maya-3 was grown on potato dex- trose agar (Sigma, St. Louis, MO, USA) at 20 °C for 10 days. Conidial suspensions of pathogen were prepared by washing the colonies with 5 mL of sterile distilled water containing 0.05% (v/v) Tween-80, quantified with a haemocytometer, and diluted to a concentration of about 10^6 conidia/mL for the infection trials.

4.2.2 Plant material

Fragaria × ananassa cv. 'Alba' plants, cultivated in pots in a glasshouse, were used for all the experiments. Standard growing conditions were maintained at 20 °C with a 16 h photoperiod. For the analysis of susceptibility, fruits (three replicates of 20 fruits each) at unripe (20 days after flowering) or ripe (30 days after flowering) stage were inoculated with *C. acutatum* by dipping the fruits for 1 min in a suspension of 10^6 conidia/mL or distilled water (mock control), and stored at 20 °C and 70% relative humidity (RH) and observed every 24 h. After 3 days, the degree of susceptibility of strawberry fruits to the pathogen was scored as the percentage of infected fruits. The fruit surface was then excised with a clean scal- pel and immediately frozen in liquid nitrogen and transferred to −80 °C until use. Total RNA was prepared as described by (Gambino et *al.,* 2008).

4.2.3 qRT PCR

For qRT-PCR experiments, first-strand cDNA was synthesized from 1 µg of total RNA in a volume of 20 µL with oligo-d(T)17 and Superscript III (Invitrogen Life Technology, Carlsbad, CA, USA), following the manufacturer's instructions. The cDNA concentration in the RT mix was quantified using a ND-1000 UV spectrophotometer (Nanodrop Technologies, Wilmington, DE, USA), and 1 µg of cDNA was used for qRT-PCR experiments, employing an MX3000 thermal cycler (Stratagene, La Jolla, CA, USA) and Platinum Sybr-Green Kit (Invitrogen Life Technology), according to the

manufacturer's instructions. The elongation fac- tor 1α gene, having constitutive expression, was used to normalize raw data using ΔΔCt method and to calculate relative transcript levels. The primer sequences used in qRT-PCR are displayed in Table 4.1.

Gene	Oligonucleotide primers for qRT-PCR	
	Forward	Reverse
C. acutatum ß-tubulin	5'TACCGACAAAGGTGGAGGAC 3'	5'AGGATGTCGAGGACCAGATG 3'
Chitinase	5'ATGAGACTGGCCACTTTTGC 3'	5'AGTACTGCTTGGCAGGGTTG 3'
Fa a 1E	5'CGAGATCCTCGAAGGAGATG 3'	5'TGGAGTGGATCTTGTGCTTG 3'
PGIP	5'ATCTCACAGGTCCCATCCAG 3'	5'GCTGAGGAAGTCAGGGACTG 3'
FaWRKY51	5' TTCCTCCACCCTTCATCATC 3'	5' AACCAACATCCCTTGTGAGC 3'
FaWRKY42	5' TTACGAAGGGAAGCACAACC 3'	5' CCTCACAGCTGCCACTGATA 3'
Elongation factor 1 α	5' GCCCATGGTTGTTGAAAGTTTC 3'	5' GGCGCATGTCCCTCACA 3'
FaRALF3	5' TGGCAAAGTCCTCTTCCATT 3'	5' AACAAAGCTCAACCCGTGAT 3'

Table4.1 Primers used for qRT PCR expression analysis.

4.2.4 Plasmid construction, *Agrobacterium* transformation and plant transformation

The full-length cDNA sequence for the *FaRALF-33- like* (*FaRALF3-1)* gene was amplified from a pool of cDNA from red strawberry fruit at 24 hpi with of *C. acutatum*, using the primers forward 5'-ATGGCAAAGTCCTCTTCCATT-3' and reverse 5'-TCAACTACGGCAGCGAGTGAT-3'. The translated peptide sequence was aligned with the *A. thaliana* RALF cDNAs using ClustalW software (https ://www.ebi.ac.uk/Tools/ msa/clust alw2/). The pK7GWIWG2(II) RNAi silencing and pK7WG2 overexpression vectors, described in Karimi et al. (2002) [VIB Department of Plant Systems Biology, Ghent University, Belgium (http://gatew ay.psb. ugent.be)], were used as destination plasmids for inducing silencing or overexpression in agroinfiltrated fruits. For this, the same pENTR/D-TOPO (Invitrogen Life Technologies) construct contain- ing the full-length sequence of the FaRALF33-like cDNA, ampli- fied with forward primer 5'-

CACCATGGCAAAGTCCTCTTCCATT-3’ and reverse primer 5’-TCAACTACGGCAGCGAGTGAT-3’, was used in GATEWAY cloning (Invitrogen Life Technologies) (Fig. 4.1).

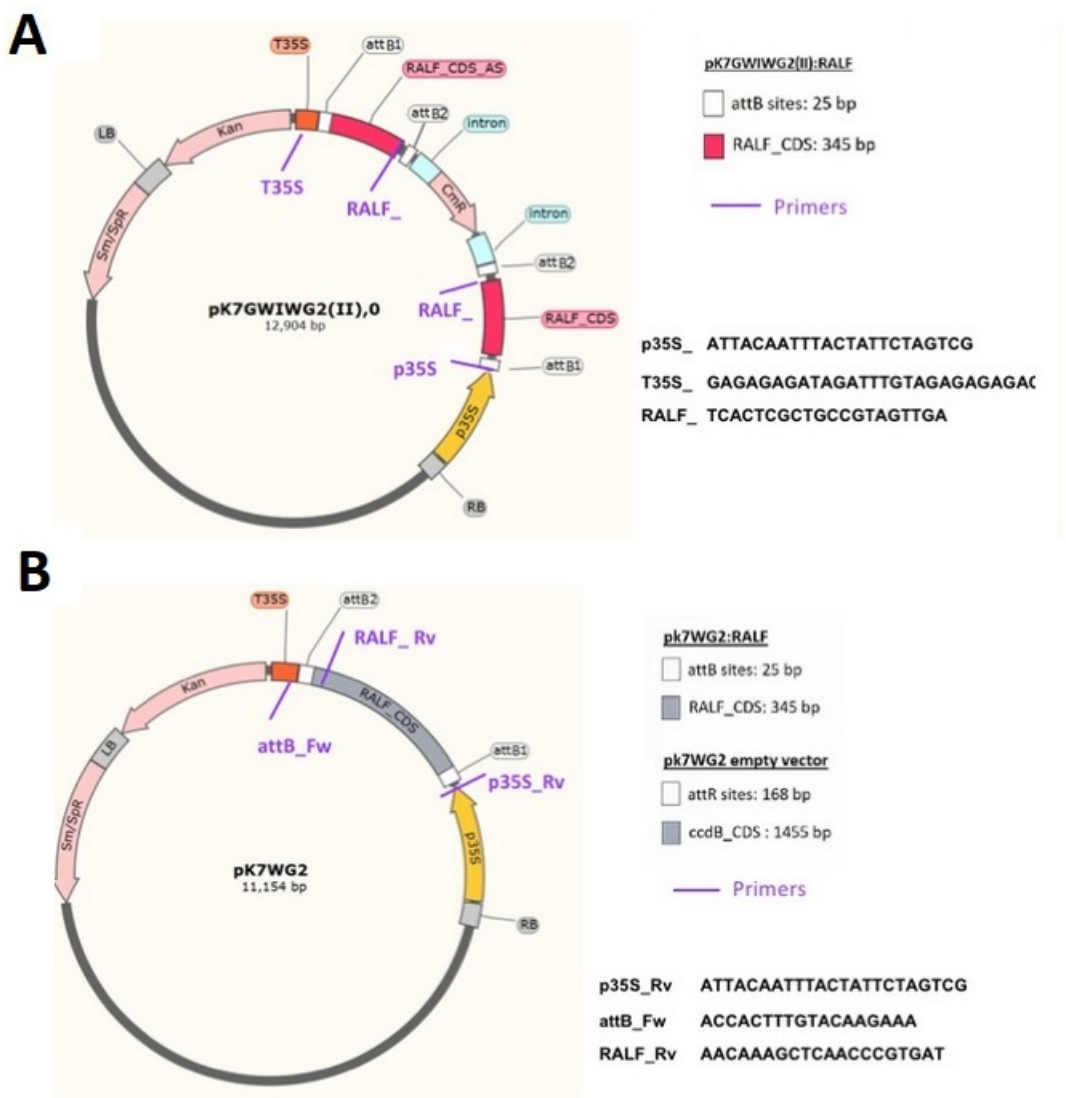

Figure 4.1. Overexpressing and silencing constructs. (a) pK7GWIWG2(II):RALF silencing construct, referred to in the text as pk7:*FaRALF-33-like*. (b) pK7WG2:RALF overexpressing construct, referred as 35S:*FaRALF-33-like.* The size of the attB and attR sites, RALF_CDS and ccdB_CDS are indicated on the right. Primers used for cloning are indicated in violet and the sequences are displayed on the right.

The plasmid constructs were checked by PCR [CaMV 35S promoter primer forward and attB2 primer reverse (5'-ACCACTTTGTACAAGAAA-3')], by digestion using restriction enzymes and by DNA sequencing. The resulting plasmids (pK7:FaRALF-33-like for silencing, 35S:FaRALF3 for overexpression) were introduced into *A. tumefaciens* strain EHA105 using the freeze–thaw shock method (Holsters et al., 1978). The *A. tumefaciens* EHA105 containing pK7:RALF33 or 35S:RALF33 were grown at 28 °C in Luria–Bertani (LB) medium with appropriate antibiotics. When the culture reached an optical density at 600 nm (OD600) of about 0.8, *Agrobacterium* cells were harvested and resuspended in a modified MacConkey (MMA) medium [Murashige and Skoog salts, 10 mM 2-(N-morpholino) ethanesulphonic acid (MES), pH 5.6, 20 g/L sucrose and 200 µM acetosyringone], according to Spolaore et *al.* (2001). After 1 h of incubation at 22 °C, the *Agrobacterium* suspension was injected into fruits still attached to the plant using a sterile syringe. After 6 days fruits were harvested and inoculated with *C. acutatum* conidia for 3 days, as described above. Tissues from the surface of the whole fruit were collected and RNA was isolated, as previously described. qRT-PCR was used to evaluate the *FaRALF33-like* (*FaRALF3-1)* transcript level, as described above.

4.2.5 FaRALF-33-like silencing and overexpression

For silencing, 44 red strawberry fruits at about 27 days after anthesis (3 days before the 'red' stage) were agroinfiltrated with pK7:FaRALF-33-like for 6 days. They were harvested and inoculated with *C. acutatum*, as described above. Twenty four of these fruits were collected 48 h after inoculation for histo- logical analysis of the fungal infection, as described by Guidarelli et *al*. (2011). The other 20 fruits were phenotypically observed at 3 days upon inoculation for anthracnose symptom evaluation and used for *FaRALF-33-like* (*FaRALF3-1)* gene expression analysis to confirm gene silencing. For this, RNA was isolated and qRT-PCR was performed, as described above. Similarly, for overexpression, 44 white fruits at about 17 days after anthesis (3 days before the 'white' stage) were agroinfiltrated with plasmid 35S:FaRALF-33- like for silencing for 6 days. They were harvested and inoculated with *C. acutatum*, as described above. The fruits were collected at 48 h after inoculation for histological analysis of the fungal infection, as described by Guidarelli et al. (2011). As controls for silencing and overexpression, the same number (44) of white and red fruits were agroinfiltrated with pK7:00 (the empty silencing vector) and 35S:00 (the empty overexpression vector) plasmids or left in the wild-type condition.

Phenotype observation, gene expression and histological analysis were performed as described above.

4.2.6 Statistics

Results were analysed for statistical significance (defined as $P < 0.05$ and indicated by asterisks in figures) by performing unpaired, two-sided Student's t-test with GraphPad Prism 7 Data Analysis Software (GraphPad Software, Inc., La Jolla, CA, USA). Mean and standard deviation (SD) values were calculated from at least three biologically and technically independent experiment.

4.3 Results

4.3.1 Silencing of FaRALF-33-like gene in ripe strawberries did not alter the susceptibility to *C. acutatum* but decreased the infection process after *C. acutatum* inoculation

To gain insightS in the possible role of *FaRALF3* gene in the response of strawberry fruits to *C. acutatum* transient transformation was used to silence the expression of this gene in red fruits. Fruits were harvested six days post agroinfiltration (pai) and inoculated with *C. acutatum* for 72 h before analysing the fruit response to anthracnose disease visual analysis of symptoms and observation of fungal infection structures by microscopy were performed to evaluate the influence of altered *FaRALF3* gene expression on fruit susceptibility. The silencing *FaRALF3* expression in red fruits is expected to render these fruits more resistant to *C. acutatum* infection. The expression of *FaRALF-33-like* gene was significantly induced 5 and 4 fold respectively, in both wild-type and control infiltrated strawberries (pK7:00) at 72 hpi with *C. acutatum*. The time (72 hpi) was chosen in order to observe the symptoms before sampling for gene expression analysis. In contrast, in pK7:FaRALF- 33-like transfected strawberries the expression of *FaRAF3* was significantly down-regulated suggesting the success of RNA interference mechanism. At phenotypic level, wild-type and pK7:00 control agroinfiltrated red strawberries at 72 hpi showed typical anthracnose symptoms with dark and sunken lesions on the fruit surface (Fig. 4.2B).

Symptom development was very similar in the pK7:FaRALF-33-like-silenced fruits, indicating that other mechanisms besides *RALF* gene induction are involved in disease susceptibility to *C. acutatum* in red ripe strawberries fruits.

The histological analysis of red fruits at 48 hpi revealed the presence of penetrated hyphae underneath the fruit surface in wild- type and mock-silenced red fruits. Similar penetrated hyphae were apparent also in *FaRALF-33-like*-silenced red fruits (Fig. 4.3A, B and C) although here tissue colonization by *Colletotrichum* hyphae appeared less deep than in control fruits. To evaluate the fungal growth, the expression of the housekeeping gene β-tubulin, specific to *C. acutatum* (Brown et al., 2008), was analysed by qRT-PCR. In *FaRALF-33-like*-silenced red fruits the fungus grows similarly to wild-type red fruits but less than in mock-silenced red fruits (Fig. 4.3D.

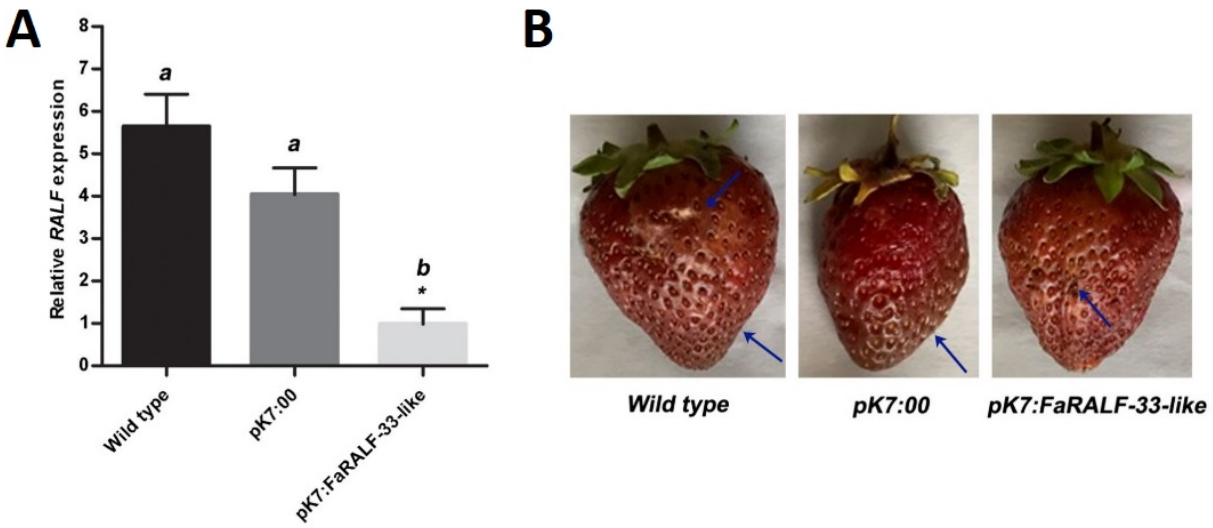

Figure 4.2. Silencing of *FaRALF-33-like* gene affects the susceptibility of ripe strawberries to *Colletotrichum acutatum.* (A) The transcript levels of *FaRALF-33-like* gene, normalized to *EF1α* transcript level, in wild-type red strawberries, mock-silenced red fruits (pK7:00) and FaRALF-33-like-silenced red fruits (pK7:FaRALF-33-like), at 72 hpi with *C. acutatum*. The data are the means and SD of three biological replicates. The letters indicate significant difference (Student's t-test) compared with wild-type or mock-treated fruits. The asterisks indicate $P < 0.05$. (B) Disease symptom analysis in wild-type infected red fruits (left), mock-silenced red fruits (pK7:00) (middle) and *FaRALF-33-like*-silenced red fruits (pK7:FaRALF-33-like) (right), at 72hpi with *C. acutatum*. One representative infected red fruit of each condition (wild-type, pK7:00, pK7:FaRALF-33-like) is shown. Arrows indicate anthracnose symptoms.

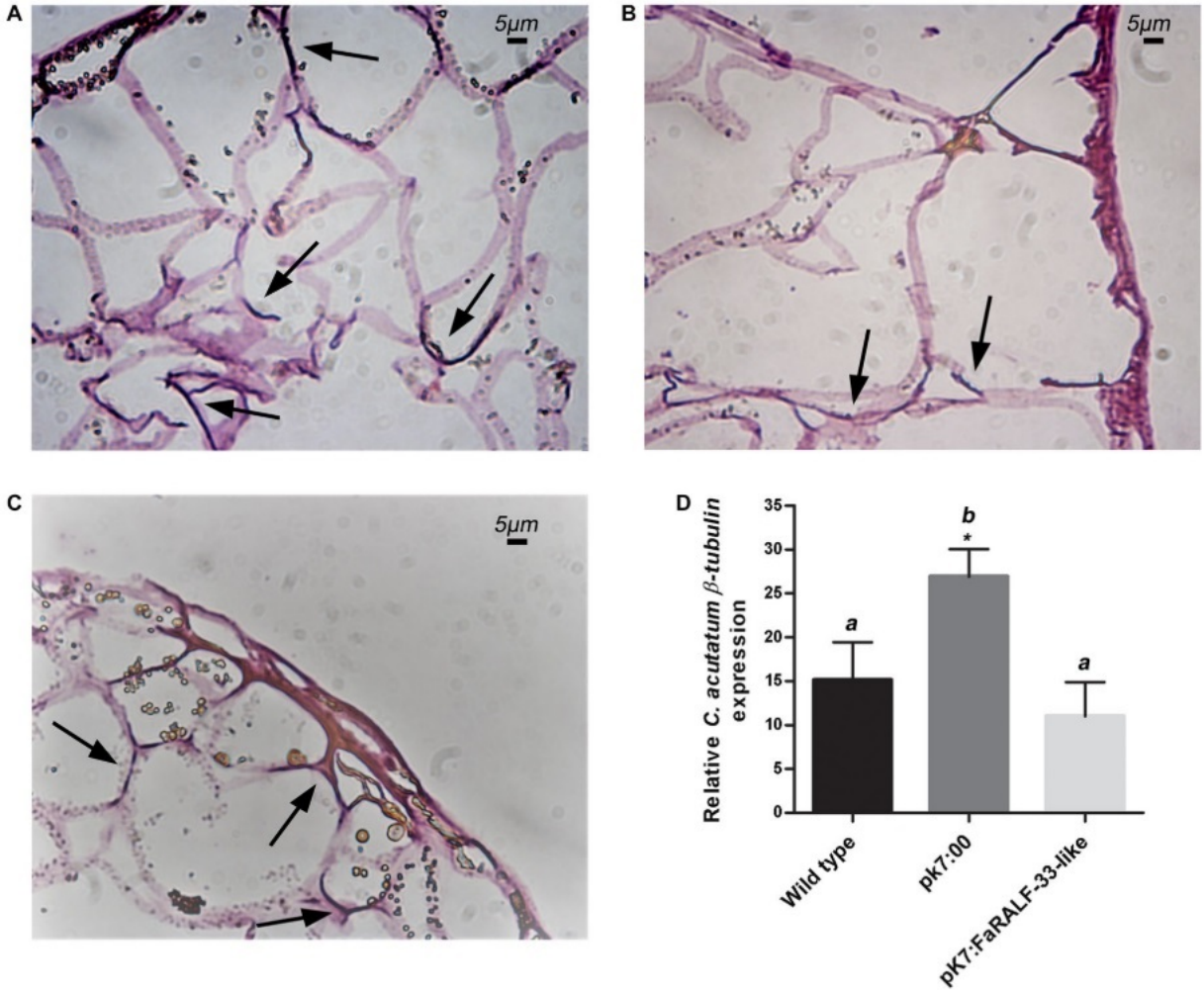

Figure 4.3. Histological analysis of *FaRALF-33-like*-silenced 48 h *Colletotrichum acutatum*-infected red fruits displays only superficial infection which correlates with *C. acutatum* similar growth in wild-type red fruits and in *FaRALF-33-like*-silenced fruits. Optical microscopy of wild-type red fruits (A), mock-silenced red fruits (B) and *FaRALF-33-like* silenced red fruits (C). Tissue slices were stained with haematoxylin and eosin. Inter-intracellular hyphae are indicated with arrows. Bar: 5 µm. (D) *Colletotrichum acutatum β-tubulin* expression in wild-type red strawberries (black bar) was compared with those of mock-silenced red fruits (pK7:00, dark grey) and *FaRALF-33-like*-silenced red fruits (pK7:FaRALF-33-like, light grey). The data are the means and SD of three biological replicates. The letters indicate significant difference (Student's t-test) compared with wild-type or mock-treated fruits. The asterisks indicate $P < 0.05$

4.3.2 Overexpression of *FaRALF-33-like* gene in white unripe strawberries led to increased susceptibility of fruits to *C. acutatum*

The overexpression of *FaRALF-33-like* was induced in white unripe strawberries by infiltration for 6 days with *Agrobacterium* carrying the plasmid 35S:FaRALF-33-like. Overexpression

in these strawberries was evaluated by qRT-PCR at 3 dpi (days post-inoculation) with *C. acutatum*. As mentioned above, the time (72 h) was chosen in order to observe the symptoms before sampling for gene expression analysis. The expression of *FaRALF- 33-like* gene increased 50-fold with respect to the control white fruit (infected wild-type or infected 35S:00) (Fig. 4.4A), indicating that overexpression was efficient and that agroinfiltration itself did not alter *FaRALF-33-like* expression.

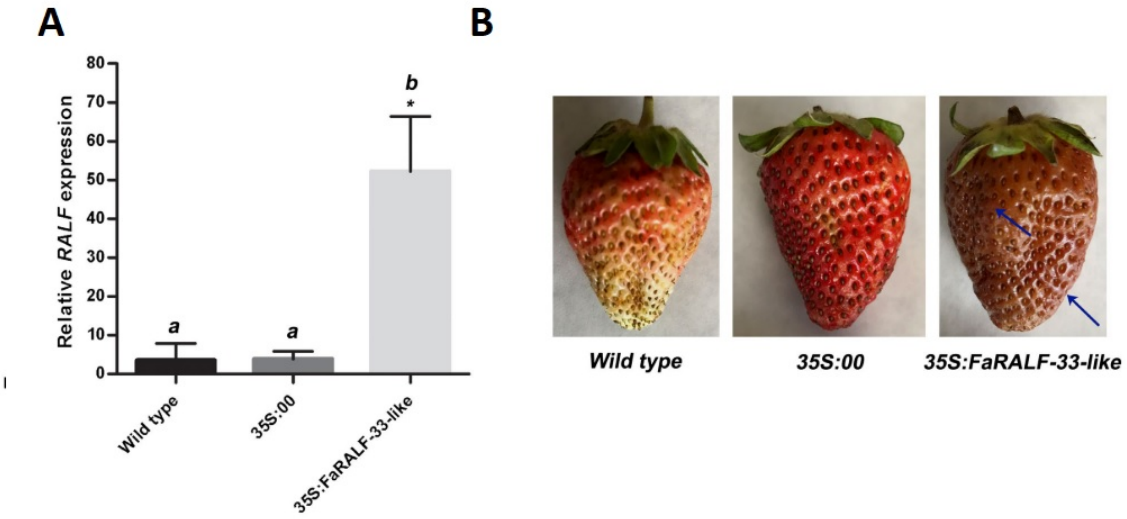

Figure 4.4. Overexpression of FaRALF-33-like gene white unripe strawberries to Colletotrichum acutatum. (A) The transcript levels of FaRALF-33-like gene in wild-type white strawberries were compared with those of mock-overexpressing white fruits (35S:00) and *FaRALF3*-overexpressing white fruits (35S:FaRALF-33-like), at 72 hpi with C. acutatum. Data were normalized to the transcript level of the housekeeping elongation factor 1α gene. The data are the means and SD of three biological replicates. The letters indicate significant difference (Student's t-test) compared with wild-type or mock-treated fruits. The asterisks indicate $P < 0.05$. (B) Disease symptom analysis in wild-type white fruits (left), mock-overexpressing white fruits (35S:00) (middle) and FaRALF-33-like-overexpressing white fruits (35S:FaRALF-33-like) (right), at 72 hpi with C. acutatum. One representative infected red fruit for each condition (wild type, 35S:00, 35S:FaRALF-33-like) is shown. Arrows indicate anthracnose symptoms.

Seventy-two hours after *C. acutatum* inoculation, wild-type white fruits did not show anthracnose symptoms, and 35S:00 agroinfiltrated control fruits showed light anthracnose symptoms, probably as consequence of agroinfiltration stress (Fig. 4.4B). On the other hand, symptom development was apparent in 35S:FaRALF-33-like white fruits, which were rotten.

The histological analysis of 48 h-infected unripe tissues showed that *C. acutatum* internal hyphae were distinguishable in the superficial layer of epidermal cells of all the three types of

fruits (Fig. 4.5A, B and C); however, in white *FaRALF-33-like*-overexpressing fruits, a higher percentage of penetration events, with deeper internal hyphae than in wild-type and mock-overexpressing white fruits, were distinguishable. Additionally, the fungus grew more in FaRALF-33- like-overexpressing white fruits compared to wild-type and mock- overexpressing fruits (Fig. 4.5D), suggesting a higher susceptibility of these fruits to *C. acutatum*.

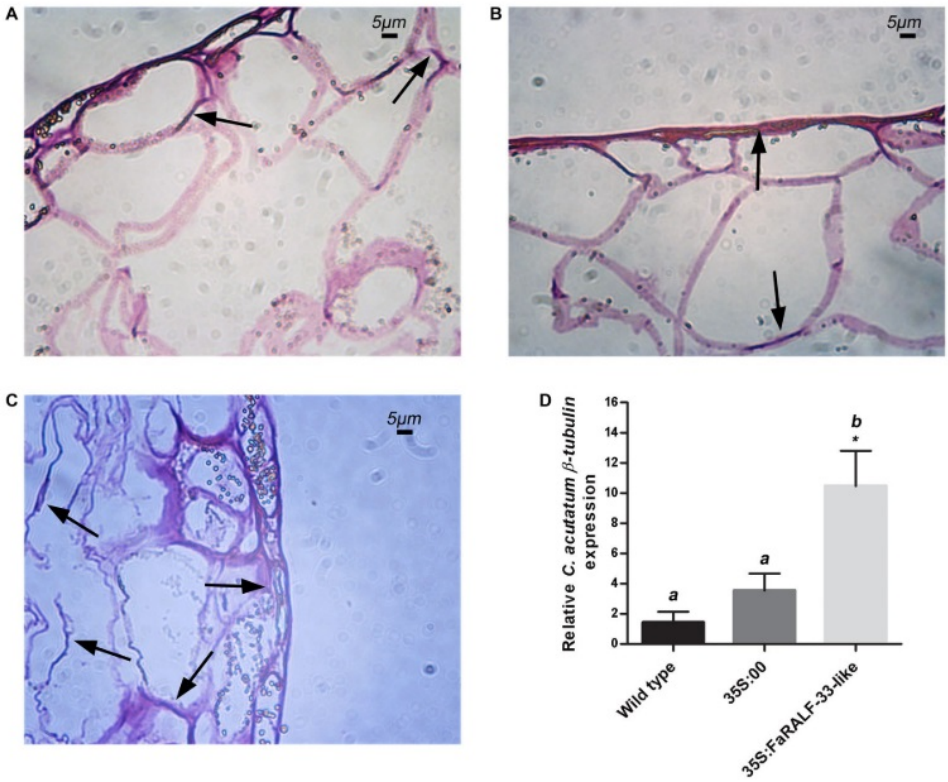

Figure 4.5 Histological analysis of *FaRALF-33-like* overexpressing 48 h *Colletotrichum acutatum*-infected white strawberry fruits. Optical microscopy of wild-type white fruits (A), mock-overexpressing white fruits (B) and *FaRALF-33-like* overexpressing white fruits (C). Tissue slices were stained with haematoxylin and eosin. Inter-intracellular hyphae are indicated. Bar: 5 µm. (D) *Colletotrichum acutatum β-tubulin* expression in wild-type white strawberries (black bar) was compared with those of mock- overexpressing white fruits (35S:00, dark grey), and *FaRALF-33-like*-overexpressing white fruits (35S:FaRALF-33-like, light grey). The data are the means and SD of three biological replicates. The letters indicate significant difference (Student's t-test) compared with wild-type or mock-treated fruits. The asterisks indicate $P < 0.05$.

4.3.3 Silencing or overexpression of *FaRALF-33-like* gene led to a different pattern expression of plant defence genes in strawberry fruits

To gain insight into the mechanism behind the susceptibility to *C. acutatum* in *FaRALF-33-like*-silencing or overexpressing fruits, the expression of genes associated with plant defence was evaluated. The genes under investigation were: a *Chitinase* gene, a gene encoding for a *PR-10* (pathogenesis-related protein 10, *Fra1E*), a gene encoding for a polygalacturonase-inhibiting protein *PGIP* and genes encoding for two transcription factors of the WRKY family (*FaWRKY51* and *FaWRKY42)*. These two WRKY genes are homologous to *A. thaliana AtWRKY 46* and *AtWRKY 33* and here they are named *FaWRKY51* and *FaWRKY42*, respectively, accordingly to the nomenclature proposed by (Wei et al., 2016). All these genes have a proved function in plant immune response to fungal pathogens (Amil-Ruiz *et al.*, 2011;De Lorenzo et *al.,* 2001; Jain, 2015; Pandey and Somssich, 2009; Sharma *et al.*, 2011) and in our previous microarray analysis were found to be differently regulated by *C. acutatum* inoculation at 24 hpi in white and red fruits (Guidarelli et al., 2011). In particular, in the microarray analysis, *Chitinase* and *FaWRKY42* were found to be upregulated in both white and red fruit upon *C. acutatum* infection, whereas *Fra a E1* and *FaWRKY51* were found to be up-regulated only in white fruits. Here, *in FaRALF- 33-like*-silenced red fruits the levels of transcripts of *Chitinase* were unaltered with respect to wild-type fruits, whereas *Fra a 1E* and *FaWRKY42* levels remained similar to the mocksilenced red fruits control, but lower than the wild-type, sug- gesting that agroinfiltration (and not RALF gene silencing) was determining a decrease in expression. On the other hand, *PGIP* and *FaWRKY51* gene expression was decreased (Fig. 4.6A) with respect to both controls (wild-type and mock-silenced fruits), as specific response associated with RALF gene silencing. When *FaRALF-33-like* was overexpressed in white fruits, the expression of *Chitinase, Fra a 1E* and *FaWRKY51* increased compared to wild-type or mock-overexpressing white fruits, whereas *PGIP* and *FaWRKY42* did not display any significant differences compared to the mock-overexpressing control. This could suggest that the white fruits that become more susceptible to *C. acutatum* by RALF gene overexpression try to arrest pathogen colonization by increasing the expression of key defence genes although with failure.

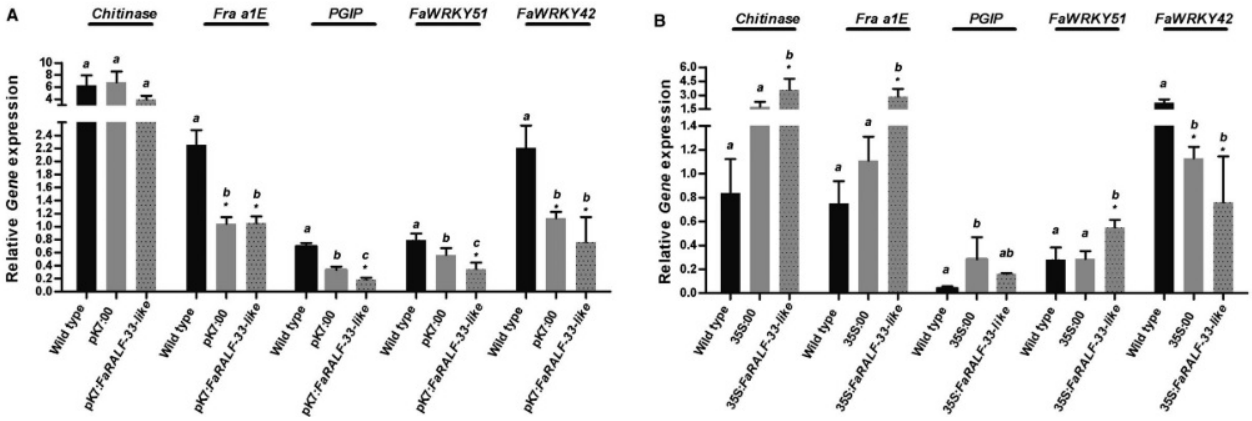

Figure 4.6. Silencing (A) or overexpression (B) of *FaRALF-33-like* gene triggers a different defence-related gene expression pattern. (A) The transcript levels of *Chitinase, Fra a 1E, PGIP, FaWRKY51* and *FaWRKY42* genes in wild-type red strawberries were compared with those of mock-silenced red fruits (pK7:00) and FaRALF-33-like-silenced red fruits (pK7:FaRALF-33-like), all inoculated for 72 h with *Colletotrichum acutatum*. (B) The transcript levels of *Chitinase, Fra a 1E, PGIP, FaWRKY51* and *FaWRKY42* genes in wild-type white strawberries were compared with those of mock-overexpressing white fruits (35S:00) and *FaRALF-33- like*-overexpressing white fruits (pK7:FaRALF-33-like), all inoculated for 72 h with C. acutatum. Data were normalized to the transcript level of the housekeeping elongation factor 1α gene. The data are the means and SD of three biological replicates. The letters indicate significant difference (Student's t-test) compared with wild-type or mock-treated fruits. The asterisks indicate $P < 0.05$.

4.4 Discussion

We have shown that silencing *FaRALF-33-like* expression in red fruits at 72 hpi (Fig. 4.2) can lead to a delay in fruit colonization by the fungal pathogen, appreciable by histological analysis of the infected tissues showing less penetrated infective hyphae than in wild-type fruit (Fig. 4.3) and a decrease in the expression of the plant defence genes *PGIP* and *FaWRKY51* genes (Fig. 4.6A). In contrast, 72 h *C. acutatum*-inoculated white unripe fruits overexpressing the *FaRALF3* gene decreased the ontogenic resistance of these fruits, leading to the appearance of disease symptoms (Fig. 4.4) and deep penetrated subcuticular hyphae (Fig. 4.5), which are generally absent in white un-ripe fruits. The different response of agroinfiltrated strawberry fruits to *C. acutatum* supports the hypothesis that *FaRALF-33*-like plays an important role in the susceptibility of fruits against the fungal pathogen *C. acutatum*.

Putative mechanisms supporting the role of *FaRALF3* in the ripe strawberry susceptibility to *C. acutatum* are the fact that its expression favours fungal pathogenicity by increasing the extracellular pH in the first stages of strawberry fruit colonization, after breaking the quiescence state (Fernandes et al., 2017) or by decreasing host defense ability, since *AtRALF23* was shown to play a role as negative regulator of plant immunity response in *Arabidopsis* (Stegmann et al., 2017). Thus, our results reinforce the hypothesis that fungi not only encode homologues of RALF genes in their genome (Masachis et al., 2016), but may also hijack the host RALF pathway by prompting RALF expression in plants, as previously shown by Dobón et al. (2015). However, the silencing of RALF in red ripe fruits while decreasing anthracnose symptoms could not prevent disease onset. Many other pathways, different from RALF signalling, may be involved in red ripe strawberry fruit susceptibility.

In summary, our results indicate that *FaRALF-33-like* gene expression plays a key role in fruit immune responses to fungal pathogens. Future research is required to elucidate the host mechanisms governing RALF expression in disease and the possible crosstalk between fungi and hosts in inducing the expression of this gene.

5. Pathogen-responsive regulatory element identification in *FaRALF3-1* promoter

5.1 Introduction

Induction of RALF genes expression upon pathogen infection was documented by microarray analysis in strawberry (Guidarelli et *al.* 2011) and subsequently confirmed by the analyses presented above which has shown that the specific upregulation of *FaRALF3* in the red ripe stage is related to fruit susceptibility to *C. acutatum* (Merino et al., 2019). A similar transcriptional regulation were observed in other host-pathogen systems, such as mature red tomato fruits (*Solanum lycopersicum)* infection by *Colletotrichum gleosporioides* and rice upon *Magnaporthe oryzae* infection (Wang et al., 2019). Furthermore, Dobón *et al.* (2015) observed that *Arabidopsis RALF23, RALF24, RALF32* and *RALF33* genes were simultaneously upregulated in four *Arabidopsis* transcription factors mutants (*at1g66810, pap2, bhlh99, zpf2)* , whose susceptibility to *B. cinerea* and *Plectosphaerella cucumerina* were increased compared to *wild type.* These findings suggest a pathogen responsive RALF gene regulation mechanism in a variety of host plants infected by different fungal agents. For these reasons the inducibility of RALF genes expression upon *Fragaria x ananassa* fruits infection with *C. acutatum* and *B. cinerea* was studied. Threfore, *In silico* analysis of the *FaRALF3-1* promoter was conducted also in order to identify putative pathogen responsive motifs. We then tested *in vivo* if progressively truncated *FaRALF3-1* promoter fragments could induce reporter genes expression in agroinfiltrated strawberry fruits infected with *C. acutatum.*

5.2 Materials and Methods

5.2.1 *In silico* analysis of predicted regulatory elements in *FaRALF3-1* promoter

For pathogen-induced predicted regulatory elements analysis, pathogen-upregulated genes were retrieved from transcriptional datasets of red strawberry (*Fragaria x ananassa)* fruits at 24 hours post infection with *C. acutatum* (Guidarelli et al., 2011) and *B. cinerea* (Xiong et al., 2018). A total of 87 predicted promoters for *C. acutatum* and 97 for *B. cinerea* were analyzed. For each gene, 1500 bp upstream the ATG start codon were analyzed from the *F.vesca* genome v4.0.a1 assembly. MotifLab software v1.08 (Klepper & Drabløs, 2013) was used for *in silico* analysis using PLACE database for Motif Scanning (Higo et al., 1998) and AlignACE algorithm for Motif Discovery (Hughes et al., 2000). Briefly, Motif Scanning were performed using Simple Scanner program with default parameters. Statistically significant known regulatory elements were calculated performing the same Motif scanning program on randomly generated DNA sequences starting from input predicted promoter sequences using a third order background model. The frequency measured for each cis-acting element on random-DNA was used as background occurrence for statistical significant evaluation using a binomial test with p-value threshold of 0.05. Motif Discovery was performed using AlignACE method with default parameters and motif significance was calculated as mentioned above for Motif scanning method.

5.2.2 In silico analysis of predicted regulatory elements in *FaRALF3*

Preliminary study on putative promoter allelic variants were conducted on *Fragaria x ananassa cv. Alba* and *cv. Florida Elyana.* Genomic DNA was extracted from leaves using Wizard® Genomic Purification kit (Promega). Plant Tissue Protocol (Manufacturer protocol 3.E.) was modified adding two consecutive chloroform:isoamyl alcohol (24:1) purification steps after Protein Precipitation solution addition and before 2-propanol precipitation. *FaRALF3-1* putative promoter was amplified using primers For 5'-TGCATCTGTTACATCATCCCTTG-3' and Rev 5'-GTAGTCGACTCTCCCATCTTG-3', cloned into pGEM®-T easy vector (Promega). Five clones for each variety were sequenced and aligned

with *Fragaria x ananassa cv. Camarosa* genomic sequence available from GDR, using Clustal Omega.

5.2.3 Progressive truncated promoter cloning and *Agrobacterium*-mediated transient transformation

FaRALF3-1 upstream sequence was PCR-amplified starting from *Fragaria x ananassa cv. Elyana* genomic DNA, using primers 5'-GGGGACCACTTTGTACAAGAAAGCTGGGTNCTGAAAGGACAAAAC ATTTTCT-3' as reverse primers for all promoter fragments, 5'-GGGGACAAGTTTGTACAAAAAAGC AGGCTNNTGCATCTGTTACATCATCCCTTG-3' as forward for whole promoter fragment (T6), 5'-GGGGACAAGTTTGTACAAAAAAGCAGGCTNNTGCTTAAGTGGCTCTCAAAG-3' as forward for 400 bp fragment (T4) and 5'-GGGGACAAGTTTGTACAAAAAAGCAGGCTNNCCGCTAAGTGGTTCAATTCA-3' as forward for 200bp fragment (T2) (Fig.4). Truncated FvRALF3 promoter constructs, and double tandem p35S promoter as positive control, were cloned into pDONR222 using Gateway BP reaction and consequently cloned into pKGWFS7 (Fig. S4) vector by LR Reaction. Obtained vectors were then introduced into chemically competent *Agrobacterium tumefaciens* strain EHA105 by heat shock transformation. Briefly, after been frozen in liquid nitrogen, cells were thawed for 5 min at 37°C, 1 µg of plasmid DNA were added, then cell were incubated at 30°C for 2 hours in agitation and plated. Positive colonies were then grown in selective media (Rinfampycin 100 µg/mL and Spectinomycin 50 µg/mL) until culture reached an OD_{600} of 0.8. Cells were then collected through centrifugation and pellet was resuspended in fresh MMS medium (Murashige and Skoog Basal Medium 4.4 g/L plus sucrose 20g/l) until an OD_{600} of 2.4 was reached, at the end acetosyringone (4'-Hydroxy-3',5'-dimethoxyacetophenone) at the final concentration of 200 µM was added to the culture. At least three white attached fruits, for each condition, were agroinfilitrated using a needle syringe until *Agrobacterium* culture filled strawberry fruit tissues. Five days after agroinfiltration, fruit were harvested and infected with *C. acutatum* conidial suspension or mock-inoculated with water, according to experimental procedure, as was described above. After 24 hours post infection fruits were

dissected and one half was used for RNA extraction and eGFP expression analysis, and the other half was used for histochemical assay of GUS activity.

5.2.4 Histochemical GUS assay

Surface tissue and longitudinal sections of infected and mock- infected fruits were cut with a razor blade and dipped in GUS staining solution [50 mM Na-phosphate (pH 7.5), 10 mM EDTA, 1 mM 5-bromo-4chloro-3-indolyl-glucuronide (X-gluc), 0.1% Triton X-100, 0.5 mM potassium ferricianide and 5% (w/v) polyvinylpyrrolidone-40 (PVP)]. Strawberry tissues were incubated overnight at 37 °C, and then kept at 4 °C in absolute ethanol until being photographed.

5.3 Results and Discussion

5.3.1 *FaRALF3* promoter analysis in *Fragaria x anannassa* subgenomes and varieties

As shown above and reported in previous studies, RALF gene expression is triggered by different biotic and abiotic stimuli, however the signaling events regulating its expression are not yet known. In particular those responding to fungal pathogen infection. Identification of the promoter elements necessary for gene induction by fungal pathogens could provide insights on the transcription factors involved in immunity signaling and ultimately provide for the necessary knowledge to develop synthetic pathogen-responsive promoters to fight infections. Among *FaRALF* family genes, *FaRALF3* has shown clear upregulation in response to pathogen, and its overexpression in strawberry fruits is related to susceptibility (Merino et al., 2019). For this reason *FaRALF3* was chosen for promoter characterization analysis.

To study *FaRALF3* putative promoter function in *Fragaria* x *ananassa*, the level of sequence conservation among the *Fxa* subgenomes of the region upstream RALF start codon was firstly assessed. *FaRALF3-1* sequence from the 3'UTR of upstream flanking gene (annotated as '*maker-Fvb2-2-augustus-gene-47.69-mRNA-1'*) and its ATG (590 bp) was used as input for BLASTn analysis against *Fragaria x ananassa cv.Camarosa* v1.0.a1. Five sequences were retrieved on Chr2-4 of *F.ii*, Chr2-1 of *F.ni* and Chr 2-3 of *F.vi* (Supplementary Fig.S1), indicating that the putative *FaRALF3* orthologs promoter sequences in the the *Fxa* subgenomes is highly conserved (Tab.2.2) except for *F. viridis,* already reported to be the most divergent and silent in octoploid genome (Edger et al., 2019).

To study allelic variability, the *FaRALF3-1* putative promoter sequence similarity was assessed also in genomes of *Fragaria x ananassa* varieties with different susceptibility to fungal pathogens, the *cv. Florida Elyana* from Florida (U.S.A.) which is resistant to anthracnose disease (Seijo, Chandler, Mertely, Moyer, & Peres, 2008)(Seijo et al., 2008), and *cv. Alba,* an italian variety which is highly susceptible to *C. acutatum* infection (*https://plantgest.imagelinenetwork.com/it/varieta/frutticole/fragola /alba/59*). The promoters wer amplified with specific primers and five clones for each variety were sequenced and aligned with that of the v1.0.a1 genome sequence *cv. Camarosa* (Supplementary Fig.S2). Only a single nucleotide polymorphism was detected between *cv.*

Alba and *Florida Elyana.* This suggests that the function associated with the *Fa*RALF3-1 5' upstream sequence in octoploid strawberry might be very important for expression regulation and also that the plant susceptibility to anthracnose disease cannot be associated with allelic polymorphisms in *FaRALF3-1* putative promoter.

5.3.2 Prediction of FvRALF3 promoter pathogen-responsive regulatory elements

The *FaRALF3-1* (from *F.ve* subgenome) putative promoter sequence was chosen for pathogen-responsive regulatory element analysis because of the reported *F. vesca* subgenome dominance in octoploid genome (Edger et al., 2019)(Edger et al., 2019). Since *Fa*- and *FvRALF3* upstream putative regulatory sequences share 99% level of identity and the available *Fxa* pathogen-responsive transcriptome data have all been mapped onto *F. vesca* genome, the analysis of the *FaRALF3-1* promoter regulatory elements responsive to pathogen infection were carried out on *F. vesca* genome *FvRALF3* promoter. For this, 656 bp of the F. vesca genomic sequence located between the stop codon of the *FvRALF3* upstream flanking gene on Chr2 and *FvRALF3* ATG starting codon, were analysed. *FvRALF3* putative promoter sequence was compared with known transcription factor binding sites of genes known to be regulated in *Fxa* strawberry fruit upon *C. acutatum* and *B. cinerea* infections (Guidarelli *et al.*, 2011 ; Xiong et al., 2018) in PLACE database (Higo et al., 1998) (Motif Scanning analysis). These latter sequences and RALF3 putative promoter were then scored for motif frequency (Motif Discovery analysis) (Fig. 5.1). Motif scanning analysis of cis-acting elements mostly represented among fungal-induced genes revealed the presence of an element initially identified as initiator of PsaDb gene promoter (INRNTPSADB, PLACE ID: S000395), lacking TATA-box, which is common to almost all the sequences analyzed and *FvRALF3* putative promoter (90% of the *C. acutatum* responsive genes promoter sequences and to 94% of *B. cinerea* ones) (Nakamura et al., 2002) (Fig. 5.1). Other TATA-like elements such as TATABOX2 (PLACE ID: S000109) and TATAPVTRNALEU (S000340), which have the role of recognition and initiator of transcription complex (Grace et al., 2004) were also found in several sequences (respectively in the 67% of *C. acutatum* and 42% of *B. cinerea* induced genes) .

A

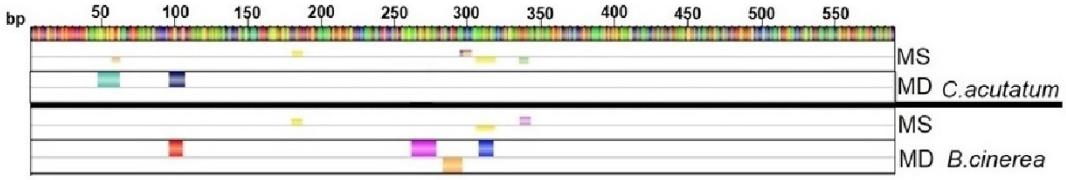

B *C.acutatum*

	ID	Name	Sequences	Total	Exp	Score	Consensus	Position (bp)	Strand	
	S000395	INRNTPSADB	78 of 87 (90%)	264	173	7.88		180-187; 306-318	+; -	MS
	S000109	TATABOX2	59 of 87 (67%)	91	51	2.82		335-341	-	
	S000167	MYBPLANT	33 of 87 (37%)	48	25	2.82		295-302	+	
	S000179	MYBZM	47 of 87 (37%)	90	56	1.76		57-62	-	
	AlignACE00085		20 of87 (23%)	21	1	7.19		47-61	+	MD
	AlignACE00098		14 of 87 (16%)	20	1	1.51		96-106	+	

C *B.cinerea*

	ID	Name	Sequences	Total	Exp	Score	Consensus	Position (bp)	Strand	
	S000395	INRNTPSADB	92 of 97 (94%)	363	295	7.11		180-187,306-318	+,-	MS
	S000340	TATAPVTRNALEU	41 of 97 (42%)	58	32	2.92		336-343	+	
	AlignACE00040		23 of 97 (23%)	25	3	3.05		262-278	+	
	AlignACE00048		15 of 97(15%)	16	1	1.86		283-295	-	MD
	AlignACE00034		16 of97 (16%)	24	4	9.87		308-317	+	
	AlignACE00021		19 of 97 (19%)	20	4	1.019		97-106	+	

Figure 5.1 In silico analysis of predicted regulatory elements in pathogen-induced Fragaria genes. （A) From the top: *FvRALF3* gene putative promoter, Motif Scanning (MS) and Motif Discovery (MD) outputs resulting from the analyses of *C. acutatum*-induced genes, and MS and MD outputs from the analysis of *B. cinerea* induced genes at 24 hour post-infection. Small colored boxes in MS indicate known regulatory elements from PLACE database found to be significantly abundant in the group of sequences analyzed and in *FvRALF3* putative promoter, while large coloured boxes in MD represent sequences found significantly enriched in the upstream sequences of genes analyzed. (B) and (C) are the color legends respectively for *C. acutatum* and *B. cinerea* reported in (A). Codes and names of regulatory elements are reported, together with elements and percentage abundance among sequences analyzed (Sequences), total count of elements found (total), element background frequency calculated as number of elements found in a third order random generated sequences (Exp), ranking score values calculated by MotifLab software using a binomial test with p-value threshold of 0.05 (Score). Consensus sequence of each element is shown along the position of the element in the putative FvRALF3 promoter (Position bp) and the strand in which it is found.

Among the group of genes upregulated by *C. acutatum*, 33% and 47% have respectively a MYBPLANT (S000167) (Merida et al., 2007) and MYBZM (S000179) (E. et al., 1994) regulatory elements, which are binding sites for MYB. Additional analysis on the putative promoters of Arabidopsis *RALF33* (*AT4G15800*) and its homologous in tomato (*S. lycopersicum Solyc09g074890.1)*, revealed the presence of the same binding site (data not shown). MYB

proteins are a large family of transcription factor involved in regulation of many processes in plants, such as phenylpropanoid metabolism (Liu, Osbourn, & Ma, 2015)(Liu et al., 2015), ABA and JA signaling (Abe et al., 2003), responses to abiotic and biotic stress (Ramírez, Agorio, et al., 2011), cell death and circadian clock. MYB proteins generally interact with basic helix-loop helix (bHLH) family member and are regulated by cytosolic WD40 repeat proteins through formation of MYB/bHLH/WD40 dynamic complexes, which regulate various gene expression pathways (Pireyre & Burow, 2015). Interestingly, MYB46 is involved in enhancing *B. cinerea* resistance through down-regulation of cell wall associated genes (CESA) during early stage infection (Ramírez *et al.,*2011)(Ramírez et al.,2011). Arabidopsis T-insertion mutants of genes regulated by MYB46, such as the a zinc-finger containing protein *gene zfp2,* the Basic Helix-Loop-Helix TF *bhlh99*, the AUX/IAA-type transcriptional repressor *pap2* and the *at1g66810 gene* coding for a Zing Finger Transcription Factor (TF), showed enhanced susceptibility to the necrotrophs fungal pathogens *B. cinerea* and *P. cucumerina* (Dobón *et al.* 2015). The transcriptional analysis of these four mutants revealed a coordinated upregulation of *RALF23, RALF24, RALF32* and *RALF33* (Dobón *et al.* 2015) supporting the hypothesis of a MYB46 regulation of RALF gene expression. A Motif Discovery analysis was performed using AlignACE algorithm (Hughes et al., 2000) on the putative promoter sequences of both FvRALF3 and the identified *C. acutatum* and *B. cinerea* strawberry upregulated genes, and significantly overrepresented motifs were assessed. The motifs identified using MotifLab software are named 'AlignACE' followed by progressive numbers. For *C. acutatum* gene group the AlignACE00085 element (consensus GxTxxxTGTGAxTTG) was found in the 23% of sequences and in *FvRALF3* putative promoter, and is partially overlapping with MYBZM elements at the position between bases 57 and 62 of *FvRALF3* putative promoter. The AlignACE00098 (xxTGGxCTTGG) element was found in the 16% of *C. acutatum* upregulated genes and aligned to the elements AlignACE00021 (TTGGxxTTGG) found in *B. cinerea* upregulated group (19% of sequences analyzed). This suggests that in this position this element might be a regulatory component important for Fv*RALF3* fungal induced expression. Furthermore in *B. cinerea* gene group the AlignACE00040 (AAxxTTGAxxGxxxAA), AlignACE00048 (TxGAAxxGGTC)and AlignACE00034 (AxTGAAxTGA), located between bases 262 and 317 in *FvRALF3* putative promoter, were found significantly overrepresented.

5.3.3 *FvRALF3 promoter Agrobacterium- medieted* reporter assay

In order to assess *FaRALF3* putative promoter function and identify possible pathogen-responsive regulatory elements, three progressive truncated fragments of *FaRALF3-1* upstream sequence consisting of the above described 588 bp sequence (T6), a 200 bp deletion (T4) and 400 bp deletion (T2) (Fig.5.2A), were cloned into pKGWFS7 vector and fused to two tandem reporter genes eGFP and β-glucoronidase (GUS) (Supplementary Fig.S3). *Agrobacterium*-mediated transient transformation of white *Fxa* fruits was performed through injection of bacteria transformed with the three constructs. Fruits were infected with *C. acutatum* and analyzed for both reporter genes activity at 24 hpi, through quantification of eGFP expression in qRT-PCR and histochemical GUS assay for β-glucuronidase activity. GUS reporter activity, visualized as blue color of fruits, showed great variability among infected and mock-infected fruits (Fig.5.2B). Consistent to this, no significant difference was shown in the eGFP transcript level quantified in *C. acutatum* infected versus control fruit. This is possibly due to the fruit response to Agrobacterium itself, independently from the fungal pathogen. Indeed Agrobacterium can be perceived as a pathogen by the fruit and stimulate similar responses as *C. acutatum*, including those leading to FaRALF3 expression. The variability affecting strawberry *Agrobacterium*-mediated transformation depending on technical and environmental conditions has recently been described (Zhao et al. 2019). It was shown that the expression level of a reporter gene is normally distributed in an population of 30 treated fruits, with huge variation among different fruits. Other important factors affecting agroinfiltration methodology are the quantity of bacteria injected for each fruits, the stage of fruit ripening and the temperature and incubation time after transient transformation. In our experiments, maybe for all these reasons, it was not possible to infer the identity of *FaRALF3-1* promoter elements inducible by fungal pathogens such as *C. acutatum*, in agrobacterium-free systems. On the other hand, with respect to the different putative promoter sequence sizes tested, clearly the GUS activity and eGFP expression controlled by T4 and T6 sequences are measurable and comparable, whereas, under control of T2 element, both the GUS and eGFP become almost undetectable, suggesting that T4, comprising 400 bp sequence upstream *FaRALF3-1* ATG, contains the minimal promoter sequence elements necessary to drive reporter gene expression in strawberry fruits. According to Motif Scanning analysis, the T4 promoter fragment includes at least two regulatory elements known to be recognized by

transcriptional activation complex, (TATA-boxes and Initiator of activation in TATA-less promoter) (Fig.5.2A and Fig.5.1). At the same time, the 200 bp sequence comprising the 3' UTR of the Low PSII Accumulation (LPA1) and Tetratricopeptide (TRP) domains containing protein genes, are probably not determinant as expression regulatory sequences.

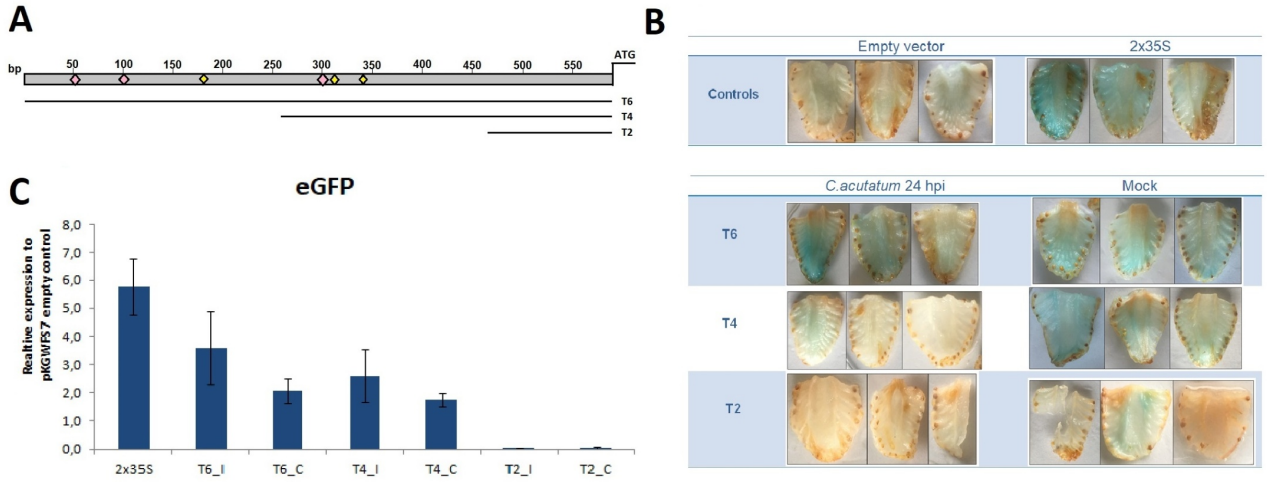

Figure 5.2 Dissection of *FaRALF3-1* promoter and *Agrobacterium*-mediated reporter assay. (A) Schematic representation of the promoter fragments used in this study. Pink squares indicate putative MYB-related regulatory elements, yellow squares indicates putative TATA-box related transcriptional activation elements. B) Histochemical GUS staining to detect β-glucoronidase activity in longitudinal fruit sections of Agroinfiltrated fruits. The figuere shows fruits transformed with negative (empty vector) and positive (double tandem p35S, 2x35S) controls. Fruits transformed with T6, T4 and T2 truncated promoter fragments were treated with *C. acutatum* or mock-treated and collected 24h post-infection. (C) Histogram showing qRT- PCR quantitative analysis of eGFP reporter expression. Each bar represents the average of three biological replicates. Expression values were normalized to pKGWFS7 empty vector infilitarted fruits. (C) Mock- tretated samples, (I) *C. acutatum* infected.

5.4 Conclusions

In conclusion, a putative involvement of a MYB transcription factor as regulator of *FaRALF3-1* based on the *in silico* promoter characterization. Furthermore, agroinfilitration-mediated *FaRALF3-1* promoter reporter assay revealed that the 400 bp upstream the start codon can drive expression in strawberry fruits. Future research, such as yeast two hybrid system analysis, and methodology optimization will be required to identify specific pathogen-responsive elements.

5.5 Supplementary Figures

Supplementary FigureS1. Blastn output of *FaRALF3-1* upstream sequence against *Fragaria x ananassa cv. Camarosa* v1.0.a1 pseudomolecule using GDR

```
> Fvb2-2
Length=24782128

 Score = 1250 bits (650),  Expect = 0.0
 Identities = 652/653 (99%), Gaps = 0/653 (0%)
 Strand=Plus/Minus

Query  1        TGCATCTGTTACATCATCCCTTGAGATTATTTGGAATAGTACTATTAGTTTACCAGATCC  60
                ||||||||||||||||||||||||||||||||||||||||||||||||||||||||||||
Sbjct  4767971  TGCATCTGTTACATCATCCCTTGAGATTATTTGGAATAGTACTATTAGTTTACCAGATCC  4767912

Query  61       ACCATTCATATTGTACCCATTCTGATATATATACAAATTGTTGATTACAGCCATTTATAT  120
                ||||||||||||||||||||||||||||||||||||||||||||||||||||||||||||
Sbjct  4767911  ACCATTCATATTGTACCCATTCTGATATATATACAAATTGTTGATTACAGCCATTTATAT  4767852

Query  121      TTCTTGTGCTTCAACACCAGCCAATTTATTTTCGGAAATTAATAGTTTGTATAAACGATT  180
                ||||||||||||||||||||||||||||||||||||||||||||||||||||||||||||
Sbjct  4767851  TTCTTGTGCTTCAACACCAGCCAATTTATTTTCGGAAATTAATAGTTTGTATAAACGATT  4767792

Query  181      AACTCAGAAAATCAAATTCTGTATGACATTGACATTGGATACACGTCTATAAGACTATAA  240
                ||||||||||||||||||||||||||||||||||||||||||||||||||||||||||||
Sbjct  4767791  AACTCAGAAAATCAAATTCTGTATGACATTGACATTGGATACACGTCTATAAGACTATAA  4767732

Query  241      CTAGGTTCGTAGTTTGAAGTCTGCTTAAGTGGCTCTCAAAGCTGTTGTAGTGCTGGATGG  300
                ||||||||||||||||||||||||||||||||||||||||||||||||||||||||||||
Sbjct  4767731  CTAGGTTCGTAGTTTGAAGTCTGCTTAAGTGGCTCTCAAAGCTGTTGTAGTGCTGGATGG  4767672

Query  301      CATAAATTCAAAGATAGTATCAGTTTCAATGATTAGTTGCATACCGACTTTATAATTGGA  360
                ||||||||||||||||||||||||||||||||||||||||||||||||||||||||||||
Sbjct  4767671  CATAAATTCAAAGATAGTATCAGTTTCAATGATTAGTTGCATACCGACTTTATAATTGGA  4767612

Query  361      ATTGTAAATGGTATTTGATAGGTCCATTTCTACTACTACGACTCGTTTTTGATATCAAGG  420
                ||||||||||||||||||||||||||||||||||||||||||||||||||||||||||||
Sbjct  4767611  ATTGTAAATGGTATTTGATAGGTCCATTTCTACTACTACGACTCGTTTTTGATATCAAGG  4767552

Query  421      ATTGCGTAAGTCACACCAATTTGCATCTAGTTATATAAATATATTCCGCTAAGTGGTTCA  480
                ||||||||||||||||||||||||||||||||||||||||||||||||||||||||||||
Sbjct  4767551  ATTGCGTAAGTCACACCAATTTGCATCTAGTTATATAAATATATTCCGCTAAGTGGTTCA  4767492

Query  481      ATTCATTTTCTTGGTAGGTTTTGAACAGGTCACGGATTTATCCAATCCAGCTTTCCTTCC  540
                ||||||||||||||||||||||||||||||||||||||||||||||||||||||||||||
Sbjct  4767491  ATTCATTTTCTTGGTAGGTTTTGAACAGGTCACGGATTTATCCAATCCAGCTTTCCTTCC  4767432

Query  541      AGCAATTGGAGCAAGGTTGAATTTTGGTGAGAGTCATTAAACTAATCAGCTTTGTTTGAA  600
                ||||||||||||||||||||||||||||||||||||||||||||||||||||||||||||
Sbjct  4767431  AGCAATTGGAGCAAGGTTGAATTTTGGTGAGAGTCATTAAACTAATCAGCTTTGTTTGAA  4767372

Query  601      CAAATGAGAAATGAGAGCTTCCAATTCCCTTAGAAAATGTTTTGTCCTTTCAG  653
                ||||||||||||||||||||||||||||||||||||||||||||||||||| ||||
Sbjct  4767371  CAAATGAGAAATGAGAGCTTCCAATTCCCTTAGAAAATGTTTTGTCCTGTCAG  4767319


> Fvb2-4
Length=26692599

 Score = 1067 bits (555),  Expect = 0.0
 Identities = 621/644 (96%), Gaps = 8/644 (1%)
 Strand=Plus/Plus

Query  12        CATCATCCCTTGAGATTATTTGGAATAGTACTAT-TAGTTTACCAGATCCACCATTCATA  70
                ||||||||||||||||||||||| ||||| ||| |||||||||||||||||||||||| |
Sbjct  21746277  CATCATCCCTTGAGATTATTTGGATTAGTAATATATAGTTTACCAGATCCACCATTCACA  21746336

Query  71        TTGTACCCATTCTGATATATATACAAATTGTTGATTACAGCCATTTATATTTCTTGTGCT  130
                ||||||   | ||||||||||||||||||||||||||||||||||   ||||||||
Sbjct  21746337  TTGTAC---TCCTGATATATATACAAATTGTTGATTACAGCCATTTATA---CTTGTGCT  21746390
```

```
Query  131       TCAACACCAGCCAATTTATTTTCGGAAATTAATAGTTTGTATAAACGA-TTAACTCAGAA  189
                 |||||||||||||||||||||||||||||| ||||||||||||||| ||||||||||
Sbjct  21746391  TCAACACCAGCCAATTTATTTTCGGAAATTAGTAGTTTGTATAAACGATTTAACTCAGAA  21746450

Query  190       AATCAAATTCTGTATGACATTGACATTGGATACACGTCTATAAGACTATAACTAGGTTCG  249
                 |||||| |||||||||||||||| ||||||||||||||||||||||||||||||||||
Sbjct  21746451  AATCAATTTCTGTATGACATTGACAATGGATACACGTCTATAAGACTATAACTAGGTTCG  21746510

Query  250       TAGTTTGAAGTCTGCTTAAGTGGCTCTCAAAGCTGTTGTAGTGCTGGATGGCATAAATTC  309
                 |||||||||||||||||||||||||||||||||||||||||||||||||||||||||| ||
Sbjct  21746511  TAGTTTGAAGTCTGCTTAAGTGGCTCTCAAAGCTGTTGTAGTGCTGGATGGCATAAACTC  21746570

Query  310       AAAGATAGTATCAGTTTCAATGATTAGTTGCATACCGACTTTATAATTGGAATTGTAAAT  369
                 ||||| |||||||||||||||||||||||||||||||||||| ||||||||||||||||
Sbjct  21746571  AAAGACAGTATCAGTTTCAATGATTAGTTGCATACCGACTTTATTATTGGAATTGTAAAT  21746630

Query  370       GGTATTTGATAGGTCCATTTCTACTACTACGACTCGTTTTTGATATCAAGGATTGCGTAA  429
                 |||||||||||||||||||||||||||||| ||||||||||||||||||||||||||||
Sbjct  21746631  GGTATTTGATAGGTCCATTTCTACTACTACTACTCGTTTTTGATATCAAGGATTGCGTAA  21746690

Query  430       GTCACACCAATTTGCATCTAGTTATATAAATATATTCCGCTAAGTGGTTCAATTCATTTT  489
                 |||||||||||||||||||||||||||| |||||||||||||||||||| ||||||||
Sbjct  21746691  GTCACACCAATTTGCATCTAGTTATATAATTATATTCCGCTAAGTGGTTCATTTCATTTT  21746750

Query  490       CTTGGTAGGTTTTGAACAGGTCACGGATTTATCCAATCCAGCTTTCCTTCCAGCAATTGG  549
                 ||||||||||||||||||||||||||||||||||||||||||||||||||||||||||||
Sbjct  21746751  CTTGGTAGGTTTTGAACAGGTCACGGATTTATCCAATCCAGCTTTCCTTCCAGCAATTGG  21746810

Query  550       AGCAAGGTTGAATTTTGGTGAGAGTCATTAAACTAATCAGCTTTGTTTGAACAAATGAGA  609
                 ||||||||||||||||||||||||||||||||||||||||||||||||||||||||||||
Sbjct  21746811  AGCAAGGTTGAATTTTGGTGAGAGTCATTAAACTAATCAGCTTTGTTTGAACAAATGAGA  21746870

Query  610       AATGAGAGCTTCCAATTCCCTTAGAAAATGTTTTGTCCTTTCAG  653
                 |||||||||||||||||| |||||||| ||||||||||||||
Sbjct  21746871  AATGAGAGCTTCCAATTCCATTAGAAAAGGTTTTGTCCTTTCAG  21746914
```

```
 Score = 1038 bits (540),  Expect = 0.0
 Identities = 621/644 (96%), Gaps = 11/644 (2%)
 Strand=Plus/Plus
```

```
Query  12        CATCATCCCTTGAGATTATTTGGAATAGTACTAT-TAGTTTACCAGATCCACCATTCATA  70
                 |||||||||||||||||||||||| ||||| ||| |||||||||||||||||||||| |
Sbjct  21731779  CATCATCCCTTGAGATTATTTGGATTAGTAATATATAGTTTACCAGATCCACCATTCACA  21731838

Query  71        TTGTACCCATTCTGATATATATACAAATTGTTGATTACAGCCATTTATATTTCTTGTGCT  130
                 ||||||   | |||||||||||||||||||||||||||||||||   ||||||||
Sbjct  21731839  TTGTAC---TCCTGATATATATACAAATTGTTGATTACAGCCATTTATA---CTTGTGCT  21731892

Query  131       TCAACACCAGCCAATTTATTTTCGGAAATTAATAGTTTGTATAAACGA-TTAACTCAGAA  189
                 |||||||||||||||||||||||||||||| |||||||||||||||| ||||||||||
Sbjct  21731893  TCAACACCAGCCAATTTATTTTCGGAAATT-ATAGTTTGTATAAACGATTTAACTCAGAA  21731951

Query  190       AATCAAATTCTGTATGACATTGACATTGGATACACGTCTATAAGACTATAACTAGGTTCG  249
                 |||||| |||||||||||||||| ||||||||||||||||||||||||||||||||||
Sbjct  21731952  AATCAATTTCTGTATGACATTGACAATGGATACACGTCTATAAGACTATAACTAGGTTCG  21732011

Query  250       TAGTTTGAAGTCTGCTTAAGTGGCTCTCAAAGCTGTTGTAGTGCTGGATGGCATAAATTC  309
                 |||||||||||||||||||||||||||||||||||||||||||||||||||||||||| ||
Sbjct  21732012  TAGTTTGAAGTCTGCTTAAGTGGCTCTCAAAGCTGTTGTAGTGCTGGATGGCATAAA-TC  21732070

Query  310       AAAGATAGTATCAGTTTCAATGATTAGTTGCATACCGACTTTATAATTGGAATTGTAAAT  369
                 ||||| |||||||||||||||||||||||||||||||||||| ||||||||||||||||
Sbjct  21732071  AAAGACAGTATCAGTTTCAATGATTAGTTGCATACCGACTTTAT-ATTGGAATTGTAAAT  21732129

Query  370       GGTATTTGATAGGTCCATTTCTACTACTACGACTCGTTTTTGATATCAAGGATTGCGTAA  429
                 |||||||||||||||||||||||||||||| ||||||||||||||||||||||||||||
Sbjct  21732130  GGTATTTGATAGGTCCATTTCTACTACTACTACTCGTTTTTGATATCAAGGATTGCGTAA  21732189

Query  430       GTCACACCAATTTGCATCTAGTTATATAAATATATTCCGCTAAGTGGTTCAATTCATTTT  489
                 |||||||||||||||||||||||||||| |||||||||||||||||||| ||||||||
Sbjct  21732190  GTCACACCAATTTGCATCTAGTTATATAATTATATTCCGCTAAGTGGTTCATTTCATTTT  21732249

Query  490       CTTGGTAGGTTTTGAACAGGTCACGGATTTATCCAATCCAGCTTTCCTTCCAGCAATTGG  549
                 ||||||||||||||||||||||||||||||||||||||||||||||||||||||||||||
Sbjct  21732250  CTTGGTAGGTTTTGAACAGGTCACGGATTTATCCAATCCAGCTTTCCTTCCAGCAATTGG  21732309
```

```
Query  550       AGCAAGGTTGAATTTTGGTGAGAGTCATTAAACTAATCAGCTTTGTTTGAACAAATGAGA  609
                 ||||||||||||||||||||||||||||||||||||||||||||||||||||||||||||
Sbjct  21732310  AGCAAGGTTGAATTTTGGTGAGAGTCATTAAACTAATCAGCTTTGTTTGAACAAATGAGA  21732369

Query  610       AATGAGAGCTTCCAATTCCCTTAGAAAATGTTTTGTCCTTTCAG  653
                 |||||||||||||||||| ||||||||| ||||||||||||||
Sbjct  21732370  AATGAGAGCTTCCAATTCCATTAGAAAAGGTTTTGTCCTTTCAG  21732413



> Fvb2-1
Length=26582685

 Score = 994 bits (517),  Expect = 0.0
 Identities = 617/657 (94%), Gaps = 15/657 (2%)
 Strand=Plus/Minus

Query  12        CATCATCCCTTGAGATTATTTGGAATAGTACTAT-TAGTTTACCAGATCCACCATTCATA  70
                 ||||||||||||| ||||||||| || || ||| ||||||||||||||||||||||| |
Sbjct  16468895  CATCATCCCTTGAGTTTATTTGGATTACTAATATATAGTTTACCAGATCCACCATTCACA  16468836

Query  71        TTGTACCCATTCTGATATATATACAAATTGTTGATTACAGCCATTTATATTTCTTGTGCT  130
                 |||||| ||||||||| ||||||||||||||||||||||||||||||||| |||||||
Sbjct  16468835  TTGTACTCATTCTGATGTATATACAAATTGTTGATTACAGCCATTTATATTTTTTGTGCT  16468776

Query  131       TCAACACCAGCCAATTTATTTTCGGAAATTAATAGTTTGTATAAACGATT-AACTCAGAA  189
                 ||||||||| ||| ||||||||||||||||||||||||||||||||| |||||||||
Sbjct  16468775  TCAACACCAACCAGTTTATTTTCGGAAATTAATAGTTTGTATAAACGATTTAACTCAGAA  16468716

Query  190       AATCAAATTCTGTATGACATTGACATTGGATACACGTCTATAA-------GACTATAACT  242
                 |||||||||||||||||||||||| ||||||||||||||||       ||||||||||
Sbjct  16468715  AATCAAATTCTGTATGACATTGACAATGGATACACGTCTATAATTTACAAGACTATAACT  16468656

Query  243       AGGTTCGTAGTTTGAAGTCTGCTTAAGTGGCTCTCAAAGCTGTTGTAGTGCTGGATGGCA  302
                 |||||| ||||||||||||||||||||||||||||||||||||||||||||||||||||
Sbjct  16468655  AGGTTCATAGTTTGAAGTCTGCTTAAGTGGCTCTCAAAGCTGTTGTAGTGCTGGATGGCA  16468596

Query  303       TAAATTCAAAGATAGTATCAGTTTCAATGATTAGTTGCATACCGACTTTATAATTGGAAT  362
                 ||||||||| ||||||||||||||||||||||||||||||||||||||||||||||||||
Sbjct  16468595  TAAATTCAACGATAGTATCAGTTTCAATGATTAGTTGCATACCGACTTTATAATTGGAAT  16468536

Query  363       TGTAAATGGTATTTGATAGGTCCATTTCTACTACTAC------GACTCGTTTTTGATATC  416
                 |||||||||||||||||||||| ||||||||||||       |||||||||| |||||
Sbjct  16468535  TGTAAATGGTATTTGATAGGTCCGTTTCTACTACTACTACTACTCGTTTTTTATATC  16468476

Query  417       AAGGATTGCGTAAGTCACACCAATTTGCATCTAGTTATATAAATATATTCCGCTAAGTGG  476
                 |||||||||| |||||||||||||||||||||||||| ||| ||||||||||||||||||
Sbjct  16468475  AAGGATTGCGCAAGTCACACCAATTTGCATCTAGTTATTTAATTATATTCCGCTAAGTGG  16468416

Query  477       TTCAATTCATTTTCTTGGTAGGTTTTGAACAGGTCACGGATTTATCCAATCCAGCTTTCC  536
                 |||| ||||||||||||||||||||||||||||||||||||||||||||||||||||||
Sbjct  16468415  TTCATTTCATTTTCTTGGTAGGTTTTGAACAGGTCACGGATTTATCCAATCCAGCTTTCC  16468356

Query  537       TTCCAGCAATTGGAGCAAGGTTGAATTTTGGTGAGAGTCATTAAACTAATCAGCTTTGTT  596
                 |||||||||||||||||||||||||||||||||| ||||||||||||||||||||||||
Sbjct  16468355  TTCCAGCAATTGGAGCAAGGTTGAATTTTGGTGAGAATCATTAAACTAATCAGCTTTGTT  16468296

Query  597       TGAACAAATGAGAAATGAGAGCTTCCAATTCCCTTAGAAAATGTTTTGTCCTTTCAG  653
                 |||||||||||||| ||| |||||||||||||| |||||||| ||||||||||||||||
Sbjct  16468295  TGAACAAATGAGAACTGATAGCTTCCAATTCCATTAGAAAAGGTTTTGTCCTTTCAG  16468239
```

```
> Fvb2-3
Length=24073015

 Score = 529 bits (275),  Expect = 2e-148
 Identities = 299/311 (96%), Gaps = 0/311 (0%)
 Strand=Plus/Minus

Query  343      ACCGACTTTATAATTGGAATTGTAAATGGTATTTGATAGGTCCATTTCTACTACTACGAC  402
                |||||  ||||||||||||||||||||||||||||||||||||||||||||||||| ||
Sbjct  8334398  ACCGATTTTATAATTGGAATTGTAAATGGTATTTGATAGGTCCATTTCTACTACTACTAC  8334339

Query  403      TCGTTTTTGATATCAAGGATTGCGTAAGTCACACCAATTTGCATCTAGTTATATAAATAT  462
                | |||||||||||||||||||| ||||||||||||||||||||||||||||||| |||
Sbjct  8334338  TAGTTTTTGATATCAAGGATTGCGCAAGTCACACCAATTTGCATCTAGTTATATAATTAT  8334279

Query  463      ATTCCGCTAAGTGGTTCAATTCATTTTCTTGGTAGGTTTTGAACAGGTCACGGATTTATC  522
                |||||  ||||||||||||  ||||||||||||||||||||||||||||||||||||||
Sbjct  8334278  ATTCCACTAAGTGGTTCATTTCATTTTCTTGGTAGGTTTTGAACAGGTCACGGATTTATC  8334219

Query  523      CAATCCAGCTTTCCTTCCAGCAATTGGAGCAAGGTTGAATTTTGGTGAGAGTCATTAAAC  582
                ||||||||||||||||||||||||||||||||||||||||||||||||| |||||||||
Sbjct  8334218  CAATCCAGCTTTCCTTCCAGCAATTGGAGCAAGGTTGAATTTTGGTGAGAATCATTAAAC  8334159

Query  583      TAATCAGCTTTGTTTGAACAAATGAGAAATGAGAGCTTCCAATTCCCTTAGAAAATGTTT  642
                |||||||||||||||||||||||||||||||||||||||||| |||| |||||||| ||||
Sbjct  8334158  TAATCAGCTTTGTTTGAACAAATGAGAAATGAGAGCTTCCACTTCCATTAGAAAAGGTTT  8334099

Query  643      TGTCCTTTCAG  653
                ||||||| |||
Sbjct  8334098  TGTCCTTCCAG  8334088

 Score = 410 bits (213),  Expect = 2e-112
 Identities = 281/305 (92%), Gaps = 12/305 (4%)
 Strand=Plus/Minus

Query  12       CATCATCCCTTGAGATTATTTGGAATAGTACTAT-TAGTTTACCAGATCCACCATTCATA  70
                |||||||||||||| ||||||||| || || ||| ||||||||||||||||||||||||
Sbjct  8334692  CATCATCCCTTGAGTTTATTTGGATTACTAATATATAGTTTACCAGATCCACCATTCACG  8334633

Query  71       TTGTACCCATTCTGATATATATACAAATTGTTGATTACAGCCATTTATATTTCTTGTGCT  130
                ||||||  ||||||||| ||||||||||||||||||||||||||||||||  |||||||
Sbjct  8334632  TTGTACTCATTCTGATGTATATACAAATTGTTGATTACAGCCATTTATATTTTTTGTGCT  8334573

Query  131      TCAACACCAGCCAATTTATTTTCGGAAATTAATAGTTTGTATAAACGATT-AACTCAGAA  189
                |||||||||||||  ||||||||||||||||||||||||||||||||||  |||||||||
Sbjct  8334572  TCAACACCAGCCAGTTTATTTTCGGAAATTAATAGTTTGTATAAACGATTTAACTCAGAA  8334513

Query  190      AATCAAATTCTGTATGACATTGACATTGGATACACGTCTATAAGACTATAACTAGGTTCG  249
                |||||||||||||||||||||||||    || |||      ||||||||||||||||||
Sbjct  8334512  AATCAAATTCTGTATGACATTGACA----ATTCAC------AAGACTATAACTAGGTTCA  8334463

Query  250      TAGTTTGAAGTCTGCTTAAGTGGCTCTCAAAGCTGTTGTAGTGCTGGATGGCATAAATTC  309
                ||||||||||||||||||||||||||||||||||||||||||||||||||||||||||||
Sbjct  8334462  TAGTTTGAAGTCTGCTTAAGTGGCTCTCAAAGCTGTTGTAGTGCTGGATGGCATAAATTC  8334403
```

Supplementary Figure S2. *FaRALF3-1* putative promoter sequence alignment in different *Fragaria x ananassa* variaties. It was considered *Fragaria x ananassa cv. Florida Elyana from Florida (U.S.A)*, the Italian variety *cv.Alba* and the sequenced *cv. Camarosa (v1.0.a1).*

```
Elyana_Fv               CATCATCCCTTGAGATTATTTGGAATAGTACTATTAGTTTACCAGATCCACCATTCATAT 60
Camarosa_Fve_v1.0.a1    CATCATCCCTTGAGATTATTTGGAATAGTACTATTAGTTTACCAGATCCACCATTCATAT 60
Alba_Fv                 CATCATCCCTTGAGATTATTTGGAATAGTACTATTAGTTTACCAGATCCACCATTCATAT 60
                        ************************************************************

Elyana_Fv               TGTACCCATTCTGATATATATACAAATTGTTGATTACAGCCATTTATATTTCTTGTGCTT 120
Camarosa_Fve_v1.0.a1    TGTACCCATTCTGATATATATACAAATTGTTGATTACAGCCATTTATATTTCTTGTGCTT 120
Alba_Fv                 TGTACCCATTCTGATATATATACAAATTGTTGATTACAGCCATTTATATTTCTTGTGCTT 120
                        ************************************************************

Elyana_Fv               CAACACCAGCCAATTTATTTTCGGAAATTAATAGTTTGTATAAACGATTAACTCAGAAAA 180
Camarosa_Fve_v1.0.a1    CAACACCAGCCAATTTATTTTCGGAAATTAATAGTTTGTATAAACGATTAACTCAGAAAA 180
Alba_Fv                 CAACACCAGCCAATTTATTTTCGGAAATTAATAGTTTGTATAAACGATTAACTCAGAAAA 180
                        ************************************************************

Elyana_Fv               TCAAATTCTGTATGACATTGACATTGGATACACGTCTATAAGACTATAACTAGGTTCGTA 240
Camarosa_Fve_v1.0.a1    TCAAATTCTGTATGACATTGACATTGGATACACGTCTATAAGACTATAACTAGGTTCGTA 240
Alba_Fv                 TCAAATTCTGTATGACATTGACATTGGATACACGTCTATAAGACTATAACTAGGTTCGTA 240
                        ************************************************************

Elyana_Fv               GTTTGAAGTCTGCTTAAGTGGCTCTCAAAGCTGTTGTAGTGCTGGATGGCATAAATTCAA 300
Camarosa_Fve_v1.0.a1    GTTTGAAGTCTGCTTAAGTGGCTCTCAAAGCTGTTGTAGTGCTGGATGGCATAAATTCAA 300
Alba_Fv                 GTTTGAAGTCTGCTTAAGTGGCTCTCAAAGCTGTTGTAGTGCTGGATGGCATAAATTCAA 300
                        ************************************************************

Elyana_Fv               AGATAGTATCAGTTTCAATGATTAGTTGCATACCGACTTTATAATTGGAATTGTAAATGG 360
Camarosa_Fve_v1.0.a1    AGATAGTATCAGTTTCAATGATTAGTTGCATACCGACTTTATAATTGGAATTGTAAATGG 360
Alba_Fv                 AGATAGTATCAGTTTCAATGATTAGTTGCATACCGACTTTATAATTGGAATTGTAAATGG 360
                        ************************************************************

Elyana_Fv               TATTTGATAGGTCCATTTCTACTACTACGACTCGTTTTTGATATCAAGGATTGCGTAAGT 420
Camarosa_Fve_v1.0.a1    TATTTGATAGGTCCATTTCTACTACTACGACTCGTTTTTGATATCAAGGATTGCGTAAGT 420
Alba_Fv                 TATTTGATAGGTCCATTTCTACTACTACGACTCGTTTTTGATATCAAGGATTGCGTAAGT 420
                        ************************************************************

Elyana_Fv               CACACCAATTTGCATCTAGTTATATAAATATATTCCGCTAAGTGGTTCAATTCATTTTCT 480
Camarosa_Fve_v1.0.a1    CACACCAATTTGCATCTAGTTATATAAATATATTCCGCTAAGTGGTTCAATTCATTTTCT 480
Alba_Fv                 CACACCAATTTGCATCTAGTTATATAAATATATTCCGCTAAGTGGTTCAATTCATTTTCT 480
                        ************************************************************

Elyana_Fv               TGGTAGGTTTTGAACAGGTCACGGATTTATCCAATCCAGCTTTCCTTCCAGCAATTGGAG 540
Camarosa_Fve_v1.0.a1    TGGTAGGTTTTGAACAGGTCACGGATTTATCCAATCCAGCTTTCCTTCCAGCAATTGGAG 540
Alba_Fv                 TGGTAGGTTTTGAACAGGTCACGGATTTATCCAATCCAGCTTTCCTTCCAGCAATTGGAG 540
                        ************************************************************

Elyana_Fv               CAAGGTTGAATTTTGGTGAGAGTCATTAAACTAATCAGCTTTGTTTGAACAAATGAGAAA 600
Camarosa_Fve_v1.0.a1    CAAGGTTGAATTTTGGTGAGAGTCATTAAACTAATCAGCTTTGTTTGAACAAATGAGAAA 600
Alba_Fv                 CAAGGTTGAATTTTGGTGAGAGTCATTAAACTAATCAGCTTTGTTTGAACAAATGAGAAA 600
                        ************************************************************

Elyana_Fv               TGAGAGCTTCCAATTCCCTTAGAAAATGTTTTGTCCTGTCAG------------------ 642
Camarosa_Fve_v1.0.a1    TGAGAGCTTCCAATTCCCTTAGAAAATGTTTTGTCCTGTCAG------------------ 642
Alba_Fv                 TGAGAGCTTCCAATTCCCTTAGAAAATGTTTTGTCCTTTCAGAATCACTAGTGAATTCGC 660
                        ************************************ ****

Elyana_Fv               ------------------------------------------------------------ 642
Camarosa_Fve_v1.0.a1    ------------------------------------------------------------ 642
Alba_Fv                 GGCCGCCTGCAGGTCGACCATATGGGAGAGCTCCCAACGCGTTGGATGCATAGCTTGAGT 720


Elyana_Fv               ----------  642
Camarosa_Fve_v1.0.a1     ----------  642
Alba_Fv                 ATTCTATAGT  730
```

Supplementary Figure S3. Map of pKGWFS7 plasmid used for promoter reporter assay. Sm/Spr, spectinomycin resistance. Kan, kanamycin resistance. FvRALF3 promoter, T6,T4,T2, empty or 2x35S promoter according to experimental procedure. eFGPand GUS, chimera reporter gene formed by eGFP and β-glucoronidase ORFs in frame. T35S, terminator.

6. FaRALF3 and FaMRLK47 proteins purification from *E. coli*

6.1 Acknowledgments

The analyses and the results presented in this chapter were conducted at the Biochemistry Department of the University of Cambridge (Sanger Building , 80 Tennis Court Road, Cambridge, CB2 1GA, United Kingdom) thanks to the supervision and kindly support of Dr. Marko Hyvönen. The research project was supported by European Molecular Biology Organization (EMBO) short fellowship program number 7779.

6.2 Introduction

RALF peptides bind to the *Catharanthus roseus* Receptor Like Kinases 1 - like family protein (CrRLK1L), characterized by two tandem malectin-like motif in the extracellular domain and known to be involved in cell expansion and reproduction throughout the plant kingdom (Galindo-Trigo *et al.,* 2016)(Galindo-Trigo et al., 2016). The large CrRLK1L receptor family includes FERONIA (FER) receptors, previously reported to interact with *Arabidopsis RALF1* and *RALF23* (Haruta *et al.*, 2014(Haruta et al., 2014; Stegmann et al., 2017)Stegmann et al., 2017) inhibiting the formation of the complex between the immune receptor kinases EF-TU RECEPTOR (EFR) and FLAGELLIN-SENSING 2 (FLS2) and their co-receptor BRASSINOSTEROID INSENSITIVE 1–ASSOCIATED KINASE 1 (BAK1), which is necessary to initiate immune signalling.

FERONIA and RALF are able to modulate different signalling pathways, functioning as a critical hub of perception and transmission of different plant cell growth and defence stimuli. This functional promiscuity makes it difficult to understand how various environmental stimuli are translated into cellular response through FERONIA at molecular level. The number of reports on the role of RALF – FERONIA signalling in plant development and immunity has increased dramatically during last years, and two crystal structures of the extracellular domains of Feronia homologs have been reported recently (Moussu et al., 2018) (Minkoff et al., 2017), however the structural bases of their interaction with RALFs are still to be elucidated. Knowledge of the structure of these two signalling components and on the way they bind each other is fundamental to understand activation of key signalling pathways through FERONIA and to elucidate the determinants the specificity in the interaction specificity between different RALFs and MRLKs.

Previous transcriptome analysis of strawberry (*Fragaria X ananassa*) fruit showed that a RALF gene homologue to *a Arabidopsis RALF33* is strongly upregulated upon interaction with a fungal pathogen Colletotrichum acutatum (Gudarelli et al., 2011), suggesting that expression of this gene is deployed by the pathogen to activate virulence factors. Furthermore, the analyses presented in the chapters above showed that among the fruit *FaRALF* genes in strawberry only one, FaRALF3, is induced by pathogen interaction at ed fruit stages. On the other hand, among the 60 strawberry MRLK receptors, of which 15 expressed during fruit ripening (Zhang et al., 2016)(Zhang et al., 2016), a FERONIA homolog, FaMLRK47, is the most expressed in red strawberry fruit, possibly acting as *FaRALF3* receptor.

In order to understand how signalling through FERONIA and RALF works and the biological role of the specificity of different RALF-FERONIA interactions, it is important to understand how these proteins interact and to reveal the key structural elements underneath.

The aim of this study was to produce active and folded FaRALF3 and FaMRLK47 by their expression in *Escherichia coli* and to analyse the interaction of the different RALF and FERONIA extracellular domain constructs using various biochemical and biophysical methods. To do this, different constructs of both RALF (in its mature and pre-forms) and of extracellular domain (itself composed of two domains,) were produced in order to identify the most suitable constructs for subsequent interaction analyses.

6.3 Materials and Methods

6.3.1 Heterologous protein expression constructs design and cloning

Predicted extracellular domain of *F. vesca* FERONIA homolog (*FvMRLK47*, XP_004302537) and pre-mature peptide of *FvRALF3* sequences were optimized for *E. coli* heterologous expression and chemically synthesized (Eurofins Genomincs) (Fig.6.1A, Fig.6.2B). Overall seven constructs for FvMRLK47 extracellular domain (EC) expression were developed, namely three different lengths forms of whole FvMRLK47-EC domain (1. 47 EC-1; 2.47 EC-2; 3. 47 EC-3), the N-terminal Malectin like domain (4. 47 MLN-1) and three lengths forms of C-terminal Malectin like domain (5. 47 MLC-1, 6.47 MLC-2, 7. 47 MLC-2) (Fig.6.1A,B). Inserts were PCR amplified from the synthetic sequence using primers listed in Fig.6.1B. For FvRALF3 expression three constructs comprising the premature RALF peptide or the mature peptide with or without the TEV protease cleavage site were amplified using primer listed in Fig.6.2. FvMRLK47 and FvRALF amplicons and pHAT2 destination vector were all digested with BamHI and HindIII (Promega) and dephosphorilated using Thermosensitive Alkaline Phosphatase TSAP (Promega) following manufacturer protocol. Restriction reactions were then loaded on 1% Agarose gel and expected lenghts bands were excised and purified using QIAGEN Gel Extraction Kit. Ligation reaction between different inserts and pHAT2 vector were then performed using Quick Ligase (NEB) following manufacturer protocol. Ligation reactions were used to transform chemically competent *E. coli DH5α.* Transformed cells were then plated on LB agar with ampicillin 100 µg/mL (amp) and resistant colonies were verified by colony PCR using primers listed in Fig.6.1B and Fig.6.2b. Positive colonies were grown in LB amp overnight and DNA was extracted using QIAGEN Plasmid mini extraction kit. Correct insertion and ligation were then certified by sequencing using primers 5'-AATACGACTCACTATAGGG-3' and 5'- CATACGATTTAGGTGACACTATAG-3'.

A

NYIPSDKIFLNCGGPQESTDADGQKWTSDVGSKFASGANSTTSPAATQ
DPSVPETPFMTARVFHSDYTYKFPVASGRIFVRLSFYPASYAGLNASGA
VFSVMVESYTVLKNFSVVQTTEALDYAFVTKEFVVNVEGESLDVTFKP
SSSVPNAYAFVNGIEVVSMPDIYSSTDGTTMIVGQSSPFYIDNSTALEN
VYRLNVGGNDISPSKDTGLLRSWYDDTAYLFGAAFGVPEFADGNMSI
AYPKDMPTYVAPEDVYKTARSMGPNNNINLNYNLTWVFSIDSGFMY
LVRLHFCEVAANITKLNQRVFDIYLNNQTAESGFDVAGITQGNGIPLYK
DYVVMVPNGSPQEDLWLALHPNPSTKPQWYDAILNGVEIFKINDTTG
NLGGPNPIPRPKQLNIDPSKAR

B

Construct ID	Primer For	Primer Rev
1) MRLK47-EC-1	tataggatccaattacatcccatctgataaaatc	tataaagcttaagtatcattgatcttgaagatctc
2) MRLK47-EC-2	tataggatccaattacatcccatctgataaaatc	tataaagcttagggacggggaataggattaggccc
3) MRLK47-EC-3	tataggatccaattacatcccatctgataaaatc	tataaagcttatctagccttagatggatcaatgtt
4) N-MLD-1	tataggatccaattacatcccatctgataaaatc	tataaagcttaaatatagaaaggacttgattgccc
5) C-MLD-1	tataggatccgataatagtacagcgctggagaat	tataaagcttaagtatcattgatcttgaagatctc
6) C-MLD-2	tataggatccgataatagtacagcgctggagaat	tataaagcttagggacggggaataggattaggccc
7) C-MLD-3	tataggatccgataatagtacagcgctggagaat	tataaagcttatctagccttagatggatcaatgtt

Figure 6.1. FvMRLK47-EC expression constructs design. a) FvMRLK47-EC sequence. In red is highlighted the first residue predicted to belong to the extracellular domain; in blue are highlighted the last residues included in respectively constructs 1)and 5), 2) and 6), 3) and 7). In green are showed the last residues included in the N-terminal Malectin-like domain construct (47-MLN 1) and the first included in The C-terminal Malectin-like domain constructs (47 MLC-1, 47 MLC-2, 47 MLC-3). b) In the table are listed the FvMRLK47-EC expression constructs developed, identified by progressive numbers (Construct ID), and primers (Primer For, Primer Rev) used to amplify by PCR.

A

GSDHGLSFVPAKSRCQGSIAECMAEDEFDMDSEINRRIL
ATTKYISYGALQRNTVPCSQRGASYYNCKPGAQANPYNRGCSAITRCRS

B

Construct ID	Primer For	Primer Rev
1) RALF-PM	tataggatccgatcacgggttgagctttgttccg	tataaagctttcaactacggcagcgagtgatggc
2) RALF-M-TEV	tataactagtaagtcgacagaaaacctgtacttccag gccaccacaaagtacatcagc	tataaagctttcaactacggcagcgagtgatggc
3) RALF-M	tataggatccgccaccacaaagtacatcagctat	tataaagctttcaactacggcagcgagtgatggc

Figure 6.2. FvRALF3 expression constructs design. a) FvRALF3 premature and mature sequence peptide. In red are indicated first residues included in the premature (G) and mature (ATTK) constructs, in green are represented conserved motif recognized and cleaved by S1P protease, in blue are highlighted the last residues. b) The table lists, construct identification name (Construct ID) and primers used to amplify sequences to insert in the expression constructs.

6.2.2. Protein expression and solubility test

To test protein expression and protein solubility in *E.coli,* the seven FvMRLK47 and the three FvRALF constructs were used to transform *E. coli* strain *Rosetta.* Transformed cells were plated on LB amp and one colony for each construct was grown in 2 mL of LB amp for 3 hours at 37°C with shaking (200 rpm). Cultures were induced with isopropyl-thiogalactopyranoside IPTG (400 µM) and grown at 37°C for 3 hours or at 15°C overnight, to test expression and protein solubility. Cells were then collected by centrifugation for 1 min at maximum speed from 500 µl of colture. Pellet cells were then broken adding 1/10 volume of BugBuster Reagent (Novagen) and 0.3µl of Lysonase™ and incubated 15 minutes at room temperature. Cell lysate was then centrifugated for 3 minutes at maximum speed and soluble fraction was isolated from the pellet. Pellet was then resuspended again in dilued BugBuster reagent (1:5). Soluble and insoluble fractions were then loaded on SDS-PAGE gel with negative control (*E.coli Rosetta* cells transformed with empty vector).

6.2.3 Refolding test from inclusion bodies in small scale

Refolding test was performed in small scale for 47-EC-1, 47-EC-3, RALF-PM and RALF-M-TEV proteins. Cell pellet from 50 ml of culture was resuspended in 4 mL of BugBuster® with 1/1000 volume of Lysonase™ and incubated at room temperature for 15 minutes. Cell lysate was collected by centrifugation in microcentrifuge for three minutes and resuspended in 50 mM Tris-HCl pH 8.0, 5 mM EDTA, 10 mm DTT, 0.5% Triton. Insoluble cell fraction was then collected by centrifugation and pellet was washed once with 50 mM Tris-HCl pH 8.0, 5 mM EDTA, 1 M NaCl, 10 mm DTT, once with 50 mM Tris-HCl pH 8.0, 5 mM EDTA, 10 mm DTT and finally resuspended 100 mM TCEP pH 7.0, adding 8 M GndHCl, 50 mM Tris pH 8.0, 10 mM EDTA solution to final GndHCl concentration of 6 M. Resuspended inclusion bodies were then incubated for 20 minutes and buffer exchanged with 6 M Urea, 20mMHCl solution using PD-10 columns. Protein refolding test in small scale was performed in a final volume of 2 mL using a set of 24 different refolding solutions (developed by Dr. Katharina Revn). Briefly, 200 µl of solubilzed and denaturated inclusion bodies in 6M Urea were added to 900 µl mq H_2O, 900 µl of refolding solution 2X (or 1,8

mL for solution number 19 Tab.6.1), 2 µl of cysteine 2 M and 2 of µl of 0.2 M cystine and incubated at 4°C for 72 hours.

No	Buffer	pH	Additive 1	Additive 2
1	Sodium phosphate	7.5		
2	Tris	8.0		
3	Tris	8.5		
4	Tris	9.0		
5	CHES	9.5		
6	CAPS	10.0		
7	Sodium phosphate	7.5	NaCL	
8	Tris	8.0	NaCL	
9	Tris	8.5	NaCL	
10	Tris	9.0	NaCL	
11	CHES	9.5	NaCL	
12	CAPS	10.0	NaCL	
13	Sodium phosphate	7.5		PPS
14	Tris	8.0		PPS
15	Tris	8.5		PPS
16	Tris	9.0		PPS
17	CHES	9.5		PPS
18	CAPS	10.0		PPS
19	Sodium phosphate	7.5	NaCL	PPS
20	Tris	8.0	NaCL	PPS
21	Tris	8.5	NaCL	PPS
22	Tris	9.0	NaCL	PPS
23	CHES	9.5	NaCL	PPS
24	CAPS	10.0	NaCL	PPS

Table 6.1. Refolding solutions used for refolding test. Solutions are listed and numbered from 1 to 24. Buffer, pH and additives are indicated. All Buffers, except for number 19 (in red) are 200mM Buffer, 1 M NaCl (if present) and 2M PPS (if present) and concentrated 2x. Refolding solution number 19 is 111.1 mM Sodium phosphate, 0.55 M NaCl, 1.11 PPS. Different colors distinguish four sets of buffers according to the presence of one, two or no additives.

6.2.4 FERONIA Ion exchange chromatography in small scale

For small scale refolding ion exchange chromatography, 2 mL of proteins in refolding solutions (100mM Tris pH 8.0 with and without PPS and 100mM CAPS pH10.0 with and without PPS) were loaded into 1 mL Hi-Trap Q Column (GE Healthcare) and eluted with 1M NaCl gradient using ÄCTA system (GE healthcare Life Sciences). Eluted fractions were collected and loaded on SDS-PAGE gel.

6.2.5 FERONIA inclusion bodies isolation, refolding and chromatography in large scale

Cells thawed from glycerol stock, were grown on LB agar amp plates at 37°C overnight. Cells were then collected from starter culture, rubbing a loop on the plate, and grown in 1 L of 2YT amp at 37°C with rotation (200 rpm) until OD_{600} reached 0.8. Expression was induced with IPTG (400 µM)
for 3 hours at 37°C. Cells were then collected by centrifugation at 4200 rpm for 15 minutes, resuspended in 50mM Tris HCl pH 8.0, 2mM EDTA, 10 mM DTT and cell lysis were performed using Emulsiflex. Dnase (400 u) and MgCl2 (4mM) were added to cell lysate and incubated for 20 minutes at room temperature in rotation. Insoluble fraction was then isolated by centrifugation for 40 minutes at 15 000 rpm at 4°C. Inclusion body pellet was then isolated and resuspended by sonication in 50mM Tris HCl pH 8.0, 2mM EDTA, 10mM DTT, 0.5% Triton x-100. Inclusion bodies were then isolated again by centrifugation at 15 000 rpm for 20 minutes at 4°C and washed once with salt solution (50mM Tris HCl pH8.0, 2mM EDTA, 10mM DTT, 1M NaCl) and once with 50mM Tris HCl pH8.0, 2mM EDTA, 10mM DTT. Isolated inclusion bodies were then resuspended in 5mL of TCEP (100mM) and with 8M GndHCl, 50 mM, Tris HCl pH 8.0, 0.5 mM EDTA up to 20 mL. Solubilzed inclusion bodies were incubated with the solution for 20 minutes at room temperature and then buffer exchanged with 6M Urea 20mM HCl using HiPrep™ 26/10. Finally, 50 mL of solubilized inclusion bodies were added to Refolding solution (100mM Tris HCl pH8.0) up to 500mL volume with cysteine (20mM) and cystine (2mM) and incubated at 4°C for two days. A small sample of refolded solutions were loaded on SDS-PAGE and an ion exchange chromatography was performed leading 140 mL of protein in refolding solution into a 5 mL Hi-trap Q column.

6.2.6 RALF-M-TEV purification from Large Scale Refolding

Inclusion bodies derived from RALF-M-TEV expression were produced and purified as described above for FERONIA. Large scale refolding was performed incubating solubilized inclusion bodies in 500 mL of 100 mM CAPS pH 10.0 at 4°C for 11 days. Protein refolding solution was loaded on XW Source RPC 5mL (GE Healthcare) for Reverse Phase

Chromatography purification using 10% Acetonitrile, 0,1% TFA to equilibrate the column and 90% Acetonitrile, 0,10 % TFA to elute. Elutions fractions were loaded onto SDS-PAGE gel and fraction containing expected molecular weight protein was loaded on a C8-RPC Column for Reverse Phase Chromatography purification. Elution fractions were then loaded again on SDS-PAGE gel.

6.2.7 Soluble-tags proteins expression constructs cloning using sequence and ligation independent cloning (SLIC)

For soluble proteins expression in *E. coli,* new FERONIA (47-EC-3) and RALF mature peptide (RALF-M) constructs were created cloning soluble expressed protein tags, as it is listed in Table 6.2 and Table 6.3. Multiple FERONIA and RALF-M constructs were created with SLIC technique (M. Z. Li & Elledge, 2007)(M. Z. Li & Elledge, 2007) using pOP vectors and customized pEXP vectors (Fig.6.3) developed by Dr. Aleksei Lulla and available in the lab (Dr. Marko Hyvonen lab group, Department of Biochemistry, University of Cambridge). Briefly, for FERONIA cloning, 47-EC-3 DNA sequence was amplified with Phusion® High-Fidelity DNA-Polymerase using primers For 5'-GAAAACCTGTACTTCCAGGGATCCAATTACATCCCATCTGATAAAATC-3' and Rev 5'-CACTATAGAATACTCAAGCTTATCTAGCCTTAGATGGATCAATGTTC-3', with two steps annealing PCR program : 98°C x30s, (98°C x 10s, 58°C x 30s, 72°C x 80s) x 20 cycles, (98°C x 10s, 65°C x 30s, 72°C x 80s) x 15 cycles, 72°C x 10 min. RALF mature peptide (RALF-M) was amplified from RALF-PM sequence using primers For 5'-GAAAACCTGTACTTCCAGGGTTCTGCCACCACAAAGTACATCAGCTATGG-3' and Rev 5'-CACTATAGAATACTCAAGCTTAACTACGGCAGCGAGTGATGGCACTAC-3' for pEXP vectors cloning (N-terminal His-tag Fig.6.3A) and with primer Rev 5'-GTGATGGTGATGAGGGCTCGAGCCACTACGGCAGCGAGTGATGGCACTAC-3' for pOP5 vector cloning (periplasmic signal sequence and C-terminal His-tag Fig.6.3B) using with two steps annealing PCR program : 98°C x30s, (98°C x 10s, 59°C x 30s, 72°C x 30s) x 20 cycles, (98°C x 10s, 66°C x 30s, 72°C x 30s) x 15 cycles, 72°C x 10 min. PCR product was loaded on Agarose 1% gel and band purified from gel using GeneJet Gel extraction kit (Thermo Scientific). pEXP and pOP5 vectors were disgested with Bsa I and Hind III, and dephosphorylated with Shrimp Alkaline Phosphatase (SAP). Insert and vector was combined with T4 DNA polymerase (NEB) following

manufacturer protocol, incubated 5 min at room temperature and reaction was stopped with 0.5 µl of 100mM dGTP. Then reactions were incubated 1min at room temperature, 5 min at 65°C, 10 min at room temperature and finally used to transform competent *E. Coli T7 express* cells (NEB). Trasformed cells were then plated on LB amp agar, grown overnight at 37°C and Colony PCR was performed to verify cloning.

	Soluble fusion protein	Construct tags	Vector
1	x	His-TEV-FER	pEXP
2	T7 epitope protein *(T7 bacteriophage)*	T7-tag-His-TEV-FER	pEXP
3	Chain A, Immunoglobulin G-binding protein (*Streptococcus sp.*)	His-GB1-TEV-FER	pEXP
4	2-oxo acid dehydrogenase subunit E2 (*Geobacillus lituanicus*)	His-Lipo-TEV-FER	pEXP
5	SUMO-tag	His-SUMO-TEV-FER	pEXP
6	Thioredoxin (*Escherichia coli*)	His-Trx-TEV-FER	pEXP
7	Translation initiation factor IF-2 (*Escherichia coli*)	His-IF2-TEV-FER	pEXP
8	Elongation factor Ts (*Escherichia coli*)	His-Tsf-TEV-FER	pEXP
9	Beta-lactamase precursor *(Chromohalobacter sp. 560)*	His-Bla-TEV-FER	pEXP
10	Maltose-binding periplasmic protein (*Escherichia coli*)	His-MBP-TEV-FER	pEXP
11	transcription termination/antitermination protein NusA (*Escherichia coli*)	His-NusA-TEV-FER	pEXP
12	Trigger factor (*Escherichia coli*)	His-TF-TEV-FER	pEXP

Table 6.2. Soluble protein tags used to create FERONIA constructs with SLIC. In the table are listed and numbered (1-12) proteins cloned at 47-EC-3 N-terminal soluble tags (Soluble fusion proteins). Additional tags are also reported (Construct tags) where His indicates 8x Histidine tag, TEV indicates *Tobacco Etch Virus* protease cleavage site, FER indicates 47-EC-3 protein coding sequence position in the construct.

	Soluble fusion protein	Construct tags		Vector
1	Chain A, Immunoglobulin G-binding protein (*Streptococcus sp.*)	His-GB1-TEV-RALF	C	pEXP
2	Thiol Disulfide Oxidoreductase A (*E. Coli)*	His-DsbA-TEV-RALF	C	pEXP
3	Thiol Disulfide Oxidoreductase C (*E. Coli)*	His-DsbC-TEV-RALF	C	pEXP
4	Thioredoxin (*Escherichia coli*)	His-Trx-TEV-RALF	C	pEXP
5	Ecotin (dimeric periplasmic protease inhibitor) *E.Coli*	ss-Ecotin-TEV-RALF-CHis	P	pOP5
6	Thiol Disulfide Oxidoreductase A (*E. Coli)*	ss-DsbA-TEV-RALF-CHis	P	pOP5
7	Subunit of trimethylamine *N*-oxide reductase I (TorA)-Monomeric Red Fluorescent Protein (mCherry)	ss-TorA-mCherry-TEV-RALF-CHis	P	pOP5
8	Thiol Disulfide Oxidoreductase C (*E. Coli)*	ss-DsbC-TEV-RALF-CHis	P	pOP5
9	Thiol Disulfide Oxidoreductase G (*E. Coli)*	ss-DsbG-TEV-RALF-CHis	P	pOP5

Table 6.3. Soluble citoplasmic and periplasmic protein tags used to create RALF-M constructs with SLIC. In the table are listed and numbered (1-9) soluble tags proteins (Soluble fusion proteins) cloned at N-terminal RALF-M. Additional tags are also reported (Construct tags) where (ss) indicates signal sequence for periplasmic extrusion, (His) indicates N-terminal 8x Histidine tag, (CHis) indicates C-terminal His-tag, (TEV) indicates *Tobacco Etch Virus* protease cleavage site, (RALF) indicates protein coding sequence position in the construct. Citoplasmic (C) and periplasmic (P) protein expression and localization in *E. Coli* is specified, and vector used to create the construct (Vector) is indicated.

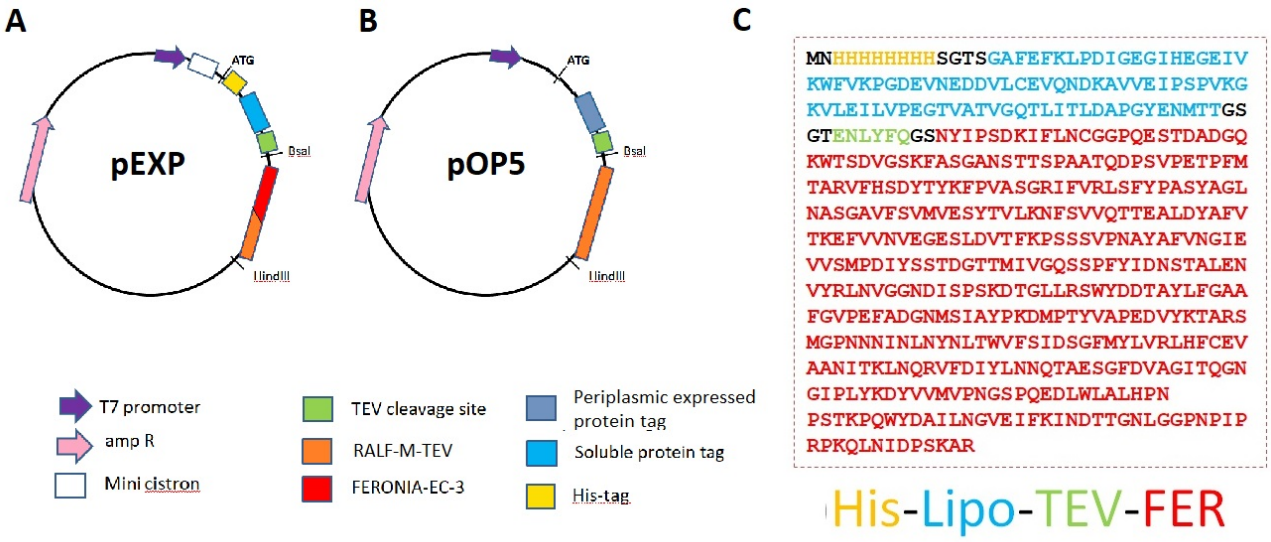

Figure 6.3. pEXP vectors scheme. A,B) The schemes show the characteristic features of pEXP (a) and pOP5 (b) vectors used to create FERONIA and RALF-M constructs trough SLIC cloning. Colored boxes indicates T7 promoter, ampicillin resistance, mini cistron, TEV cleavage site, FERONIA (47-EC-3) and RALF (RALF-M) coding sequences, the position of citoplasmic expressed soluble protein tag listed in Tables 6.2 (light blue) and periplasmic expressed protein tag listed in Table 6.3. Start coding sequence (ATG) and cloning sites (HindIII, BsaI) are reported. C) In this vector series the 8xHis tag (yellow) is at the C-terminal of RALF-M coding sequence (orange). c) Amino acid sequence of His-Lipo-TEV-FER pEXP protein construct (number 4 in table 6.2) as example of fusion protein tags composition. In Yellow is represented 8x His tag, in light blue soluble expression tag in *E.coli,* in green TEV protease cleavage site and in red FERONIA extracellular domain (47-EC-3).

6.2.8 Soluble tags-FERONIA protein expression and purification

FERONIA-pEXP constructs expression test was performed growing transformed *E. coli T7 express* in 5 mL LB amp for 3 hours at 37°C with shaking (200 rpm). Cultures were induced with isopropyl-thiogalactopyranoside IPTG (400 µM) and then expression and protein solubility were tested at 18°C overnight. Cells were then collected by centrifugation for 1 min at maximum speed from 500 µl of colture. Pellet cells were then broken adding 1/10 volume of BugBuster Reagent (Novagen) and 0.3µl of Lysonase™ and incubated 15 minutes at room temperature. Cell lysate was then centrifugated for 3 minutes at maximum speed and soluble fraction was isolated from the pellet. Pellet was then resuspended again in dilued BugBuster reagent (1:5). Total lysate and soluble fraction were then loaded on SDS-PAGE gel with negative control (*E.coli T7 express* cells not transformed). Soluble protein expressing constructs were selected and grown in large scale (2 L each) at 37°C with rotation up to OD_{600} reached 0.8, induced with IPTG (400 µM) and expressed at 18°C overnight. Cells were collected by centrifugation, resuspended in Lysis Buffer (50mM TrisHCl pH8.0, 500mM NaCl, 20mM Imidazole), Dnase (800 u), MgCl2 (4mM) and Protease inhibitor cocktail (Promega) were added. Cell suspension was lysated with Emulsiflex, passing the cell suspension four times through the pomp. Surnatant was isolated after centrifugation at 4°C for 40 minutes at 15 000 rpm and loaded onto a 2 mL Ni sepharose excel column (GE healthcare) equilibrated with Lysis buffer. His-tagged proteins were then eluted with Elution Buffer (50mM Tris HCl, 500mM NaCl, 300mM Imidazole) in five fractions of 1mL each and loaded on SDS-PAGE. The fractions containing more protein of expected molecular weight were then buffered exchanged with 50mM TrisHCl, 500mM NaCl using P10 columns (GE healthcare), later incubated overnight at 4°C with TEV (150 µg) and loaded again on SDS-PAGE with control (aliquots without TEV). In the case of FERONIA derived from TEV cleavage of His-Bla-TEV-FER, protein was concentrated using Millipore Amicon® Ultra-15 centrifugal filter concentrators and loaded Superdex 200 Increase 10-300 column (GE healthcare) equilibrated with (20mM HEPES pH 7.5, 500mM NaCl, 10mM TCEP) for Gel Purification Chromatography. Elution fractions were then loaded on SDS-PAGE gel.

6.2.9 Soluble tag-RALF expression and purification from cytosolic and periplasmic fraction

Cytoplasmic expression test for protein-tag RALF pEXP constructs (1-4, Table 6.3) and RALF-pOP5 (5-9, Table 6.3) was performed as described for protein-tag-FERONIA-pEXP constructs. For protein purification from periplasma, the cells, once collected by centrifugation, were resuspended in Sucrose Buffer (20mM Tris HCl pH 8.0, 1mM EDTA, 20% sucrose), incubated 30 minutes on ice, centrifugated at maximum speed, resuspended again in Extraction Buffer (5mM $MgCl_2$) and centrifugated again to collect surnatant. Both surnatant derived from Sucrose Buffer and $MgCl_2$ Buffer resuspensions were loaded on SDS-PAGE gel.

6.3.10 3D modelling of FaRALFs interaction with MRLK and LLG2 proteins

Homology models of Fxa RALF3, RALF8 and RALF13 in complex with FERONIA and LLG2 were generated using Modeller (Sali & Blundell, 1994)(Sali & Blundell, 1994) (v9.19) package using the complex of *A. thaliana* RALF23, LLG2 and FERONIA (PDB: 6a5e) as the template. ClustalX was used to create alignments of different components of the complex: FaRALF3, *Fragaria x ananassa* FERONIA MRLK47 and Fxa LLG2 with the *A. thaliana* proteins in the *A. thaliana* complex and models with all the different combinations of Fxa RALFs and FERONIAs were generated using the default modelling script of Modeller package. PyMOL (Schroedinger LLC) was used for the analysis of the homology models and the figures.

6.4 Results

6.4.1 FERONIA extracellular domain heterologous expression in *E. Coli*

FERONIA belongs to *Catharanthus roseus* Receptor Like Kinases 1-like (CrRLK1-like) family proteins, which are plasmalemma-anchored receptor-like kinases (RLKs) known to be involved in different plant signaling pathways and cell-wall sensing mechanisms, characterized by two malectin-like motifs in the extracellular domain.

In order to purify *F. vesca* FERONIA homologous MRLK47 (Jia et al., 2017)(Jia et al., 2017) and test the interaction with mature RALF peptide, seven constructs expressing the whole MRLK47 extracellular domain (MRLK47-EC-1,2,3) or N-terminal (N-MLD-1) or C-terminal (C-MLD-1,2,3) Malectin like Domain, were designed and created (Tab.6.4). For MRLK47-EC and C-MLD three expressing constructs coding for proteins differing few residues, were designed to maximize the possibilities of protein expression and purifications.

Construct ID	Schematic sequence	MW (kDa)
MRLK47-EC-1	GS-NYI.. ……KINDT	42
MRLK47-EC-2	GS-NYI.. ……PIPRP	43
MRLK47-EC-3	GS-NYI.. ……SKAR	44
N-MLD-1	GS-NYI.. ……PFYI	20
C-MLD-1	GS-DNS.. ……KINDT	22
C-MLD-2	GS-DNS.. ……PIPRP	23
C-MLD-3	GS-DNS.. ……SKAR	24

Table 6.4. FERONIA extracellular domain constructs and calculated molecular weight. FERONIA constructs names are listed (Construct ID) and a schematic map of cloned FERONIA extracellular domain is represented (Schematic sequence) as a green line. In red and blue are shown respectively first and last residues of expressed proteins. Molecular Weight in kDa (MW kDa) was calculated for each construct. Extracellular Domain (EC), N-terminal Malectin like domain (N-MLD), C-terminal Malectin-like Domain (C-MLD).

FERONIA expression was first tested in *E.coli* in small scale at 37°C for three hours and at 15°C overnight. The SDS-PAGE gels in Fig.6.4 show that all the FERONIA proteins except N-MLD-1 were expressed at 37°C as inclusion bodies in the insoluble fraction, and absent in the soluble fraction. When expressed at 15°C, bands corresponding to expected molecular weight were observed in the insoluble fraction for C-MLD-1 (22 kDa), C-MLD-2 (23 kDa) and C-MLD-3 (24 kDa), while for MRLK47-EC-1, MRLK47-EC-2, MRLK47-EC-3 and N-MLD-1 no visible bands were detected neither in the soluble nor in the insoluble fraction.

In conclusion, all the FERONIA extracellular domain proteins, besides N-MLD-1, are expressed in *E. coli* in the insoluble cell lysate fraction, and none of them could be recovered from soluble fraction neither at 37°C nor at 15°C.

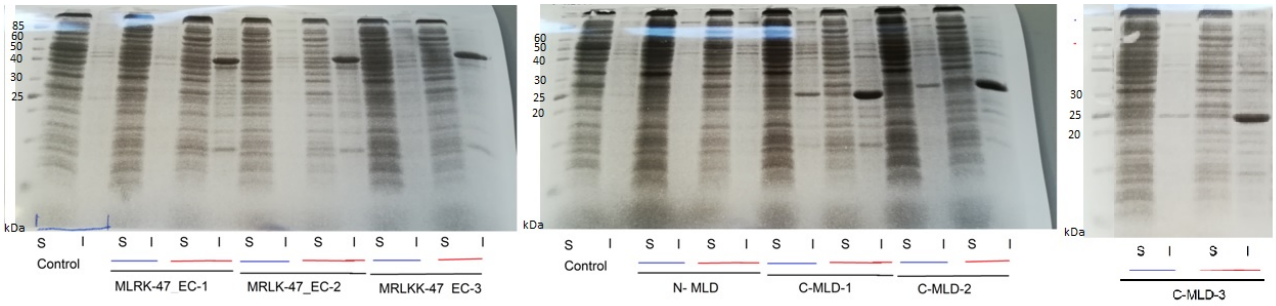

Figure 6.4 FERONIA extracellular domain expression test in *E. Coli.* SDS-PAGE gels of FERONIA constructs (Tab.4.4) expression at 37°C (red line) and 15°C (blue line) in small scale. Soluble fraction (S) and insoluble fraction (I) were loaded for each construct at both the temperatures tested. Protein Marker (kDA) and control (*E. coli Rosetta cells* transformed with pHAT2 empty vector) were loaded for each gel.

6.4.2 FERONIA protein refolding and purification from inclusion bodies

Since expressed FERONIA proteins are insoluble in *E. coli*, proteins were recovered from solubilised inclusion bodies to perform refolding. To determine which could be the optimal buffer condition to properly purify native state protein, a refolding test in small scale was performed for MRLK47-EC-1 and MRLK47-EC-3 proteins using 24 different buffer conditions varying in pH and additives (NaCl and or PPS).

SDS-PAGE gels (Fig.6.5) of FERONIA proteins incubated for 72 hours in refolding buffer, did not show significantly differences among all the condition tested. In particular for

MRLK47-EC-1 three distinct bands are visible at 13-14 kDa, between 40 and 50 kDa (presumably corresponding to FERONIA-EC) and between 85-90 kDa (Fig.6.5A). Similarly, MRLK47-EC-3 refolding protein shows, three bands in every condition tested: one above 15 kDa marker band, one near to 50 kDa and a double band corresponding to 85-100 kDa (Fig. 6.5B).

Since buffer conditions do not seem to affect protein refolding, four pH conditions, two at lower pH (100mM Tris HCl pH8; 100mM Tris HCl pH8, 1 M PPS) and two at higher pH (100mM CAPS pH 10.0; 100mM CAPS pH 10.0, 1M PPS) buffers were arbitrary chosen to perform ion exchange chromatography in small scale (Fig.6.6). Chromatograms of FERONIA refolded in pH 8.0 buffers show a single wide peak (Fig.6.6A,B) corresponding to the same three band on SDS-PAGE gel (Fig. 6.6 C) observed after refolding test (Fig. 6.5B).

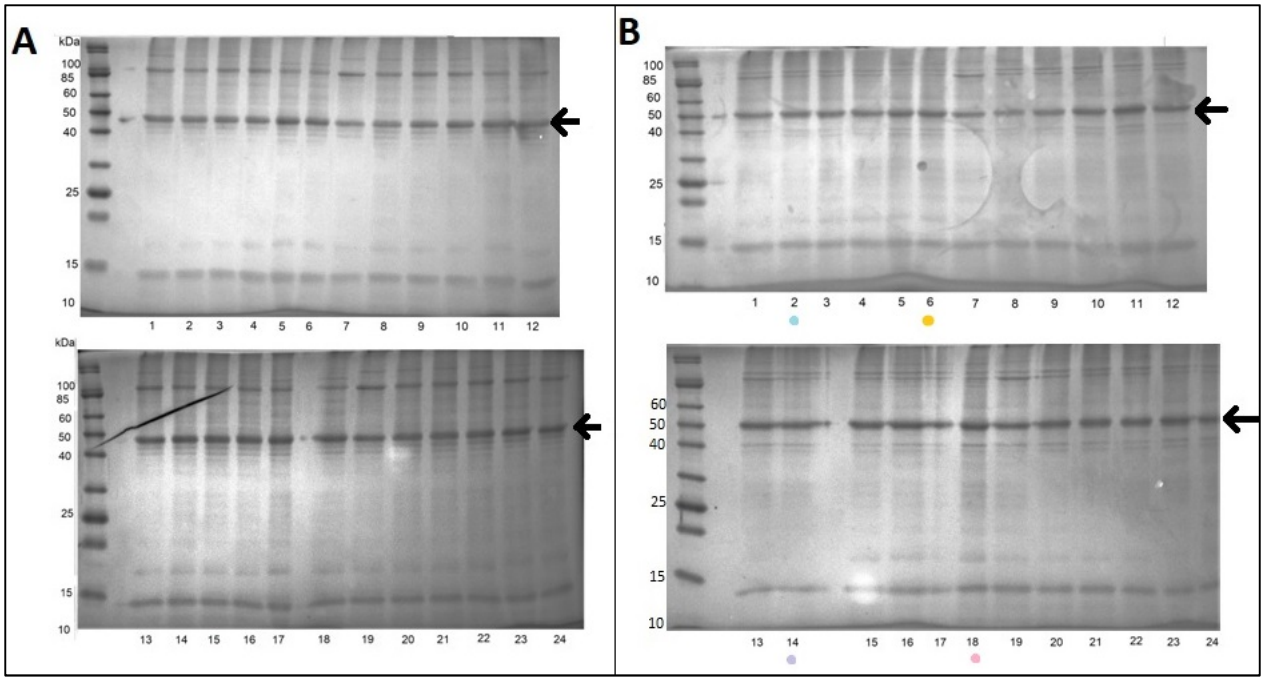

Figure 6.5. MRLK47-EC-1 and MRLK47-EC-3 refolding test in small scale. SDS-PAGE gels showing small scale refolding performed for MRLK47-EC-1 (A) and MRLK47-EC-3 (B). Arrows indicate bands corresponding to expected molecular weight 42 kDa (MRLK47-EC-1) and 44 kDa (MRLK47-EC-3). Numbers from 1 to 24 indicate refolding buffers. 100mM Sodium phosphate pH 7.5 (1,7,13,19); 100mM Tris HCl pH 8.0 (2,8,14,20); Tris HCl pH 8.5 (3,9,15,21); 100 mM Tris pH 9.0 (4,10,16,22); 100 mM CHES 9.5 (5,11,17,23); 100 mM CAPS pH 10.0 (6,12,18,24); 500 mM NaCl (7-12); 1M PPS (13-18); 500mM NaCl 1M PPS (19-24). Light blue (pH 8.0), Yellow (pH10.0), violet (pH8 +PPS) and pink (pH10 +PPS) points indicate proteins refolding buffer used to ion exchange chromatography in small scale.

Chromatogram of proteins in buffer at pH 10 (Fig.6.6 D,E) show one tight peak, which is not visible on SDS-PAGE gel (Fig.6.6F) probably due the low protein concentration.

Since at low volumes was not possible to detect eventually aspecific contaminations in protein recovered from inclusion bodies, culture and refolding solutions volumes were increased.

FERONIA refolding was performed in 100mM Tris pH 8.0 and 100mM CAPS pH 10.0 without additives and a small aliquots was loaded on SDS-PAGE gel (Fig.6.7A) before running ion exchange chromatography (Fig.6.7B). High volume refolding FERONIA presents a different profile from small scale refolding, (Fig.6.7A) showing one thick band at 45-50 kDa, corresponding to expected MRLK47-EC-3 MW, and many tiny contamination bands in both buffer conditions analyzed. Ion exchange chromatogram (Fig.6.7B) presents three distinct peaks named A,B and C which, once loaded on SDS-PAGE gel (Fig.6.7C) do not show FERONIA corresponding band. However, the unbound fraction loaded on the gel shows that protein bound to the column and was not lost in the flow-through fraction. Furthermore high 260nm and 230nm absorbance was observed in chromatogram, probably due to DTT (used in inclusion bodies isolation buffers), which presents an high 260 nm absorbance when it is oxidized.

In conclusion, it was not possible to purify native FERONIA extracellular domain from refolded inclusion bodies in the conditions tested.

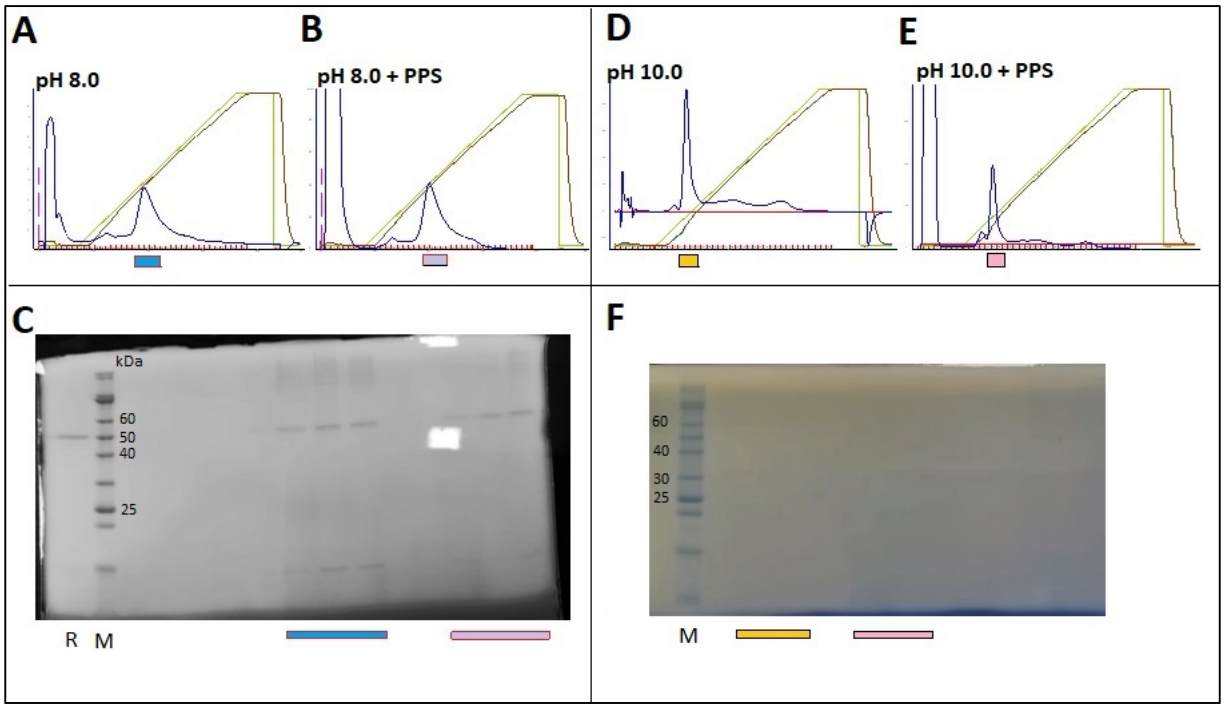

Figure 6.6. MRLK47-EC-3 ion exchange chromatography after refolding in small scale. A,B,D,E) Chromatograms of ion exchange chromatography performed on MRLK47-EC-3 protein refolded in A) 100mM Tris HCl pH 8.0, B) 100mM Tris HCl pH 8.0, 1 M PPS, d) 100 mM CAPS pH 10.0, E) 100 mM CAPS pH 10.0, 1M PPS refolding buffers. Blue lines show 280 nm absorbance, green lines show NaCl concentration gradient for elution, brown lines show conductivity, and red small lines separate elution fractions. Colored boxes indicate elution fractions loaded on SDS-PAGE gel C,D). Reduced MRLK47-EC-3 protein (R) and Marker (M) were loaded.

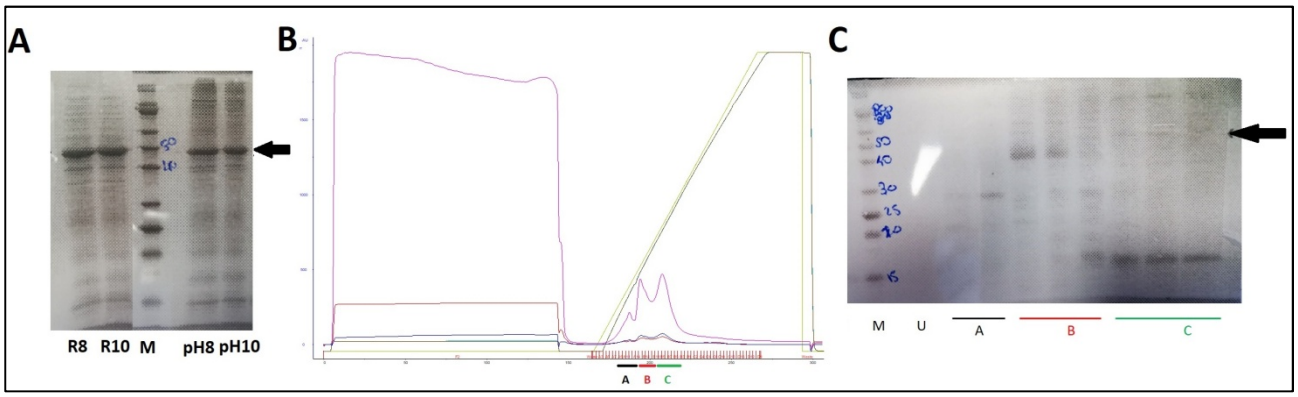

Figure 6.7. MRLK47-EC-3 ion exchange chromatography after refolding in large scale. A) SDS-PAGE gel of MRKL-47-EC-3 after 72h in refolding solution 100mM Tris HCl pH 8.0 (pH 8.0) and 100mM CAPS pH 10.0 (pH 10.0). Respectively reduced samples were loaded on the gel (R8, R10). Arrow indicates expected molecular weight MRLK47-EC-3 band. B) Ion exchange chromatography of protein refolded in large scale in 100 mM Tris HCl pH 8.0. Absorbance at 280 nm (blue), 260 nm (red) and 230 nm (violet) are shown. Green line shows NaCl elution gradient and brown line shows conductivity. Peaks are named with letters (A,B,C). C) SDS-PAGE gel of ion exchange chromatography elution fractions corresponding to peaks A, B and C. Unbound fraction was loaded on the gel (U).

6.4.3 FERONIA-soluble-protein-tag expression and purification

Since it was not possible to purify FERONIA from refolded inclusion bodies, another strategy was undertaken developing 11 additional constructs for FERONIA expression in *E. coli.* To increase FERONIA recovery and purification from cell lysate soluble fraction, the constructs were designed to express N-terminal His-tag FERONIA fused to proteins tags soluble in *E. coli* (Table 6.2).

Expression test (Fig.6.8) revealed that six out of eleven constructs developed, are expressed in the soluble fraction in small scale, namely FERONIA fused to *Streptococcus sp.* chain A, Immunoglobulin G-binding protein (3. His-GB1-FER), *Geobacillus lituanicus* 2-oxo acid dehydrogenase subunit E2 (4. His-Lipo-FER), *E. coli* translation initiation factor IF-2 (7. His-IF-2-FER), *E. coli* elongation factor Ts (8. His-Tsf-FER), *Chromohalobacter sp.* Beta-lactamase precursor (9. His-Bla-FER) and *E. coli* transcription termination/antitermination protein NusA (11. His-NusA-FER). Soluble protein expressing constructs were then scaled up to higher volume culture and purified through Ni affinity chromatography (Fig.6.9A).

A

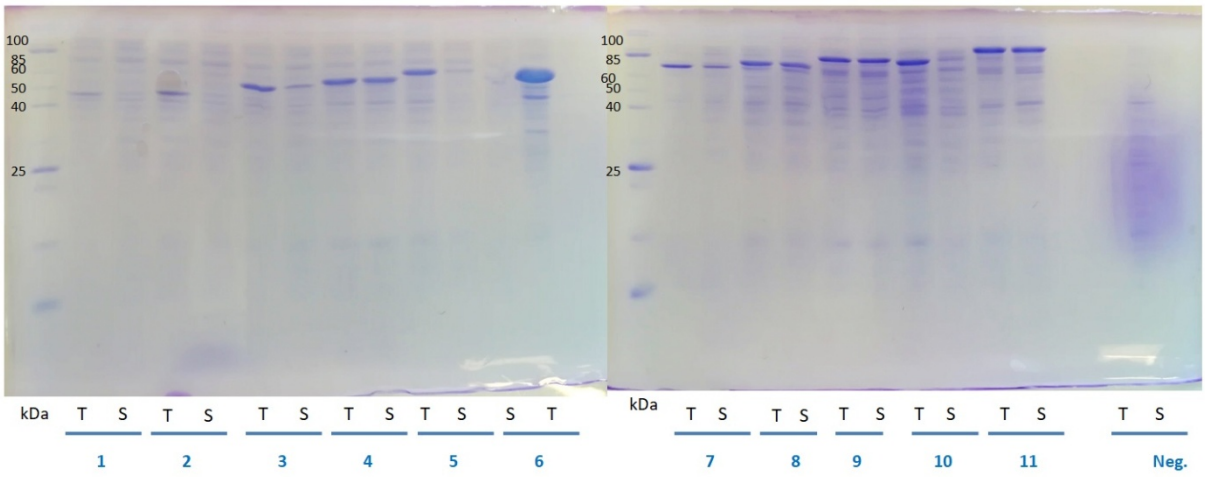

B

1	2	3	4	5	6	7	8	9	10	11	
Cis-N His TEV: FER	T7 tag-His TEV: FER	HIs.-GB1-TEV: FER	His-Lipo-TEV :FER	His-SUMO-TEV :FER	His-Trx TEV :FER	His-IF2 TEV :FER	His-Tsf-TEV : FER	His-Bla - TEV:FER	His x MBP TEV :FER	His NusA TEV :FER	T7 negative control
47,7 kDa	48,76 kDa	54,2 kDa	57,4 kDa	59,1 kDa	59, 8 kDa	65,7 kDa	78,4 kDa	87,5 kDa	88,2 kDa	102,8 kDa	

Figure 6.8. FERONIA-soluble protein tag expression in small scale. a) SDS-PAGE gels of MRLK47-EC-3-soluble-protein-tags constructs expression in *E.coli* in small scale. For each construct (numbered from 1 to 11) and T7 express *E.coli* negative control (Neg.), total lysate (T) and soluble fraction (S) were loaded on the gel. Protein marker is reported (kDa). Gels were stained in Blue-Coomassie. b) Table lists FERONIA-protein tag constructs tested, reporting associate construct number (first row), construct composition (second row), estimated molecular weight in kDa (third row). His: N-terminal His-tag; T7tag, GB1, Lipo, SUMO, Trx, IF2, Tsf, Bla, MBP, NusA: soluble proteins tag (ref. Table 4.2); TEV: TEV cleavage site; FER: FERONIA. Blue background indicate expression in the soluble fraction.

A

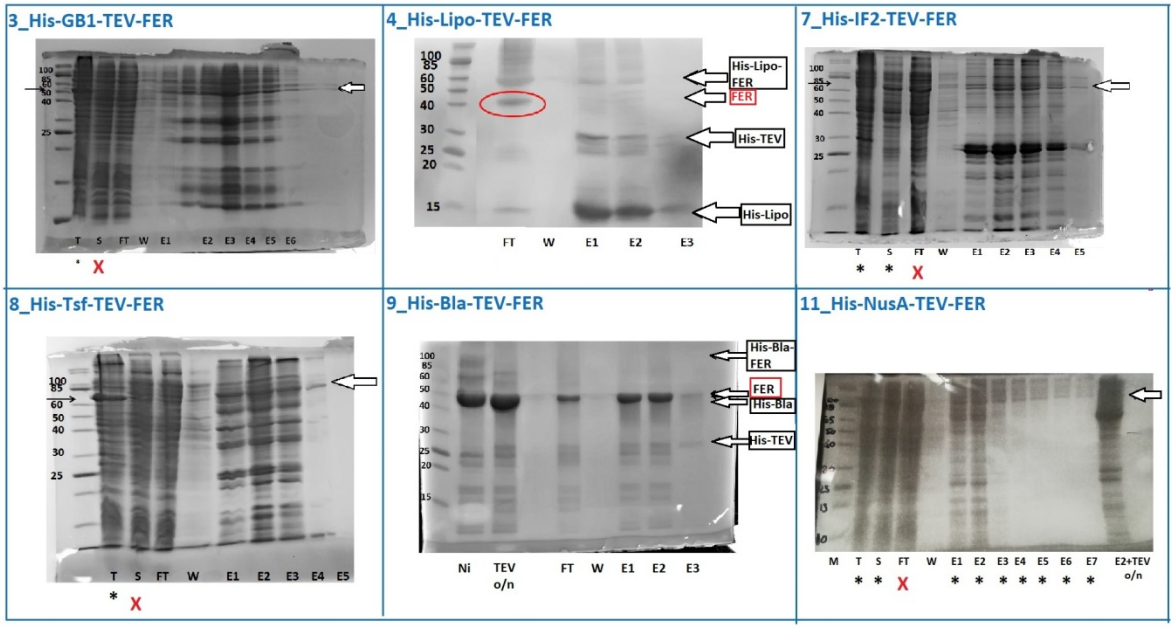

B

pEXP construct	Large Scale Soluble expression	Protein in the Flow trough (FT)	Protein in the Elutions fractions	TEV cleavage
4_His-Lipo-FER	√ →	√ →	√ →	√
11_His-NusA-FER	√ →	√	√ few	X
3_His-GB1-FER	X			
7-His-IF2-FER	√ →	√	√ few	
8-His-Tsf-FER	X			
9-His-Bla-FER	√ →	√ →	√ →	√

Figure 6.9. FERONIA-soluble tag expression and affinity chromatography in large scale. a) Ni column affinity chromatography SDS-PAGE gels of respectively His-GB1-TEV-FER, His-Lipo-TEV-FER after TEV cleavage, His-IF2-TEV-FER, His-Tsf-TEV-FER, His-Bla-TEV-FER after TEV cleavage, His-NusA-TEV-FER before and after TEV cleavage. Total lysate (T), unbound flow through (FT), wash (W) and elutions (E1,2,3…) were loaded. In 9_His-Bla-TEV-FER, Ni column purification elutions before (Ni) and after (TEV o/n) TEV cleavage were loaded on the gel. Arrows indicate 54 kDa (3-His-GB1-FER); from the top His-Lipo-FER (57kDa), FER (44kDa), His-TEV (29 kDa), His-Lipo (10kDa); His-IF2-FER (66kDa); His-Tsf-FER (78kDa); His-Bla-FER (87kDa), His-Bla (43kDa); His-NusA-FER (103kDa). Red circle in 4-His-Lipo-FER indicates FER corresponding band in the flow through fraction. Asterisks indicate fractions in which band corresponding to expected protein MW was detected. Red crosses under (S) indicate that protein was not recovered from the soluble fraction when expressed in large scale, red crosses under (FT) indicate that protein or part of it was lost in the unbound fraction. b) FERONIA Ni column purifications summarizing table. Positive result is indicated by (√), positive but not sufficient by (√ few) and negative by (X). The table report if protein was expressed in the soluble fraction in large scale (first column), if protein was lost in the unbound fraction (second column), if it was possible recover some protein from elution fraction (third column), if it was possible to purify protein in denaturing condition with 8M Urea supplemented buffers (fourth column), if protein was cut by TEV protease (fifth column).

Unlike positive expression in small scale, it was not possible to obtain high yield of His-GB1-FER and His-Tsf-FER proteins from soluble fraction when expressed in large scale, since a small band was observed in the elutions fractions after Ni affinty chromatography (Fig.6.9A, B). On the other hand, all the protein-tag-FERONIA expressed, showed low affinity in binding column, since proteins corresponding bands were detected in the flow through fraction (Fig.6.9). This could be caused by proteins aggregation and formation of agglomerates which could eventually hide His-tag and affect proteins binding affinity to Ni column. However, the most efficient result was obtained with His-Lipo-FER and His-Bla-FER, which, after affinity chromatography, were cleaved with TEV protease overnight. A second Ni affinity chromatography allowed FERONIA protein purification after cleavage, isolating it from His-tagged soluble protein–tag (Lipo and Bla). In fact, SDS-PAGE gels of Ni chromatography after cleavage (Fig.6.9A_4.Lipo,9.Bla) show His-tag free FERONIA presence in the unbound fraction (FT) and His-tagged Lipo, His-tagged Bla and His-tagged TEV protease used for the cleavage reaction, in the elutions fraction. Protein recovered after TEV cleavage was then further purified through Gel Purification chromatography (Fig.6.10). The chromatogram generated shows a tight and high peak of absorption at 280nm (underlined in red in Fig.6.10A), which corresponds on SDS-PAGE to FERONIA molecular weight band (Fig.6.10B) and lower contaminant bands.

In conclusion, it was not possible to purify high yield and high purity FERONIA protein to test the interaction with RALF ligand. Further analyses and tests will be necessary to perform FERONIA purification, possibly considering an eukaryotic hetorologous expression system.

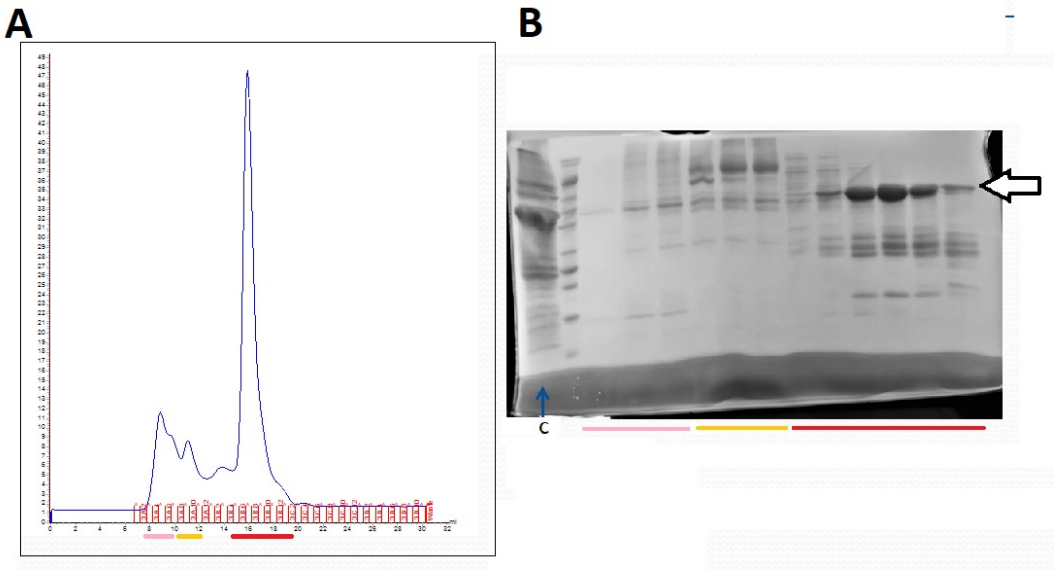

Figure 6.10. FERONIA purification after His-Bla-FER TEV cleavage. a) FERONIA gel purification chromatography after His-Bla-FER TEV cleavage. Pink, yellow and red lines underline fractions loaded on SDS-PAGE gel (b). b) Arrow indicates FER corresponding band. Protein fraction before gel purification chromatography was loaded on the gel (C).

6.4.4 RALF protein purification from refolded inclusion bodies

To purify native and active RALF peptide, the same procedure initially used to express and purify FERONIA extracellular domain in *E.coli* was followed. In this case three constructs were designed to produce respectively His-tagged, pre-mature RALF peptide (RALF-PM), mature RALF peptide (RALF-M) and mature RALF peptide with N-terminal TEV cleavage site (RALF-M-TEV) (Table 6.5).

Construct ID	Schematic sequence	MW (kDa)
RALF-PM	GSDH.. .....CRS	12
RALF-M	GS-ATTK.. .....CRS	5.5
RALF-M-TEV	STENLYFQATTK.. .....CRS	8.1

Table 6.5. RALF constructs. RALF constructs names (Construct ID) and a schematic map of cloned RALF sequences are listed. In red are represented first residues included in the constructs for pre-mature RALF peptide RALF-PM (GSDH), for mature RALF peptide RALF-M (GSATTK); in blue are represented TEV protease recognition cleavage motif (STENLYFQ) and at the end of blue line, last residues included in all constructs (CRS). Molecular Weight for each construct were calculated (MW, kDa).

First, expression in small scale allowed to test RALF proteins production and solubility in *E. coli*. Small scale expression SDS-PAGE gels (Fig.6.11) shows that RALF-M peptide is not expressed neither at 37°C nor at 15°C, since bands observed in RALF-M are similar to negative control. On the other hand RALF-PM (12 kDa) and RALF-M-TEV (8.1kDa) proteins seem to be highly expressed at 37°C and barely at 15°C in the insoluble fractions. Interestingly, RALF-M-TEV expressed protein presents two bands corresponding to higher molecular weight compared to calculated mass. This could be related to differential protein migration in non reducing condition or to protein degradation products.

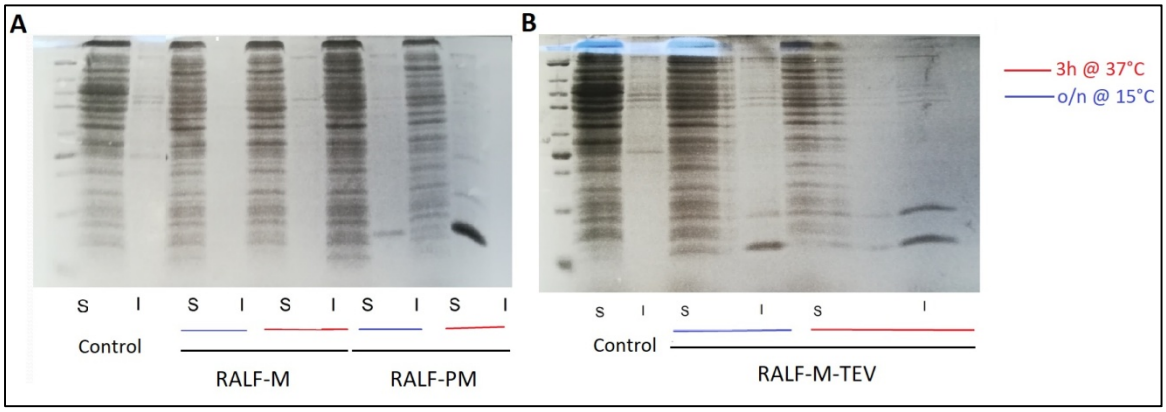

Figure 6.11. RALF constructs expression test. a,b) SDS-PAGE gels of RALF-M, RALF-PM (a) and RALF-M-TEV (b) constructs (Tab.4.5) expression at 37°C (red line) and 15°C (blue line) in small scale. Soluble fraction (S) and insoluble fraction (I) were loaded for each construct at both the temperatures tested. Protein Marker (kDA) and control (*E. coli Rosetta cells* transformed with pHAT2 empty vector) were loaded for each gel.

Subsequently, RALF-PM and RALF-M-TEV have been subjected to protein refolding test in small scale using 24 buffers differing in pH and additives compositions (Fig.6.12). No significantly differences among buffers conditions tested were observed in the SDS-PAGE gels for RALF-M-TEV (Fig.6.12A) and RALF-PM (Fig.6.12B) proteins, after two days of incubation in refolding solution. Therefore, 100mM CAPS pH 10 buffer (condition number 6), was arbitrary chosen to test RALF-M-TEV refolding in large scale.

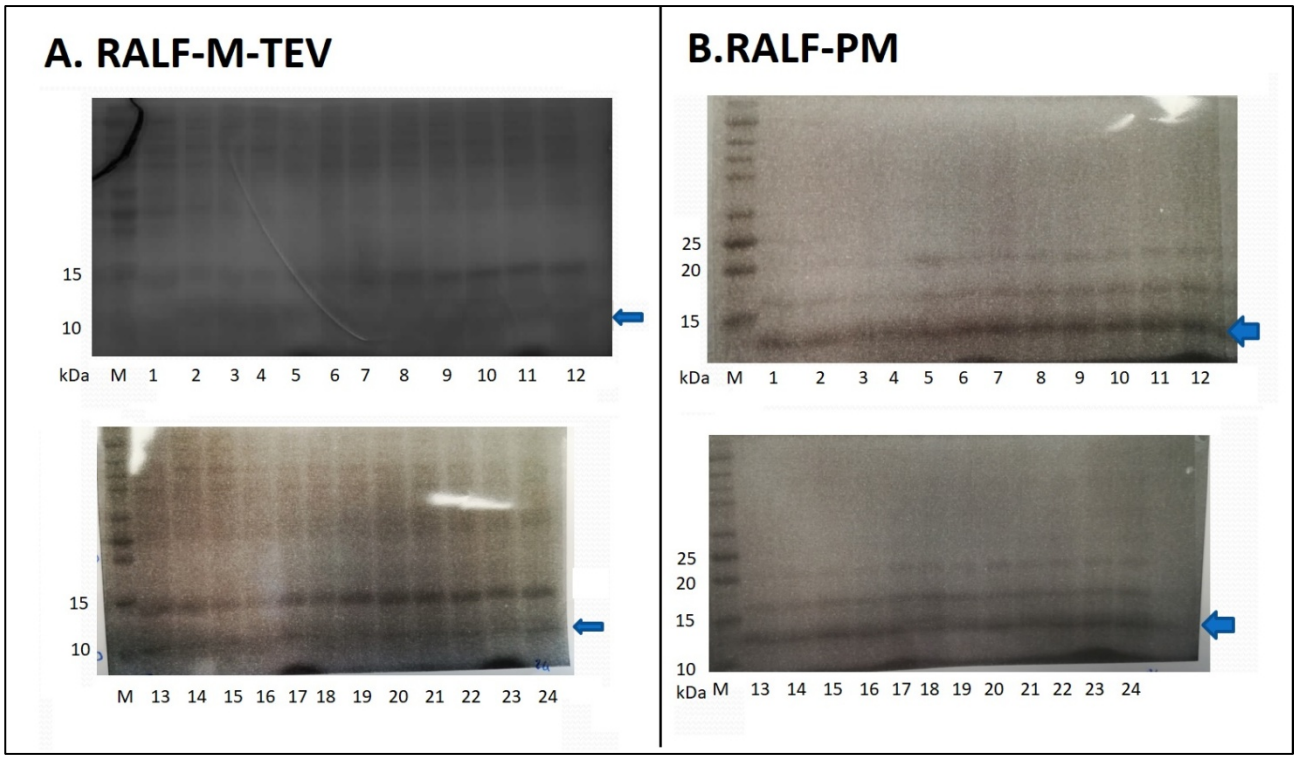

Figure 6.12. RALF-M-TEV and RALF-PM refolding test in small scale. SDS-PAGE gels showing small scale refolding performed for RALF-M-TEV (a) and RALF-PM (b). Arrows indicate bands corresponding to expected molecular weight 8 kDa (RALF-M-TEV) and 12 kDa (RALF-PM). Numbers from 1 to 24 indicate refolding buffers. 100mM Sodium phosphate pH 7.5 (1,7,13,19); 100mM Tris HCl pH 8.0 (2,8,14,20); Tris HCl pH 8.5 (3,9,15,21); 100 mM Tris pH 9.0 (4,10,16,22); 100 mM CHES 9.5 (5,11,17,23); 100 mM CAPS pH 10.0 (6,12,18,24); 500 mM NaCl (7-12); 1M PPS (13-18); 500mM NaCl 1M PPS (19-24). Light blue (pH 8.0), Yellow (pH10.0), violet (pH8 +PPS) and pink (pH10 +PPS) points indicate proteins refolding buffer used to ion exchange chromatography in small scale.

Reverse phase Chromatography was then performed on refolded RALF-M-TEV in large scale. The chromatogram generated by purification (Fig.6.13A) shows different peaks. The highest peak corresponding fractions (Fig.6.13A: cells A4 and A5), once loaded on SDS-PAGE gel (Fig.6.13B), shows the same two bands previously observed in small scale RALF-M-TEV expression test (Fig.6.11B). In particular fraction A5 corresponds to the thin higher band (above 10kDa marker) and the wide lower band (below 10kDa marker), while fraction A4 presents only the wide lower band. Due to differentially migration caused by eventually RALF disulfide bonds or protein degradation during purification, it is not possible to determine which band out of the two observed, corresponds to RALF-M-TEV protein.

In order to further isolate and characterize native RALF-M-TEV protein, fraction A5 was then purified using Reverse phase chromatography (Fig.6.14). The chromatogram obtained (Fig.6.14A) shows that was not possible to separate A5 fraction components, since only one tight peak corresponding to a double band on SDS-PAGE gel (Fig.6.14B) was observed.

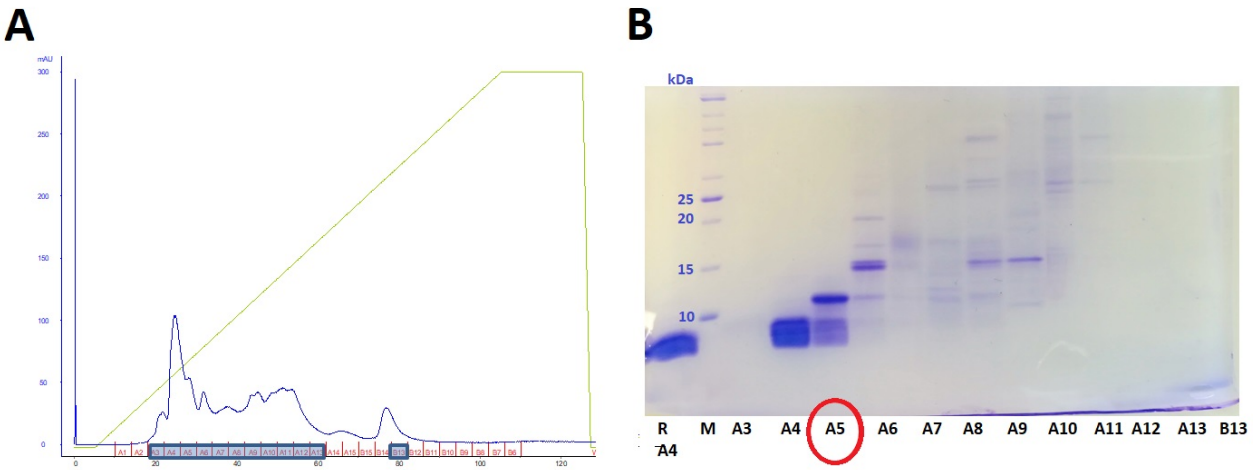

Figure 6.13. RALF-M-TEV Reverse Phase Chromatohgraphy purification. a) Chromatogram illustrates RALF-M-TEV purification trough XW Source RPC 5mL column. Blue line shows $A_{280,}$ green line shows elution buffer concentration gradient, in red are represented elution fractions in the order: A1 to A15 and from B15 to B6. Blue boxes highlight peak corresponding fractions (A3-A13 and B13) loaded on SDS_PAGE gel (b). b) Red circle indicates fractions subsequently purified by another RPC. On the gel was loaded a reduced aliquot of A4 fraction (R A4) and protein marker (M). Gel was stained in Coomassie Brilliant Blue.

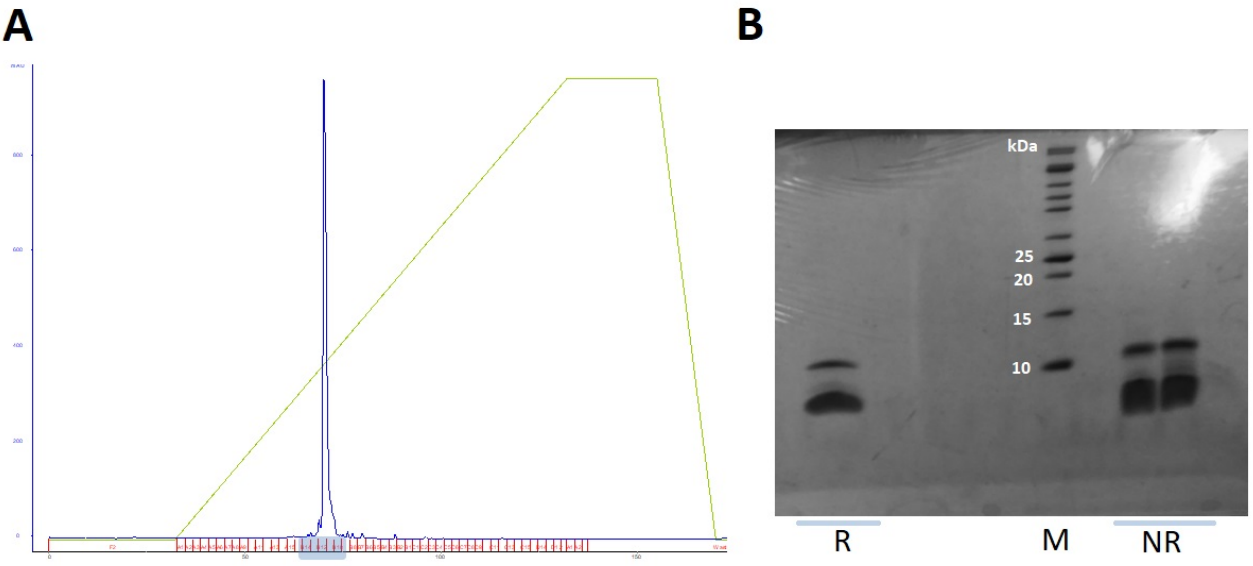

Figure 6.14. RALF-M-TEV second Reverse Phase Chromatohgraphy purification. a) Chromatogram illustrates fraction A5 (RALF-M-TEV) purification trough C8 column . Blue line shows $A_{280,}$ green line shows elution buffer concentration gradient, in red are represented elution fractions. Blue boxes highlight peak corresponding fractions loaded on SDS_PAGE gel (b). b) On the gel a reduced (R) and not reduced (NR) aliquots and protein marker (M) ere loaded. Gel was stained with Coomassie Brilliant Blue.

To determine proteins identities of the double bands observed, SDS-PAGE gel was excised and bands were analyzed by Liquid chromatography-Mass Spectrometry (LM-MS). Results summarized in Figure 6.15, revealed that higher band corresponds to a peptide whose sequence matchs 75% with RALF-M-TEV sequence, while lower band corresponds to smaller peptides which overall cover 41% of RALF-M-TEV peptide sequence. Then, it is reasonable to consider the higher band as the complete RALF-M-TEV peptide and the lower band as a mixture of degradeted small RALF-M-TEV peptides.

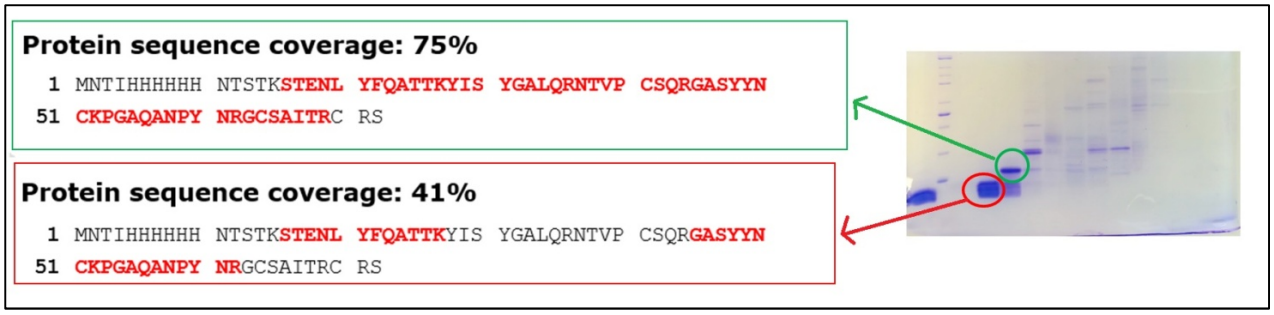

Figure 6.15. RALF-M-TEV bands MASS SPEC results. His-RALF-M-TEV amino acid sequence is represented and matched peptides found by MASS SPEC analysis are shown in bold red. Green squared sequence, with 75% of His-RALF-M-TEV matching sequence coverage corresponds to higher small band, while red squared sequence with 41% of His-RALF-M-TEV matching sequence coverage corresponds to lower wide band.

Since it was not possible to separate full RALF-M-TEV peptide from degraded RALF-M-TEV peptides, similarly to FERONIA-EC, another expression and purification strategy was tested, developing soluble-tag proteins-RALF-M expressing constructs in *E.coli* (Fig. 6.16B). Furthermore, in addition to cytosolic *E. coli* expressed proteins, five different constructs including signal sequence for protein translocation in the periplasmic space were developed (Fig.6.16B :5-9).

First, expression was tested in small scale, extracting proteins both from soluble fraction after cell lysis (cytosol) (Fig.6.16A) and from periplasma using different buffers (Fig.6.16C). Cytosol expressed constructs His-GB1-RALF-M, His-DsbA-RALF-M, His-DsbC-RALF-M and His-Trx-RALF-M proteins were all expressed and recovered in the soluble fraction, however all the samples contained proteins corresponding to the double band associated to RALF-M protein degradation (Fig.6.16A). On the other side, periplasmic signal sequence proteins ss-Ecotin-TEV-RALFM-Chis, ss-TorA-TEV-RALFM-CHis and ss-DsbG-TEV-RALFM-CHis are not efficiently

expressed and recovered in the soluble fractions, while ss-DsbA-TEV-RALFM-CHis and ss-DsbC-TEV-RALFM-CHis were expressed, soluble and correspond to double bands. As was observed with cytosolic extraction, periplasmic extraction performed with sucrose and $MgCl_2$ buffers revealed that ss-Ecotin-TEV-RALFM-Chis, ss-TorA-TEV-RALFM-CHis and ss-DsbG-TEV-RALFM-CHis were not efficiently recovered neither with sucrose nor with $MgCl_2$ buffers, while ss-DsbA-TEV-RALFM-CHis and ss-DsbC-TEV-RALFM-CHis are expressed and recovered with both buffers, but present RALF-M degradation characteristic band.

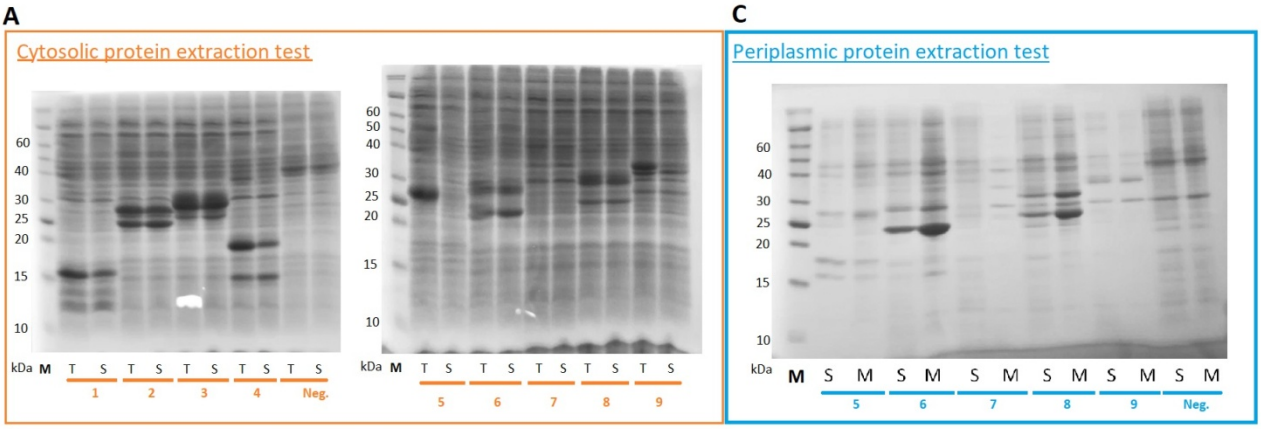

B

Cytosolic expressed constructs

1	His-GB1-TEV-RALF-M	14,2 kDa
2	His-DsbA-TEV-RALF-M	29,3 kDa
3	His-DsbC-TEV-RALF-M	31,6 kDa
4	His-Trx-TEV-RALF-M	19,7 kDa

Periplasmic expressed constructs

5	ss-Ecotin-TEV-RALF-Chis	27,7 kDa
6	ss-DsbA-TEV-RALF-Chis	30,3 kDa
7	ss-TorA-mCherry-TEV-RALFCHis	36,5 kDa
8	ss-DsbC-TEV-RALF-Chis	32,9 kDa
9	ss-DsbG-TEV-RALF-Chis	35,1 kDa

Figure 6.16. Cytoplasmic and periplasmic protein-tagged-RALF-M expression test. a) SDS-PAGE gels of protein-tagged-RALF-M expression in small scale. Total lysate (T) and soluble fraction (S) were loaded on the gel for constructs listed in table (b) and negative control (Neg.). Marker (M). b) The table lists constructs and corresponding molecular weight in kDa. Proteins-tag included in constructs 1,2,3 and 4 are expressed in *E. coli* cytoplasmic space, while 5,6,7,8 and 9 include signal sequence peptide (ss) for expression in the periplasmic space and have C-terminal His-tag (CHis). c) SDS-PAGE gel of periplasmic protein extraction performed with sucrose buffer (S) and $MgCl_2$ buffer (M). Marker and negative control (Neg.) were loaded.

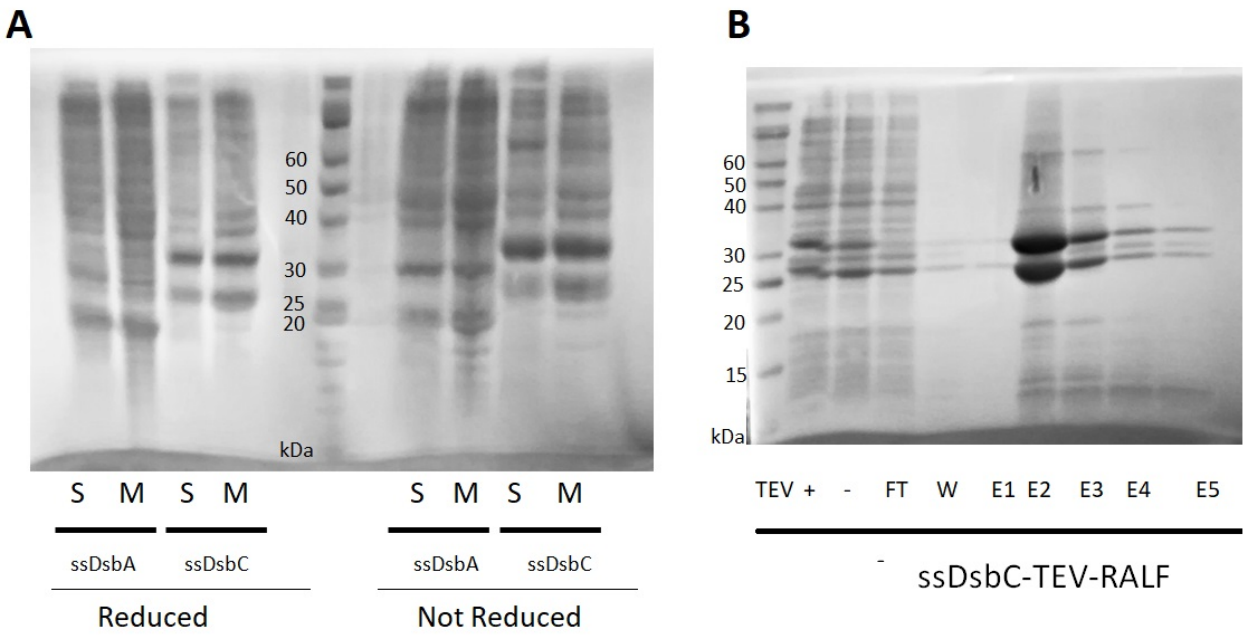

Figure 6.17. Large scale ss-DsbA-RALF-CHis and ss-DsbC-RALF-CHis periplasmic expression. a) SDS-PAGE gel of periplasmic protein extraction using sucrose (S) and $MgCl_2$ (M) buffers. Reduced (Reduced) and not reduced (Not Reduced) proteins extracts were loaded on the gel. b) TEV cleaved ssDsbC-RALFM-CHis Ni affinity chromatography SDS-PAGE gel. From left to right sample was loaded before (TEV -) and after (TEV +) TEV cleavage; Ni column unbound (FT), wash (W) and 1mL elution

RALFM-CHis expression and Ni affinity chromatography purification were performed. Extraction (Fig.6.17A) and purification (Fig.6.17B) SDS-PAGE gels show that proteins were efficiently expressed, isolated and purified in large scale. However the band corresponding to degraded RALF-M peptide is still present and the intensity is comparable to full length RALF-M peptide band.

In conclusion it was not possible to purify high yield and purity native RALF-M peptide to test the interaction with the receptor FERONIA (MRLK47).

6.5 Discussion

At the beginning of this project in 2018, the crystal structure of RALF-FERONIA complex had not been resolved yet. However, recently Xiao *et al.* (2019) purified and resolve the crystal structure of RAF23-FERONIA-LLG2 complex in *Arabidopsis* showing that LLG1 and LLG2 proteins directly bind RALF23 to induce the complex assembly with FERONIA and inhibit immunity response. Furthermore, it has been showed that N-terminal mature peptide fragment (residues 1-17) is sufficient to bind and nucleate the complex. In particular YISY and LRRL motifs were identified as interacting residues crucial for RALF-FERONIA-LLG2 interaction and are conserved in most of the AtRALF and FaRALF peptides (Fig. 18A) suggesting that this mechanism may be conserved in other RALF binding complexes.

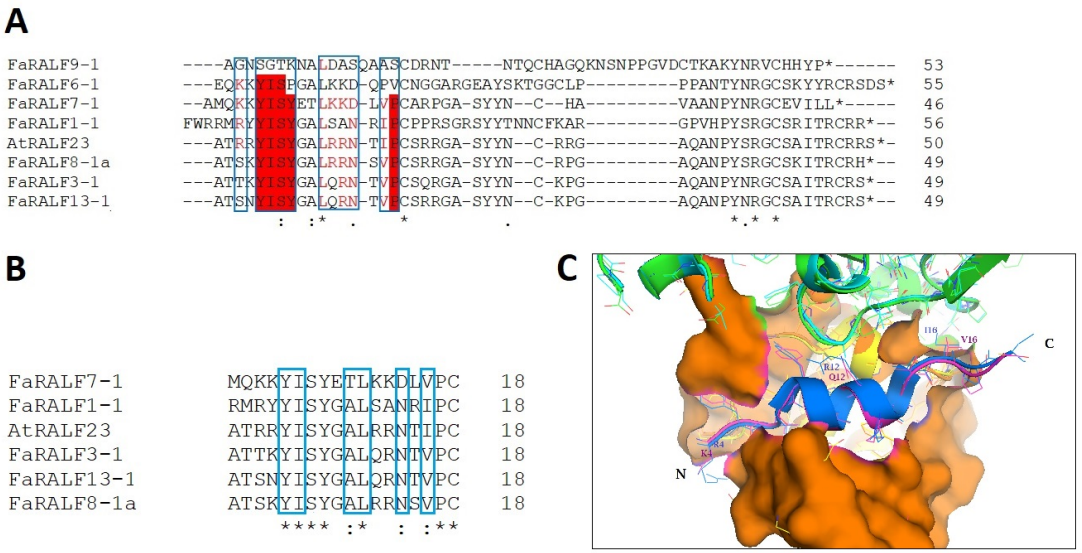

Figure 6.18: Interaction residues conservation among *Fragaria x ananassa* RALF peptides expressed in fruits.(a) Mature FaRALF peptides alignment; conserved amminacid are highlighted in red and similar amminoacids are in red font. Blue boxes indicate conserved motifs characteristic of subfamily 1 classification according to Xiao et al., 2019. (b) Subfamily 1 FaRALF peptide N-terminal sequences alignment, boxes indicate important residues for AtRALF23 binding to LLG2-FER complex. Homology model of FaRALF3-1-FaLLG2-MRLK47 complex based on AtRALF23-LLG2-FER structure in *Arabidopsis* (Xiao et al., 2019)*;* in cyan FER, in blue AtRALF23, in yellow LLG2, in green FaMRLK47 (*Fxa* FER homolog), in magenta FaRALF3-1, in orange FaLLG2 (*Fxa* LLG2 homolog). N-terminal (N) and C-terminal (C) are indicated. Only N-terminal helix of RALF peptides (4-17 residues) are shown and residues differences between AtRALF23 and FaRALF3-1 are indicated.

Structural data, developed by Xiao et *al.,* (2019) also show that RALF23 recognition is dependent on the conformationally flexible C-terminal of LLG1, LLG2 and LLG3. Thus, it has been supposed, that diverse RALF peptides may regulate multiple processes, through perception by distinct heterocomplexes of CrRLK1L receptor kinases and GPI-anchored proteins of the LRE and LLG family.

Since FaRALF3-1 presents the same conserved N-terminal sequence of AtRALF23 (Fig. 6.18B), it has been developed an homology binding proteins model in strawberry using FaRALF3, FaMRLK47 and FaLLG1 (Fig 6.18C). Consistently with motif conservation, the strawberry binding model follows the *Arabidopsis* complex interaction structure. However further analyses will be required to confirm the effective interaction between FaRALF3 and FaMRLK47 in strawberry.

7. Genotypic and phenotypic characterization of *F. vesca* transgenic RNAi plants silenced for *FvRALF13* gene

7.1 Acknowledgments

The analyses presented in this chapter were started at the Horticultural Science Department of the University of Florida (Fifield Hall, Hull Road, Gainesville, Florida 32611, USA), thanks to the supervision and kindly support of Prof. Kevin M. Folta and Dr. Kevin O' Grady. The project I have been working was previously aim of the research of Dr. Mithu Chatterjee, Dr. TingTing Zhang and Dr. Mohamad Mad Atari at the University of Florida. In particular Dr. Mithu Chatterjee has developed transgenic RALF RNAi plants, Dr.TingTing Zhang has performed the first phenotypic characterization and Dr. Mohamad Mad Atari has grown and maintained transgenic lines through the years. Furthermore the phonotypic characterization presented in this chapter was realized thanks to the kindly help of Dott. Alessandra Sbizzera and presented in her Master Degree Dissertation in 2019.

7.2 Introduction

A previous work, conducted by Dr. Mithu Chatterjee , Dr. TingTing Zhang and Dr. Kevin Folta in 2012 at the University of Florida (U.S.A.), allowed the identification of a partial *FaRALF13-1* transcript (from here called *7b01*) trough random Sanger sequencing of a flower cDNA library produced from *Fragaria × ananassa cv. Festival* (Zhang, 2012). The aim of this study was to characterize new genes involved in strawberry development regulation. For this reason *Fragaria x ananassa* flower cDNA sequences were introduced into RNAi silencing constructs and used to transform *F. vesca Hawaii-4* plants, which are more easy to regenerate and transform. Transgenic lines were then screened for interesting developmental defective traits and other transgenic lines were produced as replicates to confirm the observed phenotype. Among transgenic lines analyzed at the University of Florida, *7b01* RNAi line was taken in consideration for further analyses due to the peculiar abnormal phenotype affecting plant canopy and flowers anatomy, which was consistent in each of the ten transgenic independent lines obtained.

Thus, the aim of this study is to characterize transgenic RNAi lines in terms of genetic variability, considering number of transgene insertion in the genome and target gene expression, and mutant phenotype, considering growth related and pathogens susceptibility traits.

7.3 Materials and Methods

7.3.1 Isolation of *FaRALF13* and generation of RNAi lines

Transgenic *FvRALF13* RNAi plants were previously generated by Dr. Mithu Chatterjee and Dr. Kevin Folta at the University of Florida (U.S.A.). Briefly, a partial *FaRALF13-1* transcript (from here called *7b01*) was isolated by random Sanger sequencing of cDNA clones from a *Fragaria × ananassa cv. Festival* library, prepared from combined flowers harvested from various developmental states. *7b01* sequence was cloned into the binary Gateway vector pK7GWIWG2D(II) (Karimi *et al.,* 2002)(Karimi et al., 2002) with standard LR Clonase II reaction conditions (Invitrogen). This construct was introduced into a *A. tumefaciens* strain GV301 by electroporation. Stable transformation of *F. vesca Hawaii-4* was then performed using a slight modification to a published protocol (Oosumi et al., 2006)(Oosumi et al., 2006), and transgenic plants were regenerated in vitro according to Chatterjee *et al.* (2011)Chatterjee et al. (2011). Kanamicyn resistant transgenic plants were screened for eGFP marker emission under a fluorescence microscope. Ten independent 7b01 transgenic lines were generated and three of them namely *7b01.1, 7b01.4b* and *7b01.7* were propagated by seeds and used for this study.

7.3.2 Plant materials and growth conditions

F. vesca wild type Hawaii-4 and transgenic lines *7b01.1, 7b01.4b* and *7b01.7* seeds were collected from self-pollination seventh generation plants. Seeds were washed in water over night and surface sterilized with ethanol 90% for 5 min, rinsed once with 1% (v/v) bleach solution for 30 min and five times with water, then plated on MS media (0.5x Murashige and Skoog medium with vitamins, 0.7% Plant agar, pH 5.8). The seeds were stratified at 4°C for 7 days under darkness and were grown for three weeks at controlled conditions at 25°C with a photoperiod of 16 h light/8 h dark. Seedlings were successively transferred in soil and acclimated before being moved to the greenhouse. Plants were grown in the greenhouse for three months at 25°C, watered twice a week and regularly fertilized with Sequestrene®NK 138Fe.

7.3.3 DNA extraction and transgene copy number analysis trough ddPCR™

Genomic DNA was extracted from stolons harvested from a population of 25 plants for each line analyzed (*Hawaii-4 wild type, 7b01.1, 7b01.4b* and *7b01.7)* using Wizard® Genomic Purification kit (Promega). Plant Tissue Protocol (Manufacturer protocol 3.E.) was modified adding two consecutive Chloroform:isoamyl alcohol (24:1) purification steps after Protein Precipitation solution addition and before 2-propanol precipitation. Genomic DNA was measured with NanoDrop™ 3300 and 1 µg of DNA was loaded into Eco RI (Promega) restriction reaction and digested for 1 hour at 37°C. Concentration after DNA digestion was measured using Qubit™ dsDNA HS Assay Kit. Silencing *7b01* RNAi construct insertion events were measured using primers 5'-GAGAGAGATAGATTTGTAGAGAGAGACTGGT-3' , 5'-AGTCAAAACGAGCTAAATAAGGAGTTACAC-3', Aldehide Dehidrogenase 1 (FvH4_2g14760) was used as single copy reference gene(DiMeglio et al., 2014) and amplified using primers 5'-TGCTGTTCTTGTGGGATTGC-3' and 5'- TCGTGGCTTGTAGTTTCCGA-3'. Copy number variation experiment was performed in ddPCR™ using QX200™ ddPCR™ EvaGreen Supermix loading 0.65 ng of digested *F. vesca* genomic DNA *(Hawaii-4 WT, 7b01.1, 7b01.4b or 7b01.7)* for each reaction. Droplets generation was performed according to manufacturer protocol and PCR was performed using program: 95°C x 5min, 95°C x 30s, 62°C x 1 min, 4°C x 5 min, 90°C x 5 min. Positive droplets were then measured by Qx200™ Droplet Reader and QuantaSoft™ Software using Absolute quantification (ABS) as Data Analysis program. Transgene copy number for genome was calculated as ratio of the *7b01* target concentration to the *ADH-1* concentration, times two (corresponding to copies of the reference gene in a diploid genome).

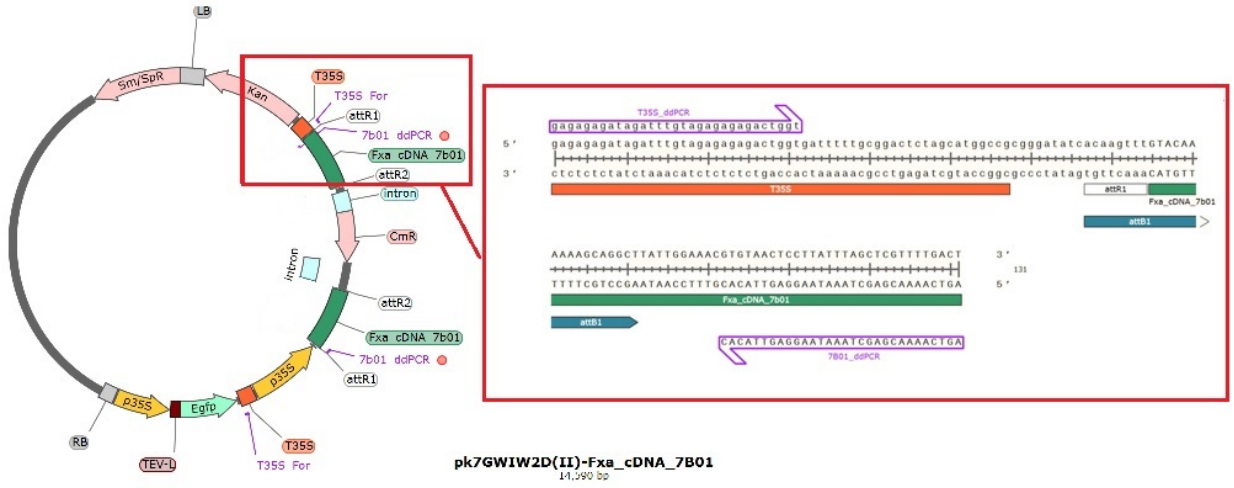

Fig. 7.1M. *7b01 RNAi* silencing construct used to transform *F. vesca Hawaii-4* plants and primers used to detect insertions in ddPCR™. At the left scheme of pk7GWIW2D(II):7b01 construct used to transform *Hawaii-4* plants. Left Border (LB) and Right Border (RB) in grey indicate ends of insertion fragment into the genome. Pink features indicate selectable marker antibiotic resistance coding sequences, kanamycin (Kan), Chloramphenicol (CmR), Spectinomycin (Sm/SpR). Yellow features indicate Cauliflower Mosaic Virus (CaMV) 35S promoter sequence, and orange CaMV T35 terminator. In cyan are represented intron sequences which allow hairpin RNAi structure formation. White background boxes represent attR1 and attR2 recombination sites. In green are represented *7b01* sequences inserts both in sense and in antisense orientation (*Fxa_cDNA_7b01).* In purple are indicated primers positions. At the right in the red box is shown primers used to detect pk7GWIW2D(II):7b01 insertion in *F. vesca* genome.

7.3.4 RNA extraction and expression analysis trough qRT-PCR

Stolons were harvested from *Hawaii-4 wild type, 7b01.1 ,7b01.4b* and *7b01.7* adult plants and immediately frozen in liquid nitrogen. RNA was extracted according to Gambino *et al.* (2008), run on an Agarose 2% gel and measured with NanoDrop™ 3300 for integrity and quality control. cDNA was made starting from 1µg of RNA using Promega ImProm-II™ Reverse Transcription system. qRT-PCR analysis was performed using ThermoFisher MAXIMA SYBR GREEN/ROX QPCR 2x supermix. *RALFs* relative expression was calculated using ΔΔCt method and Elongation Factor gene (*EF1*) as reference (XM_004307362.2). Relative *RALF* expression was calculated as ratio between transgenic and wild *F. vesca* Hawaii-4 type expression. Primers used to measure RALFs gene expression are listed in Table 7.1.

Gene name	Primer For	Primer Rev
FvRALF3	TGGCAAAGTCCTCTTCCATT	AACAAAGCTCAACCCGTGAT
FvRALF4	GGTCTCAAACACAGCCGC	ACGGACATTATTTGCCATCAGT
FvRALF7	TCCAAACTCAGAGACAATCCCA	TGAGTGCATTGAGGTCCAGA
FvRALF13	GCTCAGGCCAACCCGTATAA	CAATAATAACAACAATACACCATCAC
EF1	GCCCATGGTTGTTGAAAGTTTC	GGCGCATGTCCCTCACA

Table 7.1. Pimers used to measure *RALFs* gene expression trough qRTPCR

7.3.5 *7b01* lines vegetative tissues growth evaluation

Plants were grown from seeds in a growth chamber with stable parameters (25°C 16hours light) for 32 weeks, and a population of 25 individuals for each lines (*Hawaii-4 WT, 7b01.1, 7b01.4b, 7b01.7)* was considered for phenotypic characterization. In particular leaves length and width were measured using a 1 mm sensitivity meterstick and considering one completely developed leaf for each individual. Petiole length was measured from plant crown to leaf, considering three petioles for plants. Analysis of variance (ANOVA) was conducted to determine significant differences among groups.

7.3.6 Flowers anatomy and flowering time evaluation

Flowers and fruits mutants phenotypes pictures were taken using Samsung Galaxy A8 smart phone camera. A population of 60 individuals for each line (*Hawaii-4, 7b01.1, 7b01.4b, 7b01.7)* was considered for mutant plant phenotype evaluation. Flowering time was measured as total number of flowers developed in 5 months (from germination) by a population of 20 plants, and as flowering plants percentage of total population, considering the appearance of the first flowering buds. The experiment was repeated three times.

7.3.7 *C. acutatum* pathogenicity assay

Pathogen assay was conducted on a population of five individuals for each transgenic line (*7b01.1, 7b01.4b* and *7b01.7)* and the control *F. vesca Hawaii-4.* The experiment was repeated four times. Adult plants (five months) were grown in the greenhouse at 25°C. *C. acutatum* (Isolate Maya-3, from CRIOF-UniBo fungi collection) was grown on Potato Dextrose Agar for eight days at 24°C, conidia were isolated from plates using distilled water supplemented with one drop of Tween-20. Each plant was sprayed with 2 mL of conidial suspension ($1x10^{-6}$ conidia mL^{-1} concentrated) on leaves, petioles, crown and stolons. Infected plants were covered with a plastic bags for 72 hours to create an high humidity environment and subsequently uncovered. Disease incidence was evaluated after 30 days on stolons, considering rate of plant stolons affected. Disease Incidence= (number of plant

symptomatic stolons/ total number of plant stolon) x 100). Disease severity was calculated considering the number of lesions on stolons (n) ranging from zero to four.

Disease Index = [Σ (number of stolons presenting n lesions × number of lesions (n)) / total number of analyzed stolons]× 100.

7.4 Results and Discussion

7.4.1 7b01 (FvRALF13) F.vesca Hawaii-4 RNAi transgenic plants

In the previous work a partial *FaRALF13-1* transcript (from here called *7b01*) was identified through random Sanger sequencing of a flower cDNA library produced from *Fragaria × ananassa cv. Festival* (Zhang, 2012). Since the octoploid strawberry genome (*Fragaria x ananassa cv. Camarosa)* was recently released, it was possible to subsequently map *7b01* sequence on *Fragaria x ananassa v1* genome, localizing it in a non coding region of chromosome Fvb7-2 (subgenome *F. vesca)* with coordinates Fvb7-2:17454553..17455322.

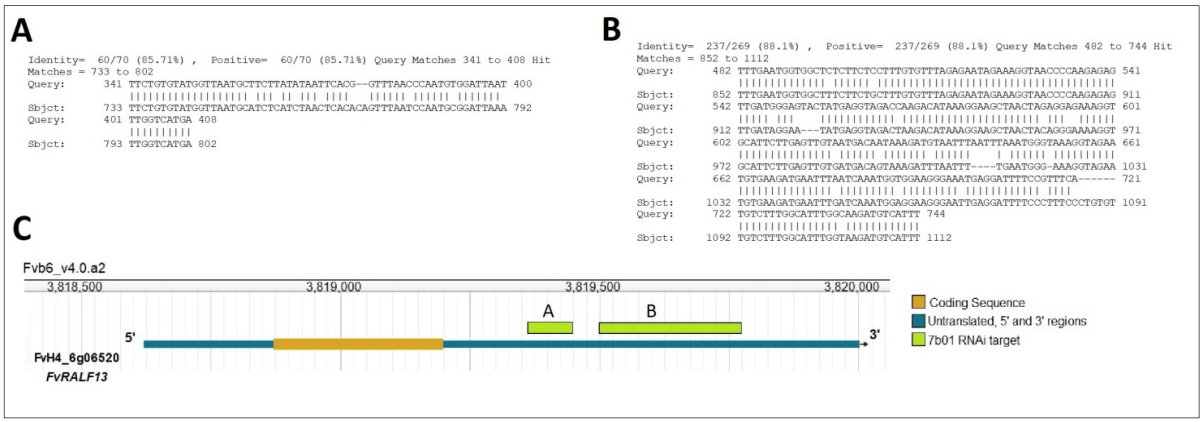

Figure 7.1. 7b01 silencing target on *FvRALF13.* a), b) 7b01 cDNA sequence was aligned with *F. vesca* v4.0.a2 transcripts database using Blastn (GDR). A single hit (*FvH4_6g06520,* here named *FvRALF13)* on chromosome 6 (Fvb6_v4.0.a2) was retrieved, formed by two complementary segments a) and b). **c)** Graphical representation of 7b01 alignment with *FvRALF13* gene and predicted sequences target of RNAi silencing. In orange is represented *FvRALF13* coding sequence, in blue 5' and 3' untranslated regions and in green complementary sequences between 7b01 and *FvRALF13*, which are predicted 7b01 RNAi silencing targets. Numbers and bars indicate nucleotides positions on Fvb6 v4.0.a2 chromosome.

Interestingly, the alignment of *7b01* sequence with Blastn against *F. vesca* v4.0.a2 transcripts database, revealed a single hit corresponding to *FvH4_6g06520* gene, here named *FvRALF13* (Fig.7.1). *7b01* sequence, derived from *Fragaria x ananassa,* has an high identity with two fragments on *F. vesca FvRALF13* 3'-untranslated (3' UTR) region, respectively of 70 nt with an identity of 85.71% (Fig.7.1A) and 269 nt with an identity of 88.1% (Fig.7.1B).Those *FvRALF13* 3'UTR regions are predicted to be target of *7b01* RNAi silencing in *F. vesca Hawaii-4* transgenic plants

(Fig.7.1C). As already reported in the previous chapters, *FvRALF13* is homologous to *Arabidopsis RALF33,* which was found to be involved in immunity response in *Arabidopsis* (Merino et al., 2019)

Since RALF peptides play an important role in roots development (Du *et al.*, 2016; Murphy *et al.*, 2016; Bergonci *et al.*, 2014; Scheer et al., 2005), and roots treatment with exogenous AtRALF1 (Pearce et al., 2001) cause root growth inhibition and reduce capacity of root acidification as much as or *AtRALF23* overexpression in *Arabidopsis* (Srivastava et al., 2009) roots phenotype was firstly analyzed (Zhang, 2012). This first report on *7b01* RNAi plant, revealed typical RALF defective traits, such as major roots growth (Fig.7.2A) and acidification of media adjacent to roots (Fig.7.2B) in transgenic lines compared to WT *Hawaii-4.* Therefore, roots phenotypes observed in *7b01* RNAi transgenic plants can be associated to *FvRALF13* silencing.

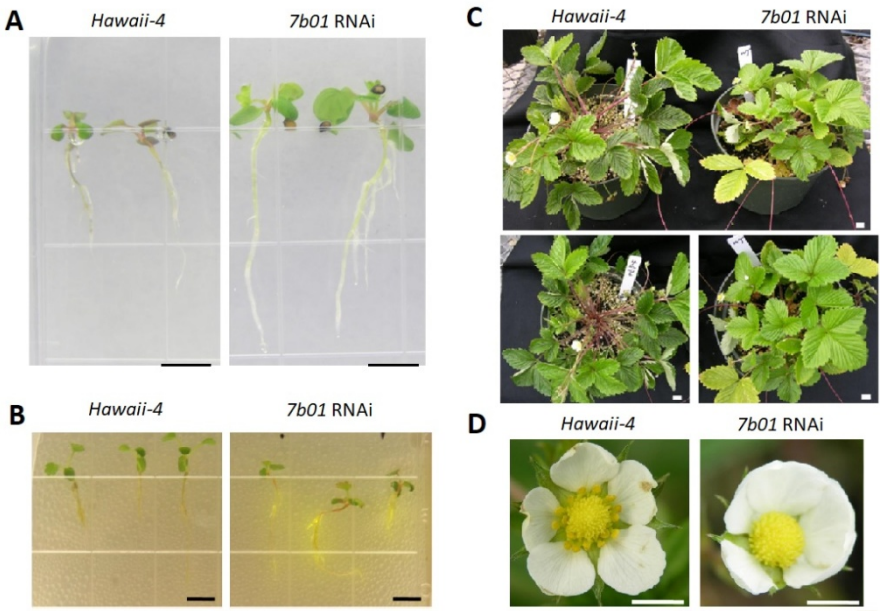

Figure 7.2. *7b01 RNAi* transgenic lines traits. a) *Hawaii-4* and *7b01* RNAi roots growth in 3 weeks strawberry seedlings.b) Acidification of the root adjacent media of *7b01* RNAi lines. Strawberry seedlings were grown vertically on B5 plates for 2 weeks, and then transferred onto plates containing 0.006% bromocresol purple (pH 6.3). The pH indicator is generally yellow below pH 5.2, and purple above pH 6.8. Bars=0.5 cm. Pictures are from Dr. Zhang TingTing PhD thesis presentation (Zhang, 2012).

On the other hand, *7b01* RNAi lines present a peculiar canopy conformation (Fig.7.2C) with longer petioles and hanging leaves which create an open plant structure compared to WT. Furthermore, some of the flowers are lacking or have non functional small stamens, indicating a putative role of *FvRALF13* in male organs development.

In order to further characterize *FvRALF13* function in *F. vesca,* the *7b01* RNAi lines were recovered from K. Folta's lab and grown in greenhouse at DISTAL UniBo and *FvRALF* genes transcriptional regulation analysis was performed together with and phenotypic characterization of flowers and leaves and *C. acutatum* pathogenicity assay.

7.4.2 Transgene copy number analysis in *7b01* trangenic plant

The analysis conducted on *7b01* RNAi woodland strawberries started in 2017 at the University of Florida, from self-pollination seventh generation plants. Due to the instability associated with transgene inheritance and transgenerational epigenetic modifications (Vain et al., 2002), the *7b01* lines were first assessed for the transgene presence and copy number variation using digital droplet PCR (ddPCR™) technique.

Line	*7b01* transgene	Reference (ADH-1)	CN
H4	0	372	0,0
RNAi_1	12,7	331	0,1
RNAi_4b	215	364	1,2
RNAi_7	254	353	1,4

Table.7.2. *7b01* transgene copy number variation among RNAi lines. Copy number was measured for WT *Hawaii-4, 7b01.1, 7b01.4b* and *7b01.7* lines, trough droplet digital PCR using primers to detect *7b01 RNAi* construct (*7b01* transgene) and Aldehide Dehidrogenase 1 gene as single copy reference gene (Reference ADH-1). Green and blue background numbers indicate respectively transgene and reference concentration calculated as numbers of positive events for reaction by QuantaSoft™ software. Copy number (CN) was calculated as ratio of the *7b01* transgene concentration to the Reference gene concentration times two, that is the reference gene copy number in a diploid genome.

According to Copy Number variation experiment (Table 7.2), *7b01.1* population has 0.1 copies of transgene for genome, meaning that only 10% of the plants carry the *7b01*

silencing construct, while 90% have lost the transgene through generations. On the other hand *7b01.4b* and *7b01.7* lines populations have 1.2 and 1.4 copies of transgene for each genome, respectively. The non- discrete transgene copy number detected in *7b01.4b* and *7b01.7* lines might indicate a non homogenous population in which some transgenic plants carry one and some two insertions, probably occurred during transgenerational genomic remodeling or duplication events. However, this analysis was conducted on tissues harvested from a population of 25 plants, thus it was not possible to detect the differences between different individuals.

7.4.3 FvRALF genes expression in *7b01* RNAi transgenic lines

In a previous work (Zhang, 2012), *FvRALF13* expression was measured in different *F. vesca Hawaii-4* tissues, namely runner tip, emerging leaves, mature leaves, flower, fruit, achene, crown, stolon, petiole and root. (Fig.7.3). The analysis showed that *FvRALF13* is highly expressed both in vegetative and in reproductive tissues in particular in fruits, achenes, flowers, stolon and petioles.

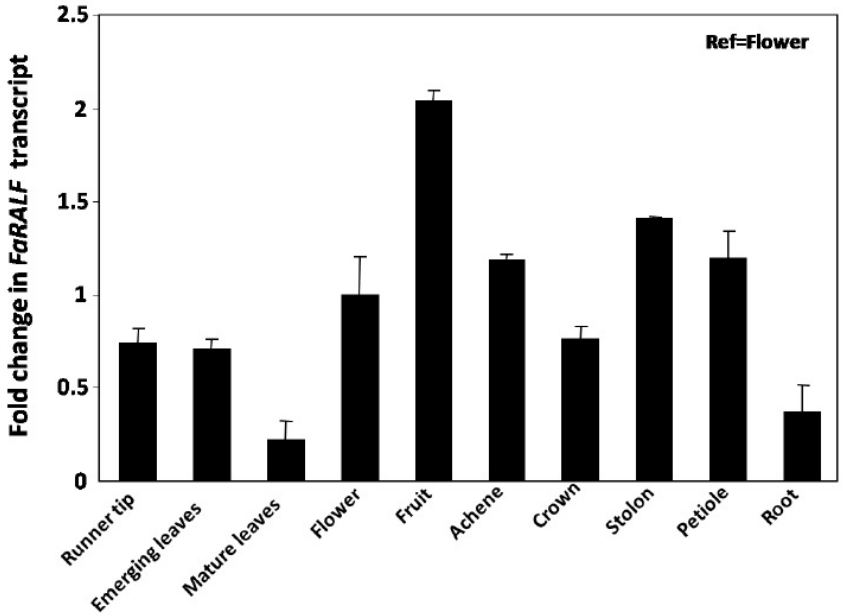

Figure 7.3. Relative expression of *FvRALF13* transcript in various *F. vesca Hawaii-4* tissues. Picture was taken from Zhang PhD dissertation (2012). The flower sample was used as reference tissue and transcripts were quantified against the reference gene using real-time qPCR. Error bars represent standard error of the mean derived from three independent replicates.

In order to assess *FvRALF13* silencing effectiveness and specificity in *7b01* transgenic lines, qRTPCR analysis was performed on stolons harvested from wild type (WT) Hawaii-4, *7b01.1, 7b01.4b* and *7b01.7,* 32 weeks old plants. Predicted RNAi target (*FvRALF13)* and the *FvRALF* family member closest to it (*FvRALF3)* were chosen for expression analysis. Furthermore, two *FvRALF* members with different expression pattern (Fig.2.3) , namely *FvRALF4* and *FvRALF7* genes, were chosen for qRTPCR analysis.

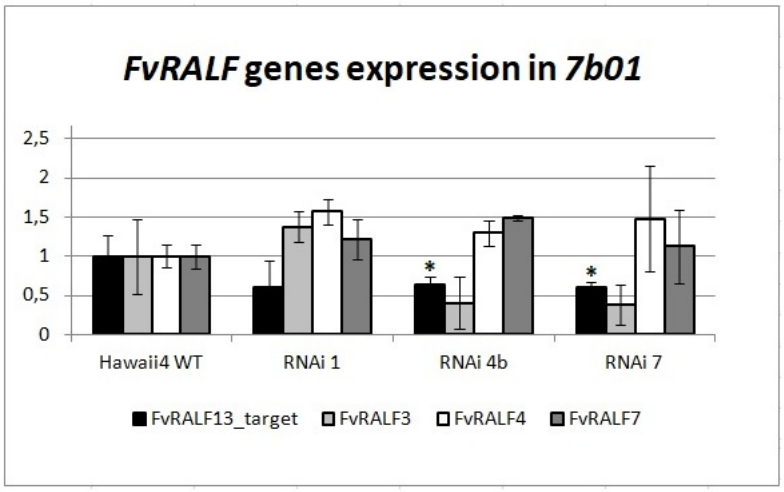

Figure 7.4. *FvRALF* genes expression in *7b01* transgenic lines. qRTPCR expression analysis conducted on wild type (WT) Hawaii-4 and *7b01.1,.4b, .7* transgenic lines. Histograms represents means calculated as fold change between transgenic line and WT expression . Bars represent three biological replicates standard deviation. * indicates t-student test $p<0.05$.

Trascriptional analysis revealed a statistically significant 40% reduction of *FvRALF13* expression in *7b01.4b* and *7b01.7* lines but not in *7b01.1* (Fig.7.4). This results, accordingly to genome analysis (Tab.7.2), reveal the variability associated with *7b01.1* population. On the other hand in *7b01.1, 7b01.4b* and *7b01.7* lines, expression of *FvRALF3, FvRAF4* and *FvRALF7* do not significantly differ from *Hawaii-4* Wild Type.

The results obtained show an effective partial silencing for two out of three transgenic lines analyzed, accordingly with the copy number variation experiment. Furthermore, it was observed a RNAi specific targeting on *FvRALF13*, since none of the other *FvRALF* genes analyzed have shown a significant expression variation.

7.4.4 Vegetative tissues phenotypic characterization

RALF peptides are known to be involved in plant growth regulation, in particular it was reported that overexpression of *AtRALF1* and *AtRALF23* causes a dwarf phenotype (Matos *et al.*, 2008Srivastava *et al.*, 2009), while external application of AtRALF19, 22, 23, 24, 31 and 33 in the medium, inhibits cell elongation in hypocotyl and root cells (Morato do Canto *et al.*, 2014; Murphy and De Smet, 2014). Furthermore, microcalli exposed to exogenous treatment with a surgacane RALF peptide homologous to *AtRALF1* showed a reduced number of elongated cells (Mingossi et al., 2010), indicating a putative role of SacRALF1 in regulating cell expansion. The mechanism behind RALF cell expansion regulation is still unclear, however it was proposed a connection between RALF-induced apoplastic alkalinisation and acid growth theory, which postulate that the precise extracellular pH modulation, plays a central role in cell wall remodelling processes and consequently cell expansion (Hocq et *al.,* 2017). Recently, it has also been reported an involvement of AtRALF1 in the FERONIA mediate signaling of Carbon / Nitrogen source metabolism, which is fundamental for plant growth regulation (Xu et *al., 2019).*

For these reasons, vegetative tissues growth was analyzed in *7b01* RNAi transgenic lines and control *Hawaii-4 WT,* measuring leaves length and width, and petioles elongation (Fig.7.5A). The analysis, conducted on a population of 25 individuals, does not reveal significant differences between transgenic lines and Wild type *Hawaii-4,* for leaves length (Fig.7.5B) and width (Fig.7.5C). Petiole length measurement revealed similar results (Fig.7.5D).

From the results reported, vegetative growth seems to be not affected by *FvRALF13* silencing in *7b01.4b* and *7b01.7* lines, however the variability observed among individuals, within the same populations, which is typical of highly inbred (Slovin et al., 2009), might have affected phenotypic evaluation.

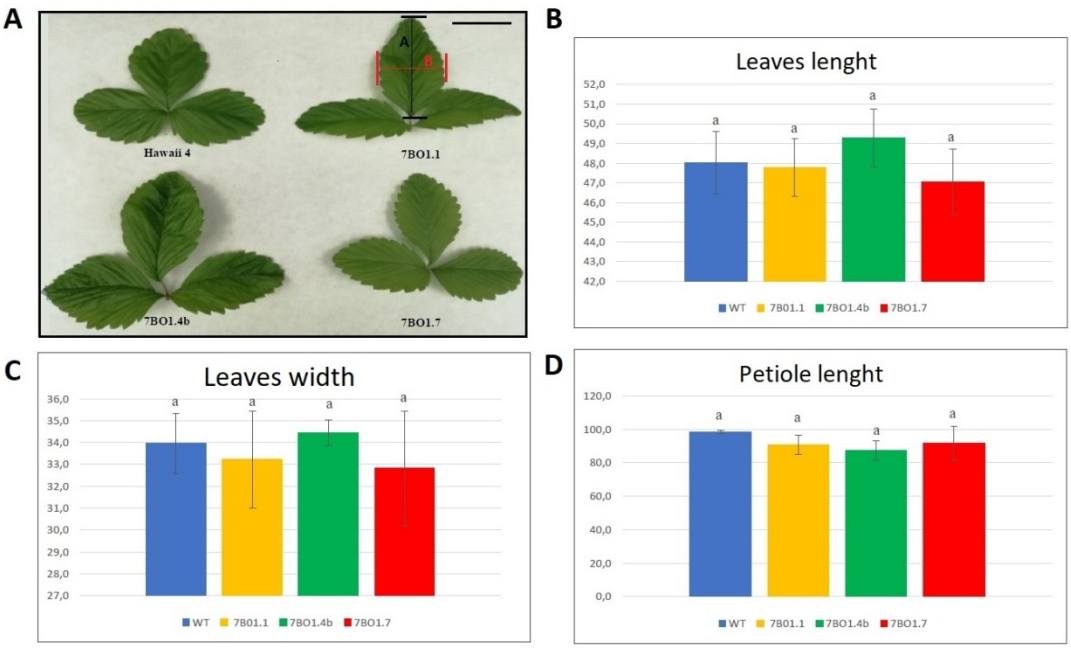

Figure 7.5 . Vegetative growth measure of *7b01* transgenic plants. a) *Hawaii-4 wt, 7b01.1, 7b01.4b* and *7b01.7* representative leaves. B) indicates length measure and C) indicates width measure and petioles length D). The histograms indicates leaves measures of a population of 25 individuals for each line. Black bars indicate standard deviation. Colors identificate different lines: blue for *Hawaii-4,* yellow for *7b01.1,* green for *7b01.4b* and red for *7b01.7.* Letters indicate analysis of variance (ANOVA) groups.

7.4.5 Mutant flower anatomy evaluation

Since in the seventh generation of *7b01* lines, it was observed the same flowers abnormalities previously reported for the first generation by Zhang (2012), it was conducted a flower anatomy evaluation, considering number of stamens and petals of *Hawaii-4, 7b01.1, 7b01.4b* and *7b01.7* lines.

F. vesca Hawaii-4 wild type flowers present five petals and two whorls of ten stamens each, which surround the receptacle. Stamens can be divided into small (S), medium (M) and tall (T) according to pistil length (Fig.7.6A). The outer whorl is formed by ten medium stamens, while the inner one is composed by small and medium alternated stamens (Fig.7.6A) (Hollender et al., 2012).

The transgenic populations analyzed present three different mutant flowers types: type I flowers are formed by ten to twelve stamens, completely developed but lacking the typical double whorl distribution, where only the medium outer stamen circle is visible

(Fig.7.6B); type II flowers show a male sterile phenotype, characterized by the total absence of developed stamens (Fig.7.6C); type III flowers characterized by the presence of one to three stamens, usually not completely formed and presumably not functional (Fig.7.6D).

Wild type *F. vesca Hawaii-4* flowers can generate, by self-pollination, yellow long conic berries (Fig.7.6E). Type I flower mutants are fertile and able to generate berries characterized by abnormal receptacle enlargement and achenes (Fig.7.6F,G). This fruit shape could be due to an inappropriate or incomplete fertilization. On the other hand type II and type III mutants flowers are sterile and in the absence of insects or human hand, they develop a swollen receptacle which will abort.

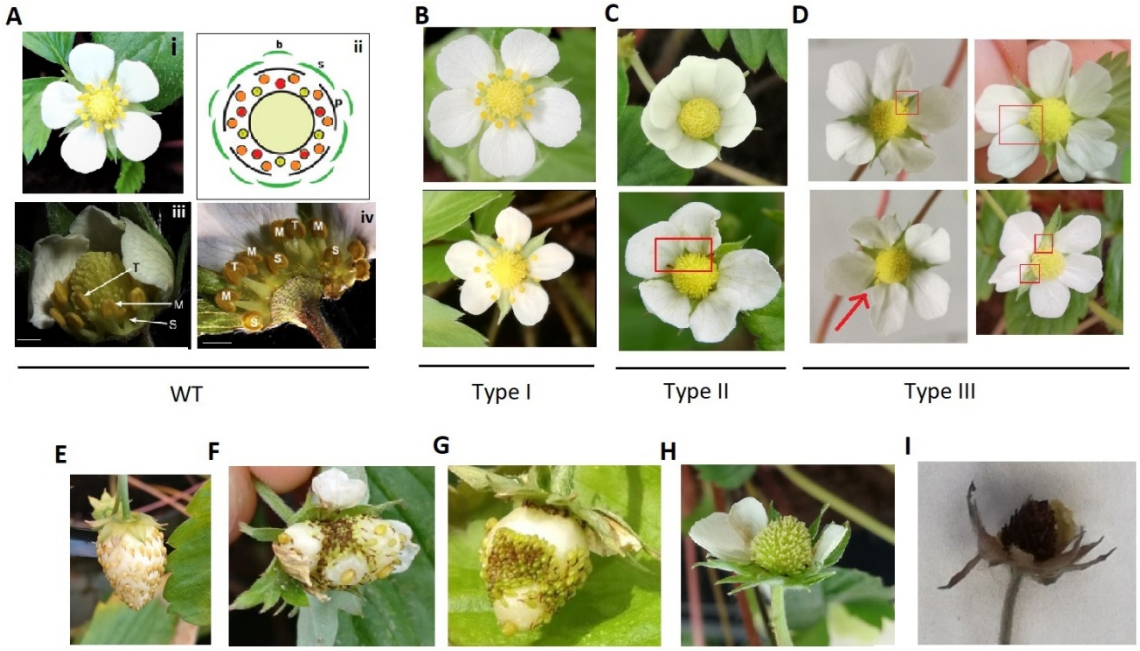

Figure 7.6. Mutants flowers and fruits anatomy evaluation in *7b01* RNAi lines. a) i. *F. vesca Hawaii-4* Wild type flower anatomy. **ii.** Schematic description of stamens organization in two concentric whorls formed by ten external medium pistil length stamens (orange) and ten internal small and long alternate stamens (yellow and red). Bracts (in green, b) petals (p) and sepals (s) are represented. **iii.** and **iv.** Close-range view and dissected view of wild type flower to illustrate tall (T), medium (M) and small (S) stamens pattern. White bars : 1 mm. Figures A.ii, iii and iv were taken from Hollender et *al.,* (2012) and modified. **b)** Type I mutant flower phenotype with ten external stamens. **c)** Type II mutant flower characterized by the absence of stamens. Red box highlight the absence of stamen. **d)** Type III mutant phenotype flower characterized by the presence of one to three stamens (highlighted by arrow and red boxes). **e)** Fruit generated by self-pollination of wild type flowers. **f,g)** Abnormal receptacle shape fruits generated by self-pollination fertilization in type I flowers. **h,i)** Development and abortion of types II and III flowers.

Since the flower anatomy evaluation revealed that individuals within the same *7b01* line population can develop different types of mutants flowers, the percentage of plants developing abnormal flowers was also evaluated, identifying four degrees of mutant phenotype severity: wild type phenotype plants, developing only wild-type flowers, mild phenotype plants developing type I flowers (Fig.7.6B), moderate phenotype plants developing types I, II and III mutant flowers (Fig.7.6B,C,D) and severe phenotype plants developing types II and III mutant flowers (Fig.7.6C,D). Therefore, wild type, mild and moderate flowers are fertile and able to develop fruits, while plants with a severe phenotype are not.

The mutant flower evaluation among individuals of *7b01* lines revealed that 100% of *Hawaii-4,* 60% of *7b01.1,* 10% of *7b01.4b* and 15% of *7b01.7* plants are wild type, developing only wild types flowers (Fig. 7.7). The percentage of plants with mild, medium and severe phenotypes plants are similar in *7b01.4b* and *7b01.7* lines with respecitively 50%, 20% and 20% in *7b01.4b,* and 58%, 18% and 18% in *7b01.7.* The percentage of mutant phenotype in each transgenic line populations associate fairly well with the transgene copy number calculated by ddPCR and with the expression profile shown in the gene expression analysis, with *7b01.1* population including less mild and medium individuals (11% and 3%) and higher number of severe phenotype plants (26%).

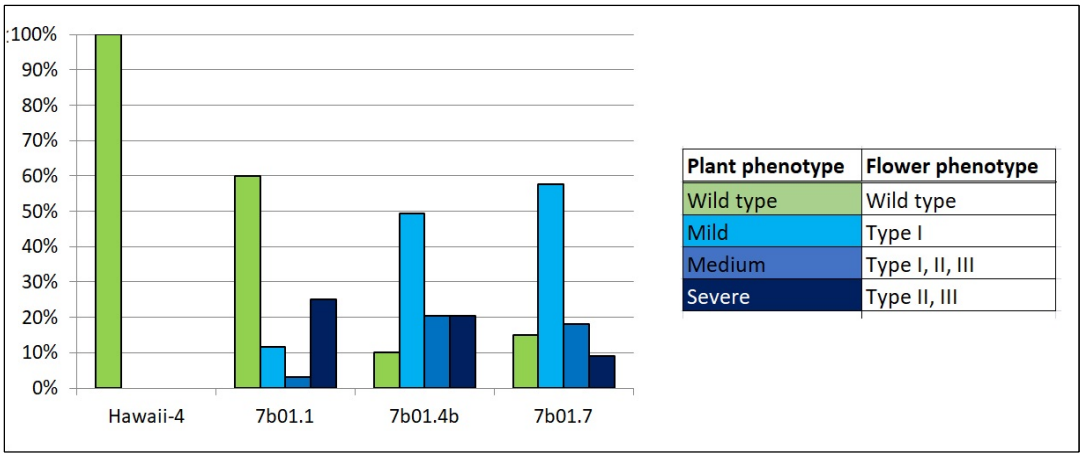

Figure 7.7 Mutants flower evaluation among individuals of *7b01* lines populations. Histogram bars represent number of individuals in terms of percentage of population, which present type I, II and three flower mutants. In particular individuals can develop wild type flower (in green), only type I mutant flower (Mild phenotype plants in cyan), all mutant phenotype types I, II and III (Medium phenotype in blue) or only types II and III phenotypes (severe phenotype in dark blue). Evaluation was done in *Hawaii-4, 7b01.1, 7b01.4b* and *7b01.7* RNAi transgenic lines.

In some cases flowers present six petals (Fig. 7.6C,D) , however this phenomenon was observed also in wild type plants and is caused by the occasionally petaloid stamen development (Hollender et al., 2012) . In some other cases, it was observed that mutant flowers of any type can present supernumerary (more than six) or less than five petals (Fig.7.8). These mutants present also an abnormal sepals and bracts development (Fig.7.8 i, ii).

Floral organs mutants have been extensively studied since Coyer and Meyerowitz proposed, in 1991, the ABC model, based on which floral organs identity determination is regulated by a unique combination of homeotic 'A', 'B', and 'C' gene activities which specifies each of the four flower whorls namely sepals, petals, stamens and pistil (Coen and Meyerowitz, 1991; Causier et *al.,* 2010, Irish, 2017).

Figure 7.8 Petals and sepals abnormalities observed in *7b01* transgenic plants. i) mutant flower type II with seven petals and supernumerary sepals. ii) mutant flower type II with four petals and five sepals. iii) Mutant flower type II with seven petals and abnormal sepals development. iv) Mutant flower type I with 8 petals and five sepals. Red bars = 0.5 cm.

The floral organ identity abnormalities observed in *7b01* transgenic lines concerning stamen and petals number, remind the homeotic mutants deficiencies and could suggest that *FvRALF13* is involved in floral fate tissue determination. However, this few considerations are not sufficient to consider this hypothesis and need to be confirmed by further analysis.

7.4.6 Flowering time and flowers abundance analysis

Timing and frequency of the transition from vegetative to reproductive state are genetically regulated mechanisms critical for genetic improvement of strawberry in order to increase flower and fruits production. For these reasons, flowering time and number of flowers, were evaluated in *Hawaii-4, 7b01.1, 7b01.4b* and *7b01.1* lines.

The flowering time analysis (Fig.7.9A) revealed that *7b01* transgenic lines flowers earlier than *Hawaii-4,* since after two months from germination flower buds are already apparent in *7b01* lines appear, while in *Hawaii-4* plants flowers develop only after four months. The flowering time rate is comparable in three transgenic lines analyzed.

The abundance of flowers observed in *7b01* lines was determined counting the number of flowers with mutant phenotype developed by each plant line (Fig.7.9B). The analysis conducted revealed that in all the three *7b01* lines the major contribution in terms of flower abundance comes from moderate and severe phenotype plants, while flowers abundance in mild phenotype plants is similar to wild type with an average of one-two flowers per plants.

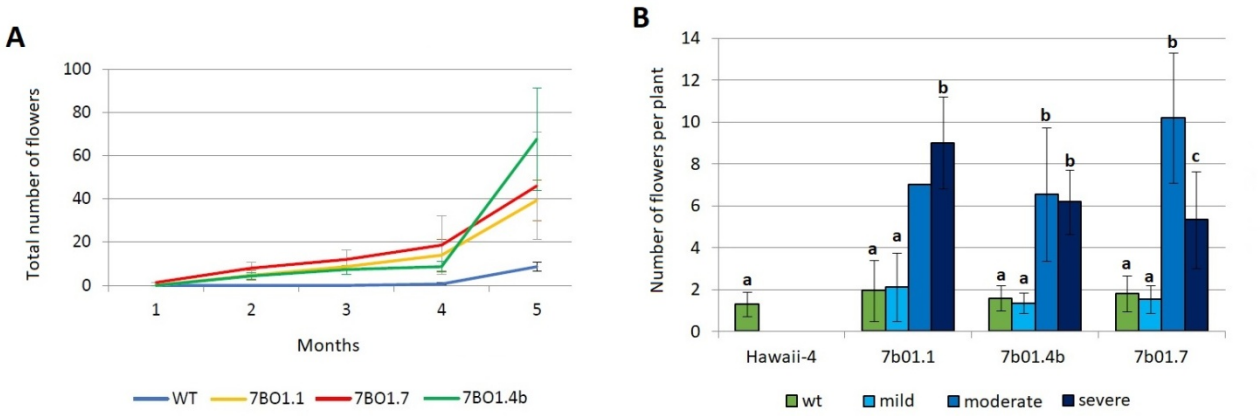

Figure 7.9 Flowering time evaluation and flowers differentiation abundance measure in *7b01* lines. a) Lines represents *Hawaii-4,7b01.1, 7b01.4b* and *7b01.7* lines total number of flowers measured once a moths for five months. **b)** Histogram bars represents total number of flowers per plants, considering mutant flower phenotype types. Individual were classified as wild type, mild, moderate or severe phenotypes. See Fig.5.6. Measures in a,b) were conducted in a population of 20 individuals, and the experiment was repeated three times. Points represents means and bars standard deviation between the three replicates. Letters indicate ANOVA homogenous groups.

The earlier flowering time and the flowers abundance observed in *7b01* plants, revealed a putative role of *FvRALF13* as negative regulator of the vegetative-reproductive phase transition, since *FaRALF13-1* expression is decreased in *7b01* RNAi plants. Furthermore, the higher rate of reproductive tissues differentiation observed in moderate and severe phenotypes plants (with types II and III mutant flowers), indicate that individuals with significant deficiencies in flower anatomy have also an abnormal flower development regulation.

Shoot meristem differentiation from a vegetative state into floral organs is a strictly regulated process, under the control of coordinated and interlinked pathways which responds to internal and environmental stimuli. Until now, five genetically defined pathways have been identified: the vernalization pathway depending on cold-exposure and mediated by chromatin remodeling and lncRNA(Heo & Sung, 2011), the photoperiod pathway, depending on day length and quality of light perceived, the gibberellins pathway regulated by gibberellic acid and the autonomous pathway depending on endogenous regulators that are independent from the photoperiod and gibberellin pathways. These flowering pathways converge on a small number of floral integrator genes, namely, *FLORAL TRANSITION (FT), SUPPRESSOR OF OVEREXPRESSION OF CONSTANS (SOC1)* and *FLOWERING LOCUS D (FD*), which initiate the early stages of flowering promoting the expression of floral meristem identity genes such as *APETALA1 (AP1),*

FRUITFUL (FUL), LEAFY (LFY), and *CAULIFLOWER (CAL)* which convert the vegetative meristem to a floral fate (Andrés & Coupland, 2012)(Andrés & Coupland, 2012).

The accelerated flowering observed in *7b01 RNAi* plants could suggest that *FvRALF13* is involved as growth regulator during cell differentiation process. This hypothesis should be tested with further analysis.

7.4.7 C. acutatum pathogenicity assay

Besides the roles of RALF peptides as growth regulator of pollen tube, leaves, roots and ipocotyl (Ge *et al.*, 2017(Ge et al., 2017; Du *et al.*, 2016; Murphy et al., 2016; Morato do Canto et al., 2014), also are implicated in the plant immune response as signaling effectros. In particular it was demonstrated that *AtRALF23* and *AtRALF33* in *Arabidopsis* are negative regulators of immunity complex formation (EFR/FLS2-BAK1) in bacterial infection (Stegmann et al., 2017)(Stegmann et al., 2017). For these reasons, the *7b01* RNAi plants susceptibility to *C. acutatum* was assessed.

Susceptibility assay was performed on *7b01.1,7b01.4b, 7b01.7* lines and *Hawaii-4* as control. At 30 days post infection, symptoms were visible on stolons as oval elongated dark lesions (Fig.7.10A), but they were not observed on leaves, flowers and fruits. Disease incidence was then evaluated as percentage of infected stolons per plant (Fig.7.10B), and disease index was calculated considering number of lesions visible on each stolon (Fig.7.10C). The analysis revealed that there are no significant differences between transgenic lines and control in disease incidence (Fig.7.10B), since plants are equally infected by the pathogen. However, the symptoms appear less severe in *7b01.7* line which presents less lesions compared to wild type (Fig.7.10C).

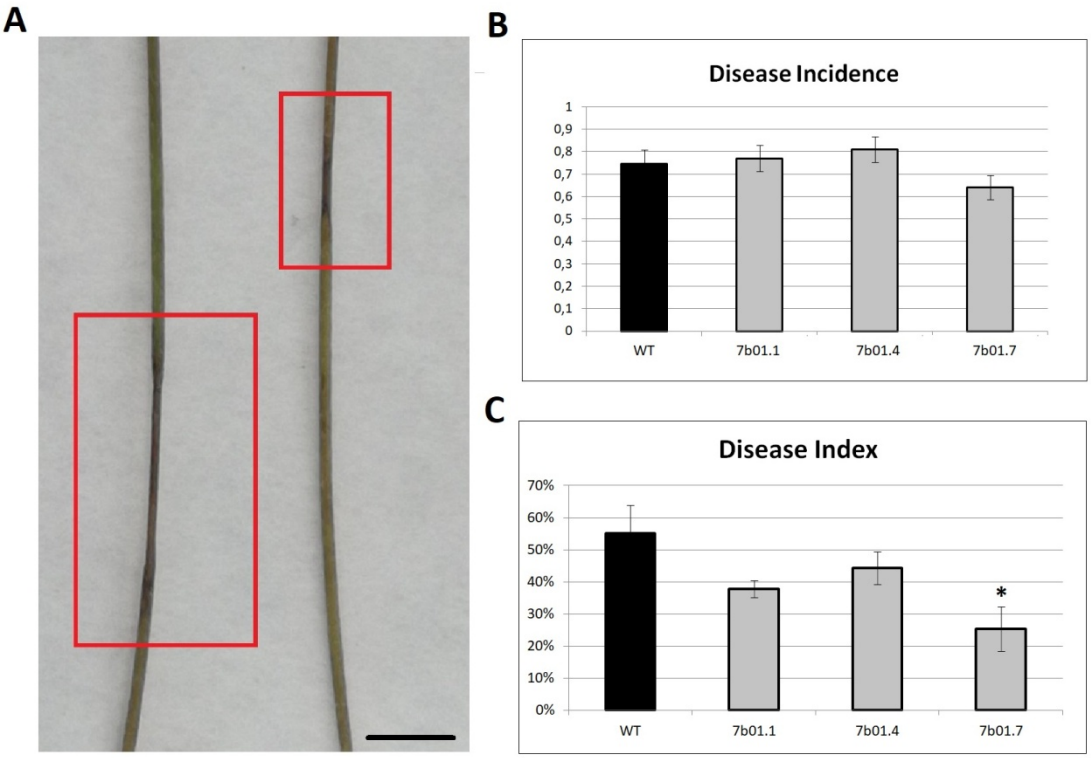

Figure 7.10. *C. acutatum* infection assay on *7b01* transgenic lines. a) *C. acutatum* symptoms on *F.vesca Hawaii-4* stolons. Lesions are indicated by red boxes. Black bar = 1 cm. b) Disease incidence is calculated as rate of symptomatic stolons on total stolons number per plant. c) Disease Index was calculated considering the number of lesions on stolons. Evaluation was conducted on five plants and repeated four times. Histogram bars represent mean values and black bars represent standard deviation. T student test p-value < 0.05 is indicated by *.

As already discussed in the previous chapters, *FvRALF* genes expression is modulated by post-harvest pathogens infection such as *C. acutatum* and *B. cinerea.* In particular *FvRALF3* is upregulated and *FvRALF1 ,6, 7, 9* are downregulated at 24 hours post infection in fruits. On the other side, *FvRALF8* and *FvRALF13* expression are not altered by pathogens attack, suggesting that it may not have a role in plant immunity response. Nevertheless, the reduced susceptibility observed as number of lesions for stolon in *7b01.7,* may indicate an indirect involvement of *FvRALF13* in pathogen infection response.

7.5 Conclusions

In conclusion, from the analyses conducted on RNAi lines silenced for *FvRALF13* gene emerge a possible involvement of *FvRALF13* in flower development regulation in terms of flowering timing and male reproductive organs formation. However, it remains unknown the mechanism behind this regulation, and further analyses will be required to further investigate RALF signalling during flower development. On the other hand, no significant growth deficiencies were detected in vegetative tissue of *FvRALF13* RNAi plants and even though the sequence similarity of *FvRALF13* with *FvRALF3,* which is involved in fruit susceptibility in *Fragaria x ananassa* (Merino et al., 2019)(Merino et al., 2019), no significant *C. acutaum* susceptibility decrease was observed during pathogenicity assay, .

8. Concluding Remarks

Rapid Alkalinization Factors are small signal peptides with multiple roles in plant growth, fertilization and immunity regulations. RALF homologues genes are also expressed by many fungal plant pathogens as infection effectors, and on the other hand RALF genes are upregulated in different plant hosts upon pathogens attack, suggesting a role as susceptibility factors during plant pathogen interaction.

This study aimed to characterize RALF genes family as susceptibility effectors in strawberry through different study approaches.

In conclusion, this study revealed that RALF gene family distribution among *Fragaria x ananassa* subgenome is consistent with octoploid polyploid genome evolution, which is characterized by subgenomes different TE activity and subsequently different genes content.

Furthermore RALF expression analysis in fruits upon *C. acutatum* and *B. cinerea* infections revealed a specific upregulation of *FaRALF3-1* gene during early stages of infections which was supported by susceptibility analyses conducted trough *Agrobacterium* mediated *FaRALF3-1* overexpression in fruits. The *FaRALF3-1* induction in white fruits allowed more fungal penetetration trough host tissue and severe symptoms development.

FaRALF3-1 predicted promoter i*n silico* analyses revealed a putative involvement of a MYB transcription factor as regulator of *FaRALF3-1* infection-inducibility. Furthermore, agroinfilitration-mediated *FaRALF3-1* promoter reporter assay revealed that the 400 bp upstream start codon can drive expression in strawberry fruits.

Since FaRALF3-1 presents the same conserved N-terminal sequence of AtRALF23 it has also been speculated that, consistently with motif conservation, FaRALF interaction with receptor FERONIA (MRLK47) and the coreceptor FaLLG2 follows the *Arabidopsis* complex interaction structure. However further analyses will be required to confirm the effective interaction between FaRALF3 and FaMRLK47 in strawberry.

Moreover, *F. vesca* RNAi transgenic lines targeting *FvRALF13* have been characterized genotipically and phenotypically, revealing a possible involvement of *FvRALF13* in flower development regulation in terms of flowering timing and male reproductive organs formation.

9. Bibliography

Abe, H., Urao, T., Ito, T., Seki, M., Shinozaki, K., & Yamaguchi-Shinozaki, K. (2003). Arabidopsis AtMYC2 (bHLH) and AtMYB2 (MYB) function as transcriptional activators in abscisic acid signaling. *The Plant Cell*.

Alkan, N., Prusky, D., Fluhr, R., Friedlander, G., & Ment, D. (2014). Simultaneous transcriptome analysis of Colletotrichum gloeosporioides and tomato fruit pathosystem reveals novel fungal pathogenicity and fruit defense strategies. *New Phytologist*, *205*(2), 801–815. https://doi.org/10.1111/nph.13087

Amil-Ruiz, F., Blanco-Portales, R., Muñoz-Blanco, J., & Caballero, J. L. (2011). The strawberry plant defense mechanism: A molecular review. *Plant and Cell Physiology*, *52*(11), 1873–1903. https://doi.org/10.1093/pcp/pcr136

Anand, L. (2019). chromoMap: An R package for Interactive Visualization and Annotation of Chromosomes. *BioRxiv*. https://doi.org/10.1101/605600

Andrés, F., & Coupland, G. (2012). The genetic basis of flowering responses to seasonal cues. *Nature Reviews Genetics*, *13*(9), 627–639. https://doi.org/10.1038/nrg3291

Atkinson, N. J., Lilley, C. J., & Urwin, P. E. (2013). Identification of Genes Involved in the Response of Arabidopsis to Simultaneous Biotic and Abiotic Stresses. *Plant Physiology*, *162*(4), 2028–2041. https://doi.org/10.1104/pp.113.222372

Bergonci, T., Ribeiro, B., Ceciliato, P. H. O., Guerrero-Abad, J. C., Silva-Filho, M. C., & Moura, D. S. (2014). Arabidopsis thaliana RALF1 opposes brassinosteroid effects on root cell elongation and lateral root formation. *Journal of Experimental Botany*, *65*(8), 2219–2230. https://doi.org/10.1093/jxb/eru099

Boa, E. (2003). Compendium of Corn Diseases, 3rd Edition. Edited by Donald G. White. 8 1 / 2 × 11 inches, 78 pp. St Paul, USA: American Phytopathological Society Press (http://www.scisoc.org), 1999. US$42. ISBN 089054 234 1 (soft covers).Compendium of Strawberry Diseas. *Plant Pathology*. https://doi.org/10.1046/j.1365-3059.2001.00529-3.x

Brown, S. H., Yarden, O., Gollop, N., Chen, S., Zveibil, A., Belausov, E., & Freeman, S. (2008). Differential protein expression in Colletotrichum acutatum: Changes associated with reactive oxygen species and nitrogen starvation implicated in pathogenicity on strawberry. *Molecular Plant Pathology*. https://doi.org/10.1111/j.1364-3703.2007.00454.x

Campbell, L., & Turner, S. R. (2017). A Comprehensive Analysis of RALF Proteins in Green Plants Suggests There Are Two Distinct Functional Groups. *Frontiers in Plant Science*, *8*(January), 1–14. https://doi.org/10.3389/fpls.2017.00037

Causier, B., Schwarz-Sommer, Z., & Davies, B. (2010). Floral organ identity: 20 years of ABCs. *Seminars in Cell and Developmental Biology*, *21*(1), 73–79. https://doi.org/10.1016/j.semcdb.2009.10.005

Chatterjee, M., Bermudez-Lozano, C. L., Clancy, M. A., Davis, T. M., & Folta, K. M. (2011). A strawberry KNOX gene regulates leaf, flower and meristem architecture. *PLoS ONE*. https://doi.org/10.1371/journal.pone.0024752

Chen, J., Yu, F., Liu, Y., Du, C., Li, X., Zhu, S., … Lan, W. (2016). *FERONIA interacts with ABI2-type phosphatases to facilitate signaling cross-talk between abscisic acid and RALF peptide in Arabidopsis*. 5519–5527. https://doi.org/10.1073/pnas.1608449113

Coen, E. S., & Meyerowitz, E. M. (1991). *The war of the whorls : genetic interactions controlling flower development*. *353*(September), 31–37.

Covey, P. A., Subbaiah, C. C., Parsons, R. L., Pearce, G., Lay, F. T., Anderson, M. A., … Bedinger, P. A. (2010). A Pollen-Specific RALF from Tomato That Regulates Pollen Tube Elongation. *Plant Physiology*, *153*(2), 703–715. https://doi.org/10.1104/pp.110.155457

De Lorenzo, G., D'Ovidio, R., & Cervone, F. (2001). The role of polygalacturonase-inhibiting proteins (PGIPs) in defense against pathogenic fungi. *Annual Review of Phytopathology*.

DiMeglio, L. M., Staudt, G., Yu, H., & Davis, T. M. (2014). A phylogenetic analysis of the genus Fragaria (strawberry) using intron-containing sequence from the ADH-1 gene. *PLoS ONE*. https://doi.org/10.1371/journal.pone.0102237

Dobón, A., Canet, J. V., García-Andrade, J., Angulo, C., Neumetzler, L., Persson, S., & Vera, P. (2015). Novel Disease Susceptibility Factors for Fungal Necrotrophic Pathogens in Arabidopsis. *PLoS Pathogens*, *11*(4), 1–30. https://doi.org/10.1371/journal.ppat.1004800

Du, C., Li, X., Chen, J., Chen, W., Li, B., Li, C., … Yu, F. (2016a). Receptor kinase complex transmits RALF peptide signal to inhibit root growth in Arabidopsis . *Proceedings of the National Academy of Sciences*. https://doi.org/10.1073/pnas.1609626113

Du, C., Li, X., Chen, J., Chen, W., Li, B., Li, C., … Yu, F. (2016b). Receptor kinase complex transmits RALF peptide signal to inhibit root growth in Arabidopsis . *Proceedings of the National Academy of Sciences*, *113*(51), E8326–E8334. https://doi.org/10.1073/pnas.1609626113

Dünser, K., Gupta, S., Herger, A., Feraru, M. I., Ringli, C., & Kleine-Vehn, J. (2019). Extracellular matrix sensing by FERONIA and Leucine-Rich Repeat Extensins controls vacuolar expansion during cellular elongation in Arabidopsis thaliana . *The EMBO Journal*, *38*(7), 1–12. https://doi.org/10.15252/embj.2018100353

E., G., B.J., D., B., B., & T., P. (1994). The myb-homologous P gene controls phlobaphene pigmentation in maize floral organs by directly activating a flavonoid biosynthetic gene subset. *Cell*. https://doi.org/10.1016/0092-8674(94)90117-1

Edgar, R. C. (2004). MUSCLE: multiple sequence alignment with high accuracy and high throughput. *Nucleic Acids Research*. https://doi.org/10.1093/nar/gkh340

Edger, P. P., Poorten, T. J., VanBuren, R., Hardigan, M. A., Colle, M., McKain, M. R., … Knapp, S. J. (2019). Origin and evolution of the octoploid strawberry genome. *Nature Genetics*, *51*(March). https://doi.org/10.1038/s41588-019-0356-4

Feliziani, E., & Romanazzi, G. (2016). Postharvest decay of strawberry fruit: Etiology, epidemiology, and disease management. *Journal of Berry Research*, *6*(1), 47–63.

https://doi.org/10.3233/JBR-150113

Feng, W., Kita, D., Peaucelle, A., Cartwright, H. N., Doan, V., Duan, Q., … Dinneny, J. R. (2018). The FERONIA Receptor Kinase Maintains Cell-Wall Integrity during Salt Stress through Ca 2+ Signaling. *Current Biology*. https://doi.org/10.1016/j.cub.2018.01.023

Fernandes, T. R., Segorbe, D., Prusky, D., & Di Pietro, A. (2017). How alkalinization drives fungal pathogenicity. *PLOS Pathogens*, *13*(11), e1006621. https://doi.org/10.1371/journal.ppat.1006621

Folta, K. M., & Barbey, C. R. (2019). The strawberry genome: a complicated past and promising future. *Horticulture Research*, *6*(1), 97. https://doi.org/10.1038/s41438-019-0181-z

Forlani, S., Masiero, S., & Mizzotti, C. (2019). Fruit ripening: the role of hormones, cell wall modifications, and their relationship with pathogens. *Journal of Experimental Botany*. https://doi.org/10.1093/jxb/erz112

Galindo-Trigo, S., Gray, J. E., & Smith, L. M. (2016). Conserved Roles of CrRLK1L Receptor-Like Kinases in Cell Expansion and Reproduction from Algae to Angiosperms. *Frontiers in Plant Science*. https://doi.org/10.3389/fpls.2016.01269

Gambino, G., Perrone, I., & Gribaudo, I. (2008). A rapid and effective method for RNA extraction from different tissues of grapevine and other woody plants. *Phytochemical Analysis*. https://doi.org/10.1002/pca.1078

Ge, Z., Bergonci, T., Zhao, Y., Zou, Y., Du, S., Liu, M. C., … Qu, L. J. (2017). Arabidopsis pollen tube integrity and sperm release are regulated by RALF-mediated signaling. *Science*. https://doi.org/10.1126/science.aao3642

Ge, Z., Cheung, A. Y., & Qu, L. J. (2019). Pollen tube integrity regulation in flowering plants: insights from molecular assemblies on the pollen tube surface. *New Phytologist*. https://doi.org/10.1111/nph.15645

Gonneau, M., Desprez, T., Martin, M., Doblas, V. G., Bacete, L., Miart, F., … Höfte, H. (2018). Receptor Kinase THESEUS1 Is a Rapid Alkalinization Factor 34 Receptor in Arabidopsis. *Current Biology*, *28*(15), 2452-2458.e4. https://doi.org/10.1016/j.cub.2018.05.075

Grace, M. L., Chandrasekharan, M. B., Hall, T. C., & Crowe, A. J. (2004). Sequence and Spacing of TATA Box Elements Are Critical for Accurate Initiation from the β-Phaseolin Promoter. *Journal of Biological Chemistry*. https://doi.org/10.1074/jbc.M309376200

Guidarelli, M., Carbone, F., Mourgues, F., Perrotta, G., Rosati, C., Bertolini, P., & Baraldi, E. (2011). Colletotrichum acutatum interactions with unripe and ripe strawberry fruits and differential responses at histological and transcriptional levels. *Plant Pathology*, *60*(4), 685–697. https://doi.org/10.1111/j.1365-3059.2010.02423.x

Haruta, M., Sabat, G., Stecker, K., Minkoff, B. B., & Sussman, M. R. (2014). A peptide hormone and its receptor protein kinase regulate plant cell expansion. *Science*, *343*(6169), 408–411. https://doi.org/10.1126/science.1244454

Heo, J. B., & Sung, S. (2011). Vernalization-mediated epigenetic silencing by a long intronic noncoding RNA. *Science (New York, N.Y.)*, *331*(6013), 76–79.

https://doi.org/10.1126/science.1197349

Higo, K., Ugawa, Y., Iwamoto, M., & Higo, H. (1998). *PLACE : a database of plant cis-acting regulatory DNA elements*. *26*(1), 358–359.

Hocq, L., Pelloux, J., & Lefebvre, V. (2017). Connecting Homogalacturonan-Type Pectin Remodeling to Acid Growth. *Trends in Plant Science*, *22*(1), 20–29. https://doi.org/10.1016/j.tplants.2016.10.009

Hollender, C. A., Geretz, A. C., Slovin, J. P., & Liu, Z. (2012). Flower and early fruit development in a diploid strawberry, Fragaria vesca. *Planta*, *235*(6), 1123–1139. https://doi.org/10.1007/s00425-011-1562-1

Howard, C. M. (1992). Anthracnose of Strawberry Caused by the Colletotrichum Complex in Florida . *Plant Disease*. https://doi.org/10.1094/pd-76-0976

Hughes, J. D., Estep, P. W., Tavazoie, S., & Church, G. M. (2000). Computational identification of Cis-regulatory elements associated with groups of functionally related genes in Saccharomyces cerevisiae. *Journal of Molecular Biology*, *296*(5), 1205–1214. https://doi.org/10.1006/jmbi.2000.3519

Irish, V. (2017). The ABC model of floral development. *Current Biology*, *27*(17), R887–R890. https://doi.org/10.1016/j.cub.2017.03.045

Jain, S. (2015). The Pathogenesis Related Class 10 proteins in Plant Defense against Biotic and Abiotic Stresses. *Advances in Plants & Agriculture Research*. https://doi.org/10.15406/apar.2015.02.00077

JARVIS, W. R. (1962). The infection of strawberry and raspberry fruits by Botrytis cinerea Fr. *Annals of Applied Biology*. https://doi.org/10.1111/j.1744-7348.1962.tb06049.x

Jia, M., Ding, N., Zhang, Q., Xing, S., Wei, L., Zhao, Y., … Jia, W. (2017). A FERONIA-Like Receptor Kinase Regulates Strawberry (Fragaria × ananassa) Fruit Ripening and Quality Formation. *Frontiers in Plant Science*, *8*(June), 1–14. https://doi.org/10.3389/fpls.2017.01099

Jones, D. T., Taylor, W. R., & Thornton, J. M. (1992). The rapid generation of mutation data matrices from protein sequences. *Bioinformatics*. https://doi.org/10.1093/bioinformatics/8.3.275

Karimi, M., Inze, D., & Depicker, A. (2002). GATEWAY^{TM} vectors for *Agrobacterium*-mediated plant transformation. *Trends in Plant Science*.

Klepper, K., & Drabløs, F. (2013). *MotifLab : a tools and data integration workbench for motif discovery and regulatory sequence analysis*.

Kumar, S., Stecher, G., Li, M., Knyaz, C., & Tamura, K. (2018). MEGA X: Molecular evolutionary genetics analysis across computing platforms. *Molecular Biology and Evolution*, *35*(6), 1547–1549. https://doi.org/10.1093/molbev/msy096

Li, C., Yeh, F. L., Cheung, A. Y., Duan, Q., Kita, D., Liu, M. C., … Wu, H. M. (2015). Glycosylphosphatidylinositol-anchored proteins as chaperones and co-receptors for FERONIA receptor kinase signaling in Arabidopsis. *ELife*. https://doi.org/10.7554/eLife.06587

Li, M. Z., & Elledge, S. J. (2007). Harnessing homologous recombination in vitro to generate recombinant DNA via SLIC. *Nature Methods*. https://doi.org/10.1038/nmeth1010

Li, Y., Pi, M., Gao, Q., Liu, Z., & Kang, C. (2019). Updated annotation of the wild strawberry Fragaria vesca V4 genome. *Horticulture Research*, *6*(1). https://doi.org/10.1038/s41438-019-0142-6

Liu, J., Osbourn, A., & Ma, P. (2015). MYB transcription factors as regulators of phenylpropanoid metabolism in plants. *Molecular Plant*, *8*(5), 689–708. https://doi.org/10.1016/j.molp.2015.03.012

Masachis, S., Segorbe, D., Turrà, D., Leon-Ruiz, M., Fürst, U., El Ghalid, M., … Di Pietro, A. (2016). A fungal pathogen secretes plant alkalinizing peptides to increase infection. *Nature Microbiology*, *1*(6). https://doi.org/10.1038/nmicrobiol.2016.43

Matos, J. L., Fiori, C. S., Silva-Filho, M. C., & Moura, D. S. (2008). A conserved dibasic site is essential for correct processing of the peptide hormone AtRALF1 in Arabidopsis thaliana. *FEBS Letters*. https://doi.org/10.1016/j.febslet.2008.08.025

Mecchia, M. A., Ringli, C., Boisson-Dernier, A., Santos-Fernandez, G., Martínez-Bernardini, A., Grossniklaus, U., … Gagliardini, V. (2017). RALF4/19 peptides interact with LRX proteins to control pollen tube growth in Arabidopsis . *Science*, *1*(December), eaao5467. https://doi.org/10.1126/science.aao5467

Merida, A., Mackay, S., Culianez-Macia, F. A., Parr, A., Roberts, K., Martin, C., & Tamagnone, L. (2007). The AmMYB308 and AmMYB330 Transcription Factors from Antirrhinum Regulate Phenylpropanoid and Lignin Biosynthesis in Transgenic Tobacco. *The Plant Cell*. https://doi.org/10.2307/3870694

Merino, M. C., Guidarelli, M., Negrini, F., De Biase, D., Pession, A., & Baraldi, E. (2019). *Induced expression of the Fragaria × ananassa Rapid alkalinization factor-33-like gene decreases anthracnose ontogenic resistance of unripe strawberry fruit stages*. 1–12.

Mingossi, F. B., Matos, J. L., Rizzato, A. P., Medeiros, A. H., Falco, M. C., Silva-Filho, M. C., & Moura, D. S. (2010). SacRALF1, a peptide signal from the grass sugarcane (Saccharum spp.), is potentially involved in the regulation of tissue expansion. *Plant Molecular Biology*. https://doi.org/10.1007/s11103-010-9613-8

Minkoff, B. B., Makino, S. I., Haruta, M., Beebe, E. T., Wrobel, R. L., Fox, B. G., & Sussman, M. R. (2017). A cell-free method for expressing and reconstituting membrane proteins enables functional characterization of the plant receptor-like protein kinase FERONIA. *Journal of Biological Chemistry*. https://doi.org/10.1074/jbc.M116.761981

Morato do Canto, A., Ceciliato, P. H. O., Ribeiro, B., Ortiz Morea, F. A., Franco Garcia, A. A., Silva-Filho, M. C., & Moura, D. S. (2014a). Biological activity of nine recombinant AtRALF peptides: Implications for their perception and function in Arabidopsis. *Plant Physiology and Biochemistry*, *75*, 45–54. https://doi.org/10.1016/j.plaphy.2013.12.005

Morato do Canto, A., Ceciliato, P. H. O., Ribeiro, B., Ortiz Morea, F. A., Franco Garcia, A. A., Silva-Filho, M. C., & Moura, D. S. (2014b). Biological activity of nine recombinant AtRALF peptides: Implications for their perception and function in Arabidopsis. *Plant Physiology and Biochemistry*. https://doi.org/10.1016/j.plaphy.2013.12.005

Moussu, S., Augustin, S., Roman, A. O., Broyart, C., & Santiago, J. (2018). Crystal structures of two tandem malectin-like receptor kinases involved in plant reproduction. *Acta Crystallographica Section D: Structural Biology*. https://doi.org/10.1107/S205979831800774X

Moussu, S., Broyart, C., Santos-Fernandez, G., Augustin, S., Wehrle, S., Grossniklaus, U., & Santiago, J. (2019). Structural basis for recognition of RALF peptides by LRX proteins during pollen tube growth. *BioRxiv*, 695874. https://doi.org/10.1101/695874

Moya-león, M. A., Mattus-araya, E., & Herrera, R. (2019). *Molecular Events Occurring During Softening of Strawberry Fruit*. *10*(May). https://doi.org/10.3389/fpls.2019.00615

Murphy, E., & De Smet, I. (2014). Understanding the RALF family: A tale of many species. *Trends in Plant Science*, *19*(10), 664–671. https://doi.org/10.1016/j.tplants.2014.06.005

Murphy, E., Smith, S., & De Smet, I. (2012). Small Signaling Peptides in Arabidopsis Development: How Cells Communicate Over a Short Distance . *The Plant Cell*. https://doi.org/10.1105/tpc.112.099010

Murphy, E., Vu, L. D., Van Den Broeck, L., Lin, Z., Ramakrishna, P., Van De Cotte, B., … De Smet, I. (2016). RALFL34 regulates formative cell divisions in Arabidopsis pericycle during lateral root initiation. *Journal of Experimental Botany*, *67*(16), 4863–4875. https://doi.org/10.1093/jxb/erw281

Nakamura, M., Tsunoda, T., & Obokata, J. (2002). Photosynthesis nuclear genes generally lack TATA-boxes: A tobacco photosystem I gene responds to light through an initiator. *Plant Journal*. https://doi.org/10.1046/j.0960-7412.2001.01188.x

Olsson, V., Joos, L., Zhu, S., Gevaert, K., Butenko, M. A., & De Smet, I. (2019). Look Closely, the Beautiful May Be Small: Precursor-Derived Peptides in Plants. *Annual Review of Plant Biology*, *70*(1), 153–186. https://doi.org/10.1146/annurev-arplant-042817-040413

Oosumi, T., Gruszewski, H. A., Blischak, L. A., Baxter, A. J., Wadl, P. A., Shuman, J. L., … Shulaev, V. (2006). High-efficiency transformation of the diploid strawberry (Fragaria vesca) for functional genomics. *Planta*. https://doi.org/10.1007/s00425-005-0170-3

Pandey, S. P., & Somssich, I. E. (2009). The role of WRKY transcription factors in plant immunity. *Plant Physiology*. https://doi.org/10.1104/pp.109.138990

Pearce, G., Moura, D. S., Stratmann, J., & Ryan, C. A. (2001). RALF, a 5-kDa ubiquitous polypeptide in plants, arrests root growth and development. *Proceedings of the National Academy of Sciences*, *98*(22), 12843–12847. https://doi.org/10.1073/pnas.201416998

Pearce, Gregory, Yamaguchi, Y., Munske, G., & Ryan, C. A. (2010). Structure-activity studies of RALF, Rapid Alkalinization Factor, reveal an essential - YISY - motif. *Peptides*, *31*(11), 1973–1977. https://doi.org/10.1016/j.peptides.2010.08.012

Pireyre, M., & Burow, M. (2015). Regulation of MYB and bHLH transcription factors: A glance at the protein level. *Molecular Plant*, *8*(3), 378–388. https://doi.org/10.1016/j.molp.2014.11.022

Prusky, D. (1996). PATHOGEN QUIESCENCE IN POSTHARVEST DISEASES. *Annual Review of Phytopathology*. https://doi.org/10.1146/annurev.phyto.34.1.413

Prusky, D., & Lichter, A. (2007). Activation of quiescent infections by postharvest pathogens during transition from the biotrophic to the necrotrophic stage. *FEMS Microbiology Letters*. https://doi.org/10.1111/j.1574-6968.2006.00603.x

Ramírez, V., Agorio, A., Coego, A., García-Andrade, J., Hernández, M. J., Balaguer, B., … Vera, P. (2011). MYB46 Modulates Disease Susceptibility to Botrytis cinerea in Arabidopsis . *Plant Physiology*. https://doi.org/10.1104/pp.110.171843

Ramírez, V., García-Andrade, J., & Vera, P. (2011). Enhanced disease resistance to botrytis cinerea in myb46 arabidopsis plants is associated to an early downregulation of CesA genes. *Plant Signaling and Behavior*. https://doi.org/10.4161/psb.6.6.15354

Sali, A., & Blundell, T. (1994). Sali, A. & Blundell, T. L. Comparative modelling by satisfaction of spatial restraints. J. Mol. Biol. 234, 779-815. *Journal of Molecular Biology*. https://doi.org/10.1006/jmbi.1993.1626

Scheer, J. M., Pearce, G., & Ryan, C. A. (2005). LeRALF, a plant peptide that regulates root growth and development, specifically binds to 25 and 120 kDa cell surface membrane proteins of Lycopersicon peruvianum. *Planta*, *221*(5), 667–674. https://doi.org/10.1007/s00425-004-1442-z

Seijo, T. E., Chandler, C. K., Mertely, J. C., Moyer, C., & Peres, N. A. (2008). Resistance of strawberry cultivars and advanced selections to Anthracnose and Botrytis fruit rots. *Proceedings of the Florida State Horticultural Society*, *121*, 246–248. Retrieved from http://strawberry.

Sharma, A., Hussain, A., Mun, B. G., Imran, Q. M., Falak, N., Lee, S. U., … Yun, B. W. (2016). Comprehensive analysis of plant rapid alkalization factor (RALF) genes. *Plant Physiology and Biochemistry*, *106*, 82–90. https://doi.org/10.1016/j.plaphy.2016.03.037

Sharma, N., Sharma, K. P., Gaur, R. K., & Gupta, V. K. (2011). Role of chitinase in plant defense. *Asian Journal of Biochemistry*. https://doi.org/10.3923/ajb.2011.29.37

Shulaev, V., Sargent, D. J., Crowhurst, R. N., Mockler, T. C., Folkerts, O., Delcher, A. L., … Folta, K. M. (2011). The genome of woodland strawberry (Fragaria vesca). *Nature Genetics*. https://doi.org/10.1038/ng.740

Slovin, J. P., Schmitt, K., & Folta, K. M. (2009). An inbred line of the diploid strawberry Fragaria vesca F. semperflorens for genomic and molecular genetic studies in the Rosaceae. *Plant Methods*, *5*(1), 1–10. https://doi.org/10.1186/1746-4811-5-15

Smith, B. J. (1990). Morphological, Cultural, and Pathogenic Variation Among Colletotrichum Species Isolated from Strawberry. *Plant Disease*. https://doi.org/10.1094/pd-74-0069

Spolaore, S., Trainotti, L., & Casadoro, G. (2001). A simple protocol for transient gene expression in ripe fleshy fruit mediated by Agrobacterium. *Journal of Experimental Botany*. https://doi.org/10.1093/jexbot/52.357.845

Srivastava, R., Liu, J. X., Guo, H., Yin, Y., & Howell, S. H. (2009). Regulation and processing of a plant peptide hormone, AtRALF23, in Arabidopsis. *Plant Journal*, *59*(6), 930–939. https://doi.org/10.1111/j.1365-313X.2009.03926.x

Stegmann, M., Monaghan, J., Smakowska-Luzan, E., Rovenich, H., Lehner, A., Holton, N., … Zipfel,

C. (2017). The receptor kinase FER is a RALF-regulated scaffold controlling plant immune signaling. *Science*, *355*(6322), 287–289. https://doi.org/10.1126/science.aal2541

Tavormina, P., De Coninck, B., Nikonorova, N., De Smet, I., & Cammue, B. P. A. (2015). The Plant Peptidome: An Expanding Repertoire of Structural Features and Biological Functions. *The Plant Cell*. https://doi.org/10.1105/tpc.15.00440

Thynne, E., Saur, I. M. L., Simbaqueba, J., Ogilvie, H. A., Gonzalez-Cendales, Y., Mead, O., … Solomon, P. S. (2017). Fungal phytopathogens encode functional homologues of plant rapid alkalinization factor (RALF) peptides. *Molecular Plant Pathology*, *18*(6), 811–824. https://doi.org/10.1111/mpp.12444

Vain, P., James, V. A., Worland, B., & Snape, J. W. (2002). Transgene behaviour across two generations in a large random population of transgenic rice plants produced by particle bombardment. *Theoretical and Applied Genetics*, *105*(6–7), 878–889. https://doi.org/10.1007/s00122-002-1039-5

van Schie, C. C. N., & Takken, F. L. W. (2014). Susceptibility Genes 101: How to Be a Good Host. *Annual Review of Phytopathology*. https://doi.org/10.1146/annurev-phyto-102313-045854

Vicente, A. R., Martínez, G. A., Civello, P. M., & Chaves, A. R. (2002). Quality of heat-treated strawberry fruit during refrigerated storage. *Postharvest Biology and Technology*. https://doi.org/10.1016/S0925-5214(01)00142-9

Wang, P., Yao, S., Kosami, K., Guo, T., Li, J., Zhang, Y., … Kawano, Y. (2019). Identification ofendogenous small peptides involved in rice immunity through transcriptomics- and proteomics-based screening. *Plant Biotechnology Journal*, 1–14. https://doi.org/10.1111/pbi.13208

Wei, W., Hu, Y., Han, Y. T., Zhang, K., Zhao, F. L., & Feng, J. Y. (2016). The WRKY transcription factors in the diploid woodland strawberry Fragaria vesca: Identification and expression analysis under biotic and abiotic stresses. *Plant Physiology and Biochemistry*. https://doi.org/10.1016/j.plaphy.2016.04.014

Williamson, B., Tudzynski, B., Tudzynski, P., & Van Kan, J. A. L. (2007). Botrytis cinerea: The cause of grey mould disease. *Molecular Plant Pathology*. https://doi.org/10.1111/j.1364-3703.2007.00417.x

Wu, J., Kurten, E. L., Monshausen, G., Hummel, G. M., Gilroy, S., & Baldwin, I. T. (2007). NaRALF, a peptide signal essential for the regulation of root hair tip apoplastic pH in Nicotiana attenuata, is required for root hair development and plant growth in native soils. *Plant Journal*. https://doi.org/10.1111/j.1365-313X.2007.03289.x

Xiao, Y., Stegmann, M., Han, Z., DeFalco, T. A., Parys, K., Xu, L., … Chai, J. (2019). Mechanisms of RALF peptide perception by a heterotypic receptor complex. *Nature*. https://doi.org/10.1038/s41586-019-1409-7

Xiong, J. S., Zhu, H. Y., Bai, Y. B., Liu, H., & Cheng, Z. M. (2018). RNA sequencing-based transcriptome analysis of mature strawberry fruit infected by necrotrophic fungal pathogen Botrytis cinerea. *Physiological and Molecular Plant Pathology*, *104*(August), 77–85. https://doi.org/10.1016/j.pmpp.2018.08.005

Yuan, H., Yu, H., Huang, T., Shen, X., Xia, J., Pang, F., … Zhao, M. (2019). The complexity of the Fragaria x ananassa (octoploid) transcriptome by single-molecule long-read sequencing. *Horticulture Research*, *6*(1). https://doi.org/10.1038/s41438-019-0126-6

Zhang, Q., Jia, M., Xing, Y., Qin, L., Li, B., & Jia, W. (2016). Genome-wide identification and expression analysis of MRLK family genes associated with strawberry (Fragaria vesca) fruit ripening and abiotic stress responses. *PLoS ONE*, *11*(9), 1–19. https://doi.org/10.1371/journal.pone.0163647

Zhao, S., Guo, Y., Sheng, Q., & Shyr, Y. (2014). Heatmap3: an improved heatmap package with more powerful and convenient features. *BMC Bioinformatics*. https://doi.org/10.1186/1471-2105-15-s10-p16